Dinoflagellate cyst stratigraphy and paleoecology of the Upper Miocene and Pliocene, Rees Borehole, Northern Belgium

Saif Al-Silwadi

Department of Earth Sciences

A thesis submitted in partial fulfillment of the degree of

M.Sc. in Earth Sciences

Faculty of Mathematics and Science, Brock University

St. Catharines, Ontario

©2017

Abstract

Correlating and dating Neogene deposits along the southern margin of the North Sea Basin have historically been complicated by the fragmentary nature of the outcrops studied, the boreal aspect of the benthic foraminifera present, and scarcity of planktonic microfossils. Dinoflagellate cysts and other palynomorphs from the Rees Borehole, Campine area of northern Belgium, are therefore used to elucidate the paleoenvironmental history of the area. The borehole contains the Upper Miocene Diest and Kasterlee, mid-Pliocene Poederlee, and Pliocene Mol and Merksplas formations. For the Diest Formation, the presence of *Achomosphaera andalousiensis andalousiensis*, *Barssidinium pliocenicum*, *Operculodinium*? *eirikianum*, *Operculodinium tegillatum*, *Selenopemphix armageddonensis* and the acritarch *Nannobarbophora walldalei* are consistent with a late Late Miocene age. The dinoflagellate cyst assemblages of the Kasterlee Formation in the Rees borehole differ from those of the Kasterlee Formation in other areas, and are more similar to assemblages of the underlying Diest Formation. This may be explained by reworking of the Diest into the Kasterlee Formation. The Poederlee Formation assemblages include *Achomosphaera andalousiensis suttonensis*, *Invertocysta lacrymosa*, *Operculodinium*? *eirikianum* and, with the absence of *Reticulatosphaera actinocoronata*, *Operculodinium tegillatum* and *Batiacasphaera minuta/micropapillata*, point to a mid- to Late Pliocene age, between 3.7 and 2.7 Ma. For the first time, dinoflagellate cysts were found in the Merksplas Formation, indicating a marine influence. The presence of *Achomosphaera andalousiensis suttonensis*, *Barssidinium pliocenicum*, *Capisocysta lyelli*, *Geonettia waltonensis*, and *Invertocysta lacrymosa* within this formation collectively point towards a Late Pliocene age. Assemblages throughout the Rees Borehole reflect neritic deposition within a restricted marine basin under temperate climates.

Acknowledgements

First and foremost, I'd like to thank my supervisor, Professor Martin J. Head. Working with him has been an incredible experience, and this project would not have been completed without his unmatched knowledge, patience and mentorship. He is truly an example to researchers, and I will forever be grateful for this privilege. I'd like to thank Professor Stephen Louwye of the University of Ghent, Belgium for suggesting this project, for collecting samples and arranging their palynological preparation, and for his crucial insight and help in so many aspects of this study. I'd also like to express my gratitude to Professor Francine McCarthy for her insight into my thesis, and Professor Rick Cheel for his help, support and good humor. My sincerest thanks also to Dr. Jan Hennissen for his help with correspondence analysis. A special thank you goes out to my fellow graduate students for their support, particularly Justin Pentesco for his feigned interest in my topic. Finally, I'd like to thank my partner, Stephanie Gunn. Her continuous encouragement, love and Excel knowledge was invaluable to completing this degree.

This research was supported by a Natural Sciences and Engineering Research Council of Canada (NSERC) Discovery Grant to Professor Martin Head. Financial support was also provided by the Faculty of Graduate Studies and the Department of Earth Sciences at Brock University.

Table of Contents

Table of Figures

Appendices

1.0 – Introduction

Neogene–Pleistocene marine deposits of northern Belgium are restricted to the north of Antwerp and the Campine area, and are characterised by nearshore deposits along the southern margin of the North Sea Basin (Figures 1–3). Biostratigraphy and regional correlation are challenging due to the fragmented and temporary nature of the outcrops available. This is further complicated by the difficulty in correlating the benthic foraminifera of the area to standard biozones owing to their boreal aspect. The expansion of Antwerp Harbour in the 1950s and 60s provided more complete and easily accessible outcrops. Further expansions of harbours in the area have since provided more outcrops for study, although there remain no permanent Neogene outcrops in the Campine area.

In recent years, studies of dinoflagellate cysts have given new insights into the Neogene and Lower Pleistocene of the southern margin of the North Sea Basin (Louwye & Laga, 1998; Louwye et al., 1999, 2007; Louwye & De Schepper, 2010; De Schepper et al., 2004; Quaijtaal et al., 2014). Studies of this nature have previously been conducted on the Diest, Poederlee and Kasterlee formations. The Rees borehole, located in the north of Belgium in the Campine area (Figure 1), was reported to penetrate these formations, along with the Mol and Merksplas formations. The borehole was therefore analysed for dinoflagellate cysts and other palynomorphs to shed new light on the biostratigraphy and paleoenvironments of the area. The findings are also compared to the framework established by previous studies in the Antwerp and Campine areas.

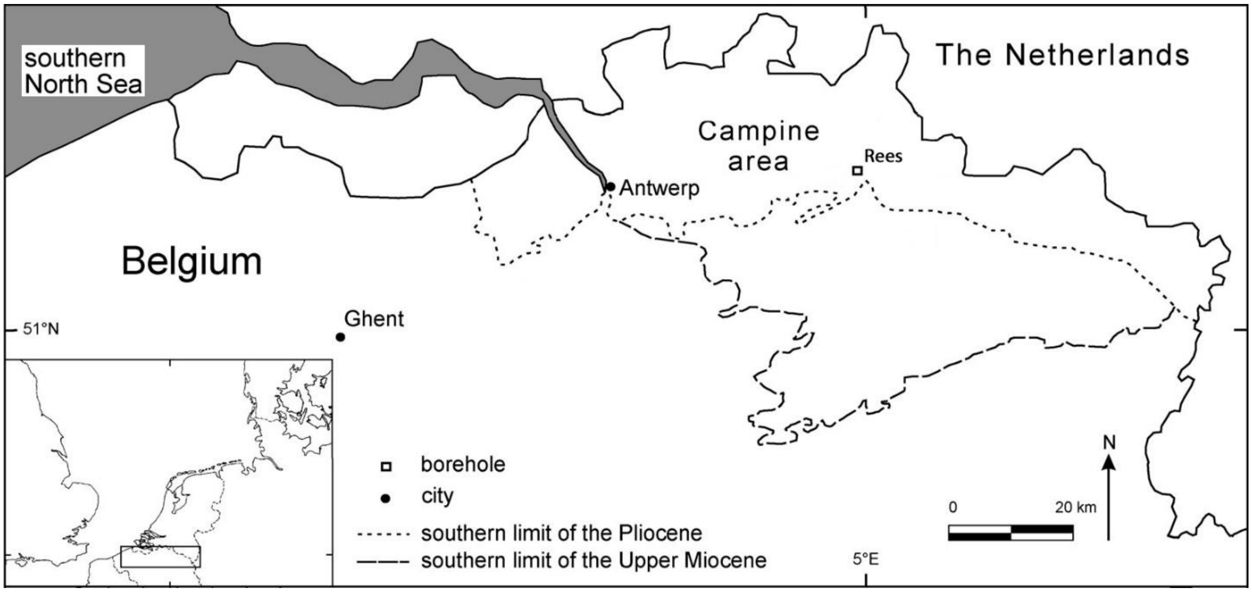

Figure 1 Northern Belgium showing position of the Rees borehole. Modified after Louwye & De Schepper (2010).

1.1 – Geological History

The geology of the North Sea Basin is complex, and has been studied extensively by oil and gas companies due to its hydrocarbon reserves. The formation of the basin has been influenced by three main events: the Caledonian, Variscan and Alpine orogenies.

The Caledonian Orogeny, which formed from the collision of the Laurentia, Baltica and Avalonia landmasses, took place during the late Silurian. Compressional forces were the dominant stresses of the area. These mountains formed part of the borders of the current day basin, as well as the basement rocks (Ziegler, 1975). At that time, the area was located south of the equator, and the arid environment allowed for high rates of erosion (Glennie, 1998). Early rifting occurred during the mid-Devonian, which resulted in erosion of the Caledonian mountains, sea level rise and deposition of marine limestones (Balson et al., 2002).

The Variscan Orogen took place during the Late Devonian to late Permian, and resulted from the collision of the Laurasia and Gondwana supercontinents. The resulting tectonism produced an extensive fault system, as well as uplift and volcanism in the northern part of the basin (Glennie, 1998). An extensional regime began, which caused a depression that was infilled with the sediment eroded from the Caledonian range (Balson et al., 2002). Eventually, the range collapsed as the Variscan range developed. The erosion of the Variscan mountains provided sediment to infill the basin. The sediment fill in the south caused subsidence, and a marine transgression occurred (Ziegler, 1978).

By the end of the Carboniferous, the supercontinent Pangea had formed, and as the continents came together, global sea level fell. The North Sea area was situated centrally in Pangea in an arid environment. As Pangea started to break up in the Triassic, global sea level rose, and the area was covered by shallow, warm sea, which allowed for the deposition of extensive thick sandstone layers (Glennie, 1998). By the end of the Triassic, major rifting was initiated in the north, and a mantle plume developed to the west of the basin, causing regional uplift and tilting. Rifting reached its peak during the Jurassic and spread southwards through the basin, forming many isolated basins (Balson et al., 2002).

During the Cretaceous, rifting had stopped and stagnation of currents allowed for the deposition of calcareous successions in the south, and deltaic siliciclastic deposits in the north. Subsidence began and continued throughout the Cretaceous, creating more accommodation for sediment deposition (Jarsve, 2014).

By the end of the Mesozoic, the North Sea Basin had moved approximately to its current location, influenced by the spreading of the Atlantic Ocean. Overall, subsidence continued and deposition of sand and mud units took place. The collision of Eurasia with the African and

Indian plates caused compressional stress on the basin (Ziegler, 1975). At this point, the Alpine Orogeny began, a tectonic phase that continues to this day. This orogeny reactivated older faults, and led to cycles of uplift and erosion, particularly at the basin margins. As the rifting slowed, regional subsidence took place and the present day intracratonic, symmetrical basin formed (Ziegler, 1975). This subsidence is thought to be due to thermal relaxation of the thinned lithosphere (Scalter & Christie, 1980).

The Cenozoic was dominated by several cycles of uplift and subsidence. The Paleocene was marked by carbonate sedimentation, followed by subsidence in the south and uplift around the remainder of the basin due to the development of the Iceland Plume. While the plume is thought to have developed quite far from the North Sea, it seems to have influenced the North Sea Basin area due to the dynamic fluid-flow field generated from the mantle in and around the ascending plume (Nadin & Kusznir, 1995). This resulted in the transport of sand-rich sediment to the southeast margin of the basin (Gibbard & Lewin, 2016). Subsidence then took place during the Early Eocene due to waning influence of the Iceland Plume, which accommodated the deposition of initially clay-rich and then sand-rich fluvial deposits (Nadin & Kusznir, 1995). Uplift then occurred in the south and west margins due to renewed collision of the African and European plates. This was then followed by subsidence and marine transgression along the southern margin of the North Sea. By the end of the Eocene, the Pyrenean tectonic phase began and created a regional hiatus in sedimentation in the south (Gibbard & Lewin, 2016).

The Oligocene began with uplift along the west and northeast margins, causing sedimentation to be more uniform and basin-centered. This was followed by a major fall in sea level in the earliest Rupelian as a result of the Oi-1 cooling event. A consequence was major erosion and extension of river systems around the basin. Another hiatus occurred at the Oligocene–Miocene boundary, caused by tectonic activity associated with the Savian Alpine phase as well as an increase in global ice volume (Mi-1 cooling event). This was followed by a widespread major marine

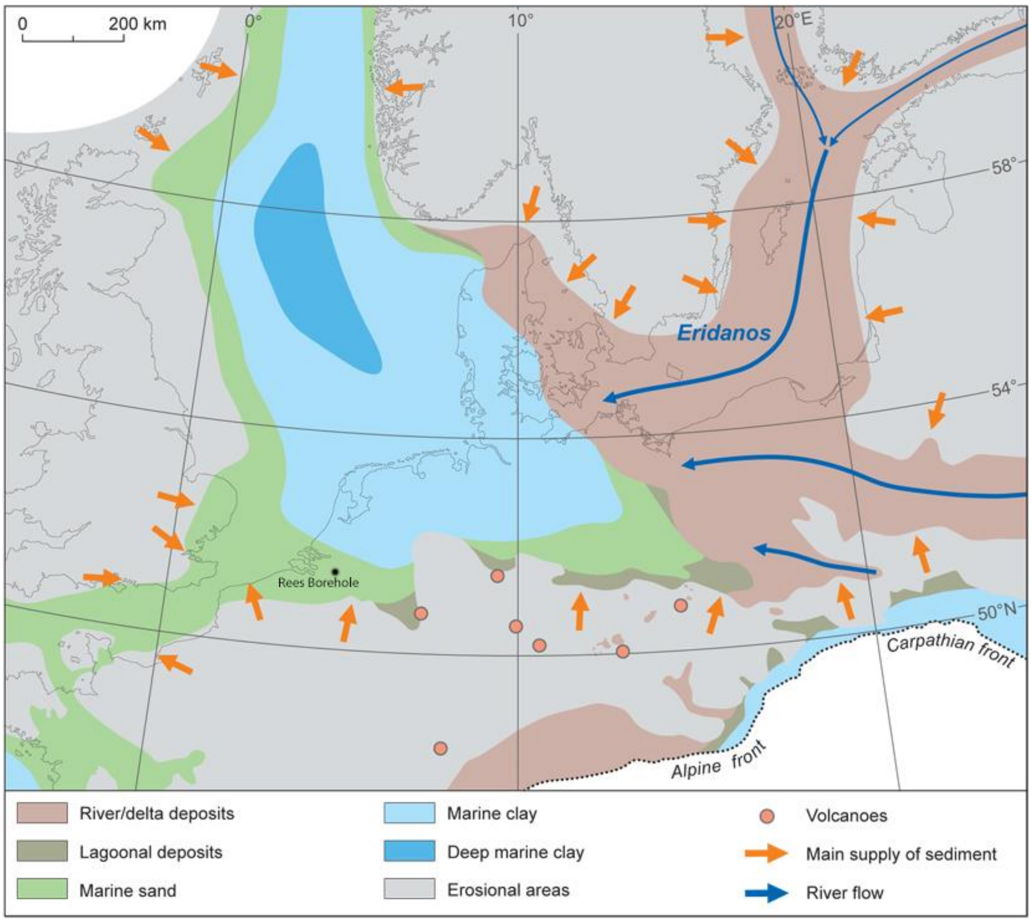

Figure 2 North Sea Basin during the mid-Miocene. Location of Rees borehole marked. Modified after Gibbard & Lewin (2016)

transgression due to the mid-Miocene climatic optimum. Subsidence then started in the southeast during the Late Miocene, followed by further regional subsidence. At this time, sediment was delivered by various rivers around the south and east of the basin, as river systems expanded. This pattern of uplift and subsidence continues to the present day, with thick sediment accumulations in the North Sea that started from the mid-Miocene. Sea level rise continued into the Pliocene, although offshore progradation of the southern shelf took place due to increased sedimentation and uplift that occurred at the same time. This was followed by more uplift, and the dominance of braided fluvial deposits (Gibbard & Lewin, 2016). Uplift began again in the Pleistocene, causing regression and further expansion of river complexes in the west and south.

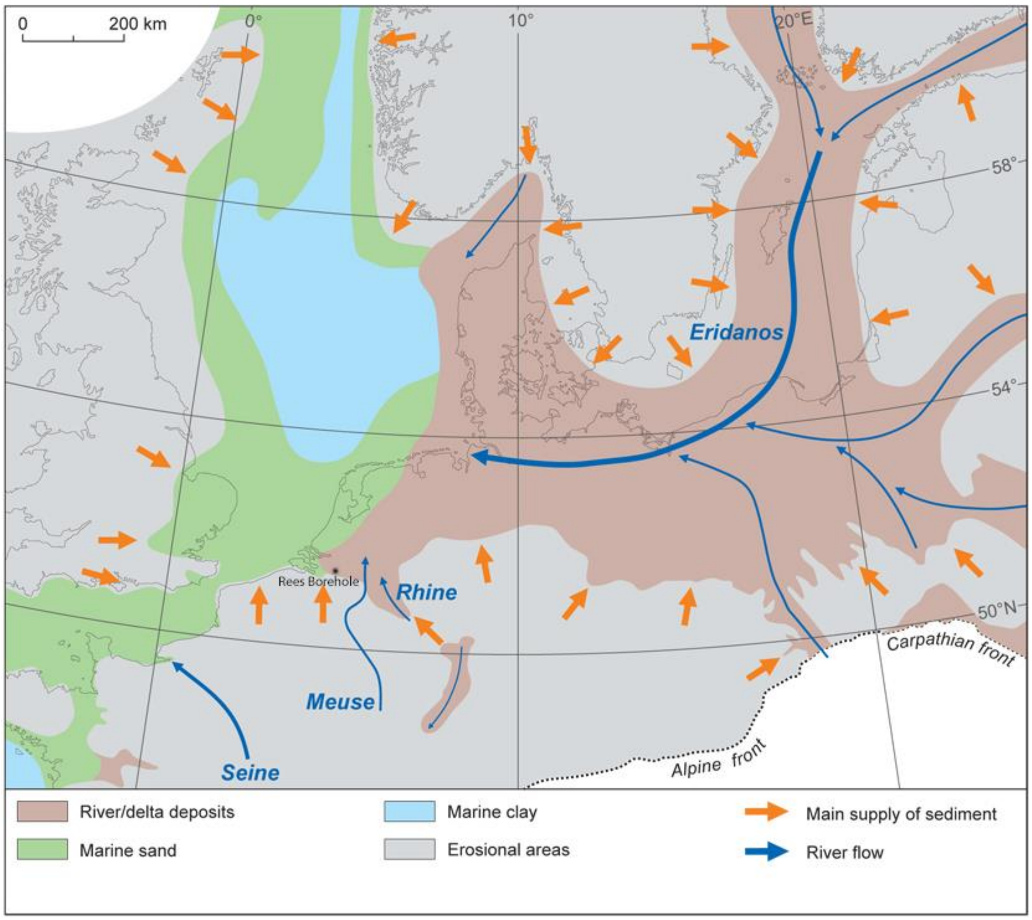

Figure 3 North Sea Basin during the Early Pliocene. Location of Rees borehole marked. Modified after Gibbard & Lewin (2016)

Glaciation occurred at approximately the Pliocene–Pleistocene transition and again through the later Pleistocene. River incision increased at this time, as did erosion as a result of the glaciation.

By the Middle Pleistocene, river and deltaic complexes had increased in size, especially in the south. Further uplift occurred which caused more sediment input into the basin. River complexes continued to dominate as sea level fell at the transition to the most recent glaciation (Gibbard & Lewin, 2016).

1.2 – Background History

The Neogene of Belgium has been studied for well over 100 years. The deposits are mostly shallow marine, and exhibit intraformational heterogeneity and lateral variability. Accordingly, the different lithostratigraphic units can share similarities and appear indistinguishable from one another, especially around transition zones. Many of the deposits also lack stratigraphically useful macrofossils. Regional correlation and establishment of a chronostratigraphic framework is therefore complicated. The most commonly accepted lithostratigraphic framework is shown in Figure 4.

Series		Antwerp Area	N	Antwerp-Campine Area	S	Campine Area
Pliocene	Upper	Lillo Formation	Lillo Formation		Poederlee Formation	Brasschaat Formation Mol Formation Poederlee Formation
	Lower	Kattendijk Formation	Kattendijk Formation			
Miocene	Upper	Diest Formation: Deurne Sands		Diest Formation: "Diest Sands", Dessel Sands	Kasterlee Formation	Kasterlee Formation Diest Formation: "Diest Sands", Dessel Sands
	Lower-Middle	Berchem Formation		Berchem Formation		Bolderberg Formation

Figure 4 Lithostratigraphic framework of the Neogene of northern Belgium. Modified in part from Louwye et al. (1999).

Dinoflagellate cysts have already been established as biostratigraphic markers and paleoenvironmental indicators throughout the world, helping to provide insight into depositional histories and environments. Various dinocyst biozonations have been erected based on specific associations of cysts that point to specific age dates. These biozonations have been shown to be correlatable interregionally, and include the biozonation of de Verteuil and Norris (1996), Dybkjaer & Piasecki (2010), Powell (1992, 1996) and Zevenboom (1995).

The first study of the dinoflagellates from the Neogene of Belgium was published by Louwye & Laga (1998). Their findings, discussed in detail in a separate section, show that dinocysts can successfully be used as indicators of age, paleoenvironment, and depositional history in the Cenozoic of Belgium. Many more studies have since been conducted on various Neogene formations in Belgium, and have been useful in understanding the complex geologic history of the area. This remains an ongoing process, however, and more formations/successions require analysis to aid correlation and gain a full understanding of the depositional history.

1.2.1 – The Diest and Kasterlee formations

The "Diestien" stage was first introduced by Dumont (1839) to describe the highly glauconiferous coarse-grained sands in north Belgium. The paucity of macrofossils hampered straightforward correlation, but the formation was included in the Pliocene based on its stratigraphic context. Vanden Broeck (1882) was the first to study the stratigraphy and depositional history of the non-fossiliferous, slightly glauconitic, fine-grained sands that overlie the coarser Diest Sands in the Kasterlee area, now known as the Kasterlee Formation. It was first thought to be the lateral equivalent of the Antwerpen "sables à Isocardia cor", now known as the Lower Pliocene Kattendijk Formation. Since there was no clear break between the Kasterlee and the underlying Diest, they were treated as the same unit, although this grouping was tentative owing to the lack of macrofossils in the two formations. Further studies (Vanden Broeck, 1902; Van Ertborn 1902) emphasised the indivisibility of these two units, placing them into the "étage Diestien", which then constituted the base of the Pliocene in Belgium. It wasn't until Halet (1935) that the two formations were first separated, and the Diest Formation was recorrelated to the Upper Miocene based on molluscan evidence. The Kasterlee was also considered to be a fluvio-marine regressive facies that followed the transgressive facies of the Diest. De Heinzelin (1955) regrouped both formations into the Upper Miocene "Diestien" Formation. A study by Gulinck (1963), however, reverted to the Vanden Broeck (1882) classification, using geometrical analysis and borehole data to correlate the formations with the Pliocene Kattendijk Formation once again.

De Meuter & Laga (1976) conducted a comprehensive study of the benthic foraminifera of the Neogene of northern Belgium. They defined six foraminiferal zones in the Antwerp area for the Miocene and Pliocene, which were correlated with deeper marine Neogene sediments in The Netherlands by Doppert et al. (1979). These studies were further expanded by Nuyts (1990) and Hooyberghs (1996) to construct a regional chronostratigraphic framework for the Neogene of Belgium. Although this helped to improve regional correlation, integration with international standard biozones proved difficult due to the boreal nature of the foraminifera of the area. Foraminiferal analysis of the Diest Formation by De Meuter & Laga (1976) led to an Upper Miocene designation. Because no new evidence had been presented since Gulinck (1963), they also assumed a correlation between the Kasterlee Formation and the Pliocene Kattendijk Formation.

It was not until the last few decades that the stratigraphy and age ranges of the different formations have been narrowed down, largely owing to dinoflagellate cyst analysis. Louwye & Laga (1998) published the first dinoflagellate cyst study on the Diest Formation. Based on the assemblage of cysts, an age range of late Tortonian to Messinian (Late Miocene) was proposed. Further studies (Louwye et al., 1999; Louwye, 2002; Louwye & Laga, 2008) were conducted on the Deurne and Dessel Sands members to analyse their dinoflagellate cyst content. The Deurne

Sands were found to be of mid- to late Tortonian age, whereas the Dessel sands were found to be early to mid-Tortonian. The diachronous nature of the members of the Diest Formation was therefore established. Louwye et al. (2007) analysed dinoflagellate cysts of the Kasterlee and Diest formations and concluded that the two formations were distinctly separate depositional cycles with different cyst assemblages, separated by a regressive phase. An age between 7.5 and 5.73 Ma was proposed for the Kasterlee Formation, thus lowering it from the Pliocene to the Upper Miocene.

1.2.1.1 – Diest Formation

The Diest Formation was formally defined by De Meuter & Laga (1976) as poorly sorted, highly glauconiferous and mostly coarse grained sands, with low clay content, occasional sandy ironstone layers, as well as being mostly barren of fossils. The type section of this formation is a series of exposures at the former fortress in the town of Diest, in the Brabant area.

The formation has been separated into three members. The Deurne Sands Member is a formally defined member found only in the Antwerp area, and consists of a basal gravel of very fine to fine grained sands, rounded pebbles with bivalve shells, bryozoans, and calcareous worm tubes (Gilbert & De Heinzelin, 1955). The formally defined Dessel Sands is also a basal gravel member, found only in the Antwerp–Campine area. It consists of glauconiferous, very fine grained sands and rounded pebbles, and is rich in calcareous microfossils (Laga & De Meuter, 1972). The Diest Sands member is the informal name of the member comprising the rest of the Diest Formation in all localities, and complies with the formal description of the formation. Although an informal name, “Diest Sands” will be used in this study to refer to the part of the Diest Formation excepting the Dessel and Deurne Sands members. The Diest Formation overlies the Lower to Middle Miocene Berchem Formation in the Antwerp and Antwerp–Campine areas, and the Lower to Middle Miocene Bolderberg Formation in the Campine area. In the Antwerp and northern Antwerp–Campine areas, the Diest Formation is overlain by the Kattendijk Formation. In the Campine and southern Antwerp–Campine areas, it is overlain by the Kasterlee Formation.

The Diest Formation was deposited in a large erosional gulley, formed during the tectonic uplift of central Belgium, following a period of non-sedimentation. This gulley was deeply incised into the Lower to Middle Miocene Bolderberg and Berchem formations, so the Diest Formation disconformably overlies these formations (Wouters & Vandenberghe, 1994). Deposition started with the Dessel Member in the deeper part of the gulley situated in the Campine area during the early Tortonian. The depocentre shifted to the marginal marine environment of the shelf, to the north of Antwerp, with the deposition the Deurne Sands during the mid- to late Tortonian (Louwye et al., 1999; Louwye & Laga, 2008).

Benthic foraminifera have been found in the Deurne and Dessel Sands, although not in the rest of the formation. The two members were characterized as being part of the *Uvigerina hosiusi deurnensis – Elphidium antoninum* Zone, of Late Miocene age (De Meuter & Laga, 1976).

The dinoflagellate cyst association of the Dessel Sands Member has been documented in the Oostmalle, Poederlee, Retie, Mol wells of the Antwerp-Campine area (Louwye et al., 1999). It is characterised by *Hystrichosphaeropsis obscura*, *Labyrinthodinium truncatum* subsp. *truncatum*, *Operculodinium*? *eirikianum*, *Palaeocystodinium golzowense*, *Pentadinium laticinctum laticinctum*, and *Sumatradinium soucouyantiae*. This correlates with both the DN8 and DN9 zones, giving an early to mid-Tortonian age. The Deurne Sands Member has been found to contain *Barssidinium wrennii*, *Bitectatodinium*? *arborichiarum*, *Habibacysta tectata*, *Labyrinthodinium truncatum truncatum*, *Operculodinium*? *eirikianum, Reticulatosphaera* *actinocoronata*, and *Sumatradinium soucouyantiae*. This association correlates with the DN8 zone of de Verteuil and Norris (1996). This, in combination with a regional correlation with northern Germany, gives a mid- to late Tortonian age for the Deurne Sands (Louwye, 2002). The Diest Sands have been documented in the Kalmthout well north of Antwerp (Louwye & Laga, 1998; Louwye et al., 1999), the Oostmalle, Poederlee, Retie, Mol and Neeroeteren wells of Antwerp-Campine and Campine areas (Louwye et al., 1999) and borehole 48W-180 near the village of Wijshagen (Louwye & Laga, 2008). It is characterised by *Achomosphaera andalousiensis andalousiensis*, *Dapsilidinium pastielsii* (as *Dapsilidinium pseudocolligerum*), *Hystrichosphaeropsis obscura, Operculodinium*? *eirikianum*, *Reticulatosphaera actinocoronata, Selenopemphix armageddonensis*, and *Selenopemphix brevispinosa*. These species correlate with both the DN9 and DN10 biozones of de Verteuil & Norris (1996), delimiting an age of Tortonian to Messinian (Louwye & Laga, 1998).

Vandenberghe et al. (2014) performed K-Ar dating on glauconite using samples from two sections of the Diest Formation in an attempt to correlate them. The ages obtained from the 28 samples varied between 13.7 ± 0.4 Ma and 17.7 ± 0.4 Ma. This differs significantly from the Tortonian age (11.6–7.2 Ma) obtained from dinoflagellate cyst analysis. Two samples from the Dessel-5 borehole in the Campine area did, however, give ages of 11.4 and 11.5 ± 0.4 Ma, which were more consistent with the dinoflagellate cyst biostratigraphy. This discrepancy is thought to be caused by large scale reworking of glauconite from older Miocene deposits. Adrieans (2016, unpublished thesis) studied several boreholes in the North Sea Basin. The pelletal glauconite of various Neogene formations was analysed, and found to have originated from the large-scale reworking of older deposits. Only the Berchem Formation found in the Antwerp area was thought to possibly have authigenic glauconite. As such, radiometric analysis of the glauconite for age estimations of other formations might be expected to give misleading results.

1.2.1.2 – Kasterlee Formation

The Kasterlee Formation is formally defined as a slightly glauconitic, micaceous, fine-grained sandy unit, with intercalations of micaceous clay and a lack of macrofossils. Outcrops occur on the hills near the "Kleine Nete" Valley, near the village of Kasterlee of the Antwerp province (De Meuter & Laga, 1976).

The shallow marine deposits of the Kasterlee Formation conformably overlie the fully marine transgressive Diest Formation, although the transition is often barely distinguishable, especially in the Campine area (Louwye et al., 2007). In the region north of Poederlee, the Kasterlee Formation is overlain by a Quaternary cover, or the Pliocene Mol or Poederlee formations.

Dinoflagellate cyst studies have been conducted on the Kasterlee Formation in the Oud-Turnhout borehole of the Campine area (Louwye & De Schepper, 2010), and the Dessel-2 borehole of the Campine area and in an outcrop near Olen (Louwye et al., 2007). Analysis points towards a shallow marine environment, characterised by *Barrsidinium taxandrianum, Reticulatosphaera actinocoronata, Selenopemphix armageddonensis*, *Trinovantedinium ferugnomatum* as well as abundant *Gramocysta verricula* near the base of the formation. Based on these species, a Messinian age of 7.5 to 5.32 Ma was given for the Kasterlee. The upper boundary of the formation was correlated with the Me2 sequence boundary of Hardenbol et al. (1998), constraining the minimum age to 5.73 Ma (Louwye et al., 2007; Louwye & De Schepper, 2010).

1.2.2 – The Poederlee Formation

The first study of the sandy deposits found in the Poederlee area is attributed to Dumont in about 1850 (Mourlon, 1882), and it included the deposits within the Diestien classification, which was then thought to be of Pliocene age. De Heinzelin (1955) separated the Poederlee from the Diest, and assigned it to the Lower Pleistocene due to similarities with a new Pleistocene unit, the Merksem Sands of the Lillo Formation. Tavernier and de Heinzelin (1962) studied the macrofossils of the Poederlee Formation, and although they were intensely limonitized and weathered, used them to correlate these deposits to the Kruischans Sands, part of what is now known as the Pliocene Lillo Formation. They also considered the Poederlee to be a transgressive unit. Further studies (Vandenberghe et al., 1998, 2004; Buffel et al., 2001) also suggested a correlation with the lower part of the Lillo Formation due to sedimentological similarities and molluscan evidence, and proposed a Piacenzian age.

A palynological study was first conducted on the Poederlee Formation by Louwye & De Schepper (2010) who suggested a mid-Piacenzian age, between 3.21 and 2.76 Ma. Comparing it to the Kasterlee Formation, the Miocene–Pliocene hiatus was determined to be of variable magnitude in the North Sea Basin, lasting 3.2 million years in the Antwerp area and 2.52 million years in the Campine area.

De Meuter & Laga (1976) formally defined the Poederlee Formation as slightly glauconitic, fine grained sands. The lower part of the formation was found to have small lenses of clays, and the upper part to consist of better sorted, more oxidised sands, sometimes including limonitic sandstones with shell moulds and traces of bioturbation. This upper section is referred to as a Heieinide facies (Buffel et al., 2001). The base of the Polderlee Formation is marked by the Hukkelberg Gravel, a basal gravel of rounded quartz, flint and silicified limestone.

The Poederlee type section is exposed on the hilltops north of the town of Poederlee in the province of Antwerp. The formation is confined to the Campine area, and unconformably overlies the Kasterlee Formation. In the north Campine area, the Poederlee is covered by the Pliocene Mol Formation or the Lower Pleistocene Brasschaat Formation (Louwye & De Schepper, 2010).

Previous dinoflagellate cyst analysis of the Polderlee Formation was conducted by Louwye and De Schepper (2010) on the Oud-Turnhout borehole in the Campine area. Their research shows a neritic paleoenvironment along with an open-ocean influence and shallowing-upwards trend near the top of the formation. The association is characterised by *Achomosphaera andalousiensis suttonensis*, *Invertocysta lacrymosa*, *Operculodinium*? *eirikianum*, and *Selenopemphix brevispinosa*. These species, along with the distinct absence of *Batiacasphaera minuta/micropapilata*, *Operculodinium tegillatum* and *Reticulatosphaera actinocoronata*, led to a Piacenzian age assignment, between 3.21 and 2.76 Ma, for the Poederlee Formation (Louwye & De Schepper, 2010).

1.2.3 – Mol Formation

Few studies have been conducted on the Mol Formation. These deposits were first studied by Mourlon (1896) and later analysed by De Meuter & Laga (1976), although no foraminifera were present.

The Mol Formation is considered Pliocene in age, and is composed of estuarine to continental white, high-quartz sands. The type section consists of sand pits that have been quarried for use in glass making, and is located near the village of Mol (National Commission for Stratigraphy, Belgium).

The formation is separated into two units, on the basis of grain size. The Mol Inferior or the Mol Donk unit is very fine and slightly glauconitic. The Mol Superior or Mol Maatheide appears coarser. The formation is confined to the northeast of the Campine area and can overlie the Diest or Poederlee formations.

Louwye & De Schepper (2010) found few dinoflagellate cysts in the Mol Formation, and no interpretation was made of their findings. Based on its stratigraphic relations, the formation was assigned a Late Pliocene age.

1.2.4 – Merksplas Formation

Few studies similarly have been conducted on the Merksplas Formation. It was first mentioned by Gulink (1962) and later analysed by De Meuter & Laga (1976), although, as with the Mol Formation, no foraminifera were present.

The Merksplas Formation was deposited in an estuarine environment, and comprises grey, medium to coarse sands that are sporadically medium-fine grained, as well as occasional gravel, silty to clayey lenses, wood fragments, shells, and shell fragments (Bogemans, 1999). The type section of the Merksplas Formation is in the northern Campine area, cropping out near the municipality of Malle. Two separate depositional facies are recognized. The first is sandy, non-calcareous, and contains silt and clay intercalations. The second is a medium-fine sand facies, and contains shell debris and few fine siliciclastic intercalations. Where both facies are present, the first overlies the second (National Commission for Stratigraphy, Belgium).

The formation overlies the Lillo Formation in the northern Antwerp–Campine area, and the Poederlee Formation in the northeast Antwerp–Campine area. In the Campine area, it overlies the Mol Formation and is overlain by the Pleistocene Malle Formation. In some eastern localities, the Mol is found to underlie the Merksplas, although this is unclear as the similarity in the lithologies of these two units obscures the boundaries between them (National Commission for Stratigraphy, Belgium).

No dinoflagellate cyst studies have been conducted on the Merksplas Formation. Based on its stratigraphic context, the base of the formation was given a Late Pliocene age, although it extends into the Pleistocene (National Commission for Stratigraphy, Belgium).

1.3 – The Rees Borehole

The present study focuses on the Rees 17E399 borehole, located in the north of the Campine area (Figure 1). The borehole was drilled by the Geological Survey of Belgium as part of a stratigraphic collection of boreholes. The stratigraphy of the top 40 m was first assessed by Buffel et al. (2001) based on geometry, grain size, and observable fossils (Figure 5). The authors interpreted the Diest Formation to be below 33.25 m based on regional correlation and grain size analysis. The Kasterlee Formation was thought to be between 33.25 m and 25.3 m, due to the higher level of sorting and finer grain-size transition from the Diest Formation, with the transition occurring at 33.25 m. The Poederlee Formation was interpreted to be between 25.5 m and 17.0 m, with a basal shell debris layer and the characteristic Heieinide facies at the top of the formation. This formation was correlated to the Oorderen Member of the Lillo Formation, based on mollusc shells. From this correlation, a Piacenzian age was assigned. The Mol Formation was interpreted between 17.0 m and ca. 9.0 m, based on the white quartz sand composition. Finally, the Vosselaar Member, part of the Malle Formation, was interpreted as being on top of the Mol.

Adriaens (2016, unpublished thesis) recently conducted a study on the Rees and other nearby boreholes, focusing on the lithology and clay mineralogical composition. In contrast to the

Buffel et al. (2001) study, the Vosselaar Member was reinterpreted as the Merksplas Formation. This is because both the Merksplas and Malle formations are present in the Campine area. In such a case, no distinction is made between the two units, and the term Merksplas Formation is used (National Commission for Stratigraphy, Belgium). The most notable difference is in Adriaens' analysis of the Kasterlee Formation. Assessment of other boreholes has found that the Kasterlee Formation has a finer grain size, and much less pelletal glauconite, siderite, muscovite, plagioclase and chlorite than the subjacent Diest Formation. It was also found that the sediment properties of the top of the Diest Formation transition into those of the Kasterlee Formation. A "reworked Diest" interval was marked in the Dessel-2 and Dessel-5 boreholes at this transition, reaching a maximum thickness of around 2 m. In the Rees borehole, however, the mineralogy of the Diest and Kasterlee formations was found to be relatively consistent. In addition, the Kasterlee Formation was found to have anomalously high pelletal glauconite concentrations, similar to those of the underlying Diest Formation. The typical Kasterlee sediments were therefore concluded to be absent from the Rees borehole. The transition between the Kasterlee and Diest interpreted by Buffel et al. (2001) is therefore based only on a change in grain size. In light of this, it was proposed that the Kasterlee Formation in the Rees borehole is in fact made up of the same "reworked Diest" as found in other boreholes, but spanning an entire 8 m.

Given the foregoing, a major objective of this study is to determine whether dinoflagellate cysts in the Rees borehole can be used to characterize the Diest and Kasterlee formations and resolve the above outlined issue. In addition, since similar studies have never been conducted on the Mol and Merksplas formations, they were also examined for dinoflagellate cysts and sporomorphs to gain a better understanding of the biostratigraphy and paleoenvironmental history of the formations. Paleoenvironmental reconstruction also gives us information on the climate of a restricted basin in response to the climate changes occurring throughout the Miocene and Pliocene. Overall, this analysis provides new information on the depositional history of the area, thereby improving understanding of the complex development of the North Sea Basin.

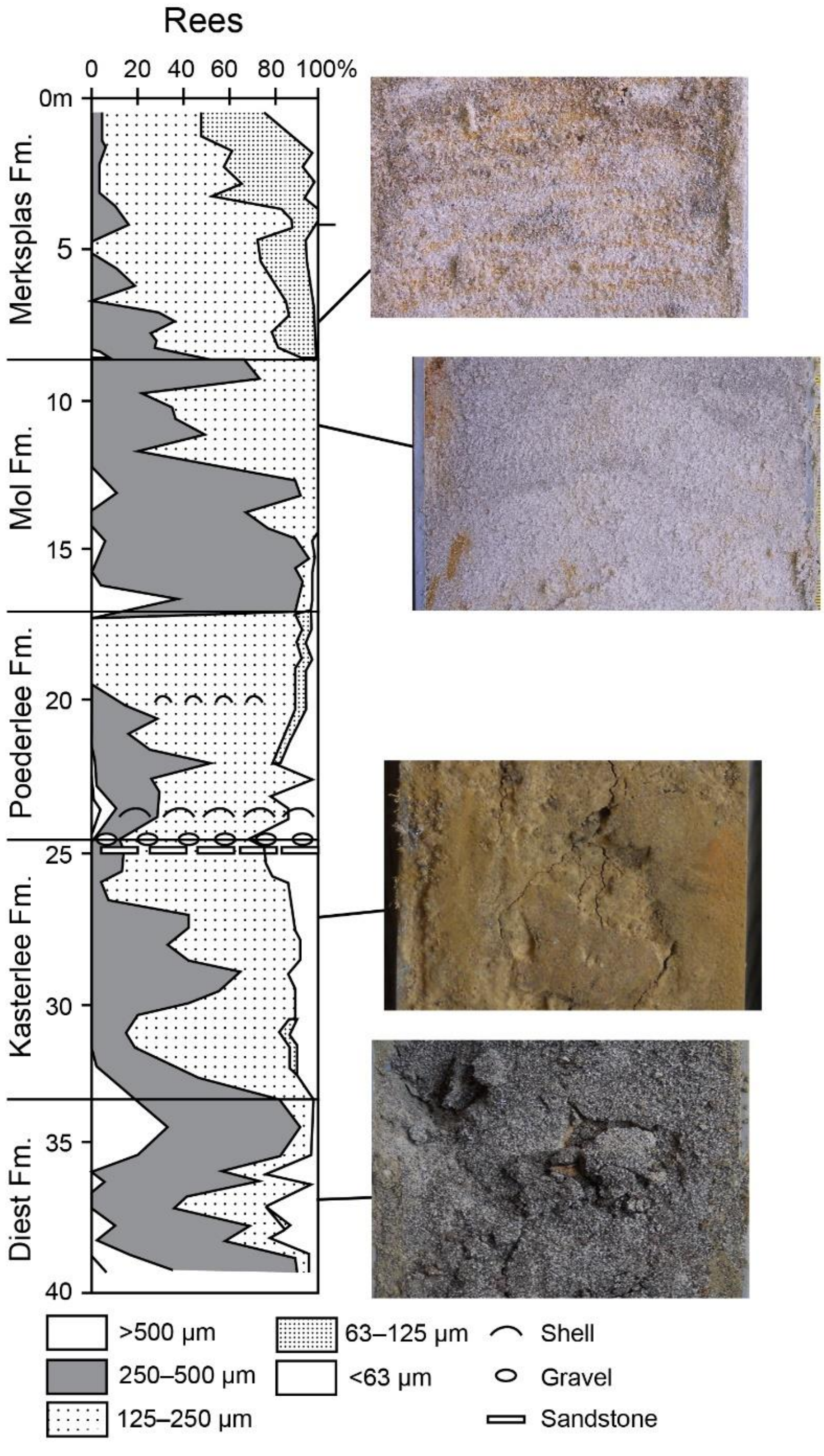

Figure 5 Lithostratigraphy of the Rees borehole, showing formations contained therein, along with pictures of the Diest, Kasterlee, Mol and Merksplas formations. Core width approximately 10 cm. Horizontal axis of the log shows percentage of grain size. Legend below. Modified after Buffel et al. (2001). Photographs courtesy of S. Louwye.

2.0 – Methods and Materials

2.1 – Preparation procedure

The Rees core is curated at the core repository of the Geological Survey of Belgium, and samples were taken from this core by Prof. Stephen Louwye. Initially, a total of 56 samples were taken, with spacing between about 20 cm and about 1.3 m, with an average of around 21 cm. After initial analysis, a second set of 25 samples was taken at higher resolution from the Merksplas Formation, with a spacing of 10 cm. Samples were processed for dinoflagellate cysts at the University of Ghent under his direction. Microscope slides were then sent to Brock University for palynological analysis. The following describes the protocol used at the University of Ghent. The samples were oven dried at 60°C, and then weighed and rehydrated with demineralised water. Weights taken were between 43 and 76g, with most being about 75g. Two *Lycopodium clavatum* tablets (batch no. 177745, X = 18,584 ± 828 was used for samples 573 to 530, and batch no. 1031, X = 20,848 ± 1546 for samples 920 to 935) were added to the material. Cold hydrochloric acid (2N) was then used to remove carbonates before the material was allowed to settle overnight. It was then rinsed with demineralised water until the pH approached neutral. A small quantity of 40% hydrofluoric acid was added for 4 hours to remove sand, followed by the stepwise addition of demineralised water and decanting. The samples were allowed to settle overnight, before being decanted again. The remaining silicates were removed by adding more hydrofluoric acid and heating in a water bath at 65° C for two days. The reaction was stopped by the addition of demineralised water. The samples were allowed to settle overnight, and were then decanted. Fluorosilicates were removed by the addition of hydrochloric acid (2N), and kept in a 65° C water bath for two days, with the hydrochloric acid being refreshed every day. The samples were then placed in an ultrasonic bath for 30 seconds to break down clumps of amorphous organic matter, before sieving using a 10 μm nylon mesh screen. The resulting residues were transferred to plastic vials, and several drops of $CuSO_4$ solution were added to prevent fungal growth. The vials were centrifuged for 5 minutes at 2000 rpm and the surplus water removed. One drop of residue was mounted on a microscope slide with one drop of glycerine jelly. The slides were covered with cover slips and sealed with nail polish, although it is noted that marine varnish gives a longer-lasting seal. The slides are stored in the Department of Earth Sciences, Brock University. For further information on the preparation procedure, see Quaijtaal et al. (2014).

Slides were initially scanned for the presence of dinoflagellate cysts in sufficient quantity to count. Those estimated to have at least 200 dinoflagellate cysts were enumerated. The slides with lower concentrations of cysts were counted, where preservation was good enough. These samples were not included in statistical analysis. Of the 81 samples processed, 14 were barren, 12 were found to have very low concentrations of dinoflagellate cysts, and 4 microscope slides (4 samples) arrived broken. At least 200 cysts were counted in each slide. After counting, the slides were scanned for rare specimens. Acritarchs, bisaccate, monosaccate and nonsaccate pollen, fern and fungal spores, green algal palyonmorphs, foraminiferal linings, invertebrate remains and incertae sedis forms were tracked and recorded during the counting process. All slides were counted with a Leica DM2500 microscope using a 400x magnification objective lens. Photomicrographs were taken with a Leica MC170 HD camera under 1000x magnification, and can be found in Appendix III.

Nomenclature follows Williams et al. (2017) for the dinoflagellate cysts, and De Schepper et al. (2004, 2014) for the acritarchs. *Achomosphaera* and *Spiniferites* species are grouped into *Spiniferites/Achomosphaera* spp. indet. due to the difficulty distinguishing between most species.

Taxa counted separately include *Spiniferites mirabilis, Spiniferites falcipedius* and *Achomosphaera andalousiensis* subsp. *andalousiensis* and subsp. *suttonensis*. *Spiniferites* species of stratigraphic value in the North Atlantic region, including *Spiniferites coniconcavus* and *Spiniferites elongatus*, were not found in this study.

Fragments of bisaccate pollen are often found in marine palynological assemblages, and need to be considered when determining the total bisaccate pollen count. In the present study, several methods were evaluated, namely counting mostly intact central bodies (CBC), counting only sacs (SC), and counting only whole grains (WGC). Using the CBC method, central bodies that are 50% intact or more are counted, while fragments less than this are ignored to prevent overrepresentation. With the SC method, only the sacs of the pollen grains are counted, whether they are attached or detached. The resulting number is then halved to obtain the bisaccate count number. Using the WGC method, only completely intact grains are counted.

To test the validity of these methods, two samples with moderate preservation (samples 536, 531) were selected and counted for bisaccate pollen using the three methods (Figure 6). The results show very similar numbers between CBC and SC, but vastly lower numbers with the WGC method. Since pollen grains will invariably become damaged by taphonomic processes, the WGC method would represent a large underestimation of bisaccate pollen amounts. When considering SC versus CBC, the difference is about 10%. Although this isn't much, the increase in sac numbers appears to be because sacs seemed to fragment more than central bodies. In their broken states, it was difficult to differentiate a broken sac from a smaller sac. As such, counting sacs would give a slight overrepresentation of bisaccates in the material here examined.

Bisaccate count	Central body count (CBC)	Sac count (SC)	Whole grain count (WGC)
Sample 536	205	459 (229.5 grains)	83
Sample 531	358	786 (393 grains)	72

Figure 6 Bisaccate counting methodology test results.

The determining factor in counting methodology seems to be the degree of degradation. In the Rees samples, central bodies break down less than sacs, and as such, the CBC method appears to give the most reliable representation. Although vegetational reconstruction is not the aim of the present study, the bisaccate – nonsaccate pollen index can be significant in marine palynological preparations because of its use as an approximate indicator of distance from shoreline, or "distality" (Versteegh, 1994; Popescu et al., 2007), as discussed below. This owes to the ability of bisaccate pollen to float (Beaudoin et al., 2007). Consistency in counting, rather than the actual method used, is therefore the key requirement.

2.2 – Univariate Statistical Analysis

2.2.1 – Estimate of concentration

Concentrations of dinoflagellate cysts were determined using the *Lycopodium clavatum* marker grain method, as per Stockmarr (1971) and Maher (1981). The following equation is used:

$$C \ = \ (D_c \times L_t \times t) \ / \ (L_c \times W)$$

Where C = dinoflagellate cyst concentration, D_c = counted dinoflagellate cysts, L_t = number of *Lycopodium* spores per tablet, t = number of tablets added, L_c = counted *Lycopodium* spores, and W = dry weight of sample.

The error is calculated according to the following equation, as per Stockmarr (1971):

$$Error = \sqrt{(e_1^2 + e_2^2 + e_3^2)}$$

Where e_1 = error in the number of *Lycopodium* spores in the added tablets, e_2 = counted dinoflagellate cyst error, and e_3 = counted *Lycopodium* spore error.

2.2.2 – Dinoflagellate cyst – pollen index

The index of dinoflagellate cysts against sporomorphs has been calculated to obtain an approximation of distance from shore. As distance from shore increases, the index increases as the dinoflagellate proportion increases and the pollen count decreases. The equation for this calculation is as follows:

$$DP = D / (D + P)$$

Where DP = dinoflagellate cyst to pollen index, D = dinoflagellate cyst count, and P = pollen grain count. This index provides an approximate indication of marine vs terrestrial influence, and may be related to distance from shore (Versteegh, 1994). Different pollen groups were used to analyse the different signals given, and were plotted on a graph. The groups of pollen included in the calculation are bisaccate pollen (DBp), nonsaccate pollen (DNp), bisaccate and nonsaccate pollen combined (DBpNp), all pollen types combined (DAp), and all sporomorph counts (DApF).

2.2.3 – Bisaccate – nonsaccate pollen index

The index of bisaccate against nonsaccate pollen (BpNp) was also calculated and plotted, in accordance with the following equation:

$$BpNp = Bp / (Bp + Np)$$

This is also thought to give an approximate distance from shore, or “distality” (McCarthy et al., 2013). Saccate pollen generally float better than nonsaccate pollen and are carried further out to sea where they then become overrepresented in the sediments, even as the total pollen count decreases. Therefore, BpNp would increase as distance from shore increases, assuming of course that other factors such as the vegetation changing over time are not involved.

2.2.4 – Species richness and diversity

Species richness is calculated and is defined as the total number of dinoflagellate species in each sample. The Shannon Index for each sample is also calculated, as per Krebs (1998), using the following equation:

$$H' = -\sum_{i=1}^{s}(p_i \ln p_i)$$

where H’ = the Shannon Index, s = number of species, and p_i = proportion of the abundance of the i^{th} species. This index acts as a measure of species diversity of each sample, based on the proportions of total abundances of each individual species. High H’ indicate high species diversity.

2.2.5 – Evenness

Evenness is then calculated as follows:

$$J' = H'/\ln S$$

Where J’ = Evenness, H’ = the Shannon Index, and S = sample richness. Sample richness (S) is defined as the number of species in a sample. This statistic is a measure of the similarity in abundances of each individual species (or taxon) within a sample as a whole (Magurran, 2004). High J' indicates that the individual species in a sample are of similar abundances.

2.2.6 – Gonyaulacoid – protoperidinioid index

The proportion of gonyaulacoid against total gonyaulacoid and protoperidinioid cysts (GP) is plotted as a measure of the trophic signal, given that protoperidiniacean dinoflagellates are heterotrophic organisms and favour environments with elevated biological productivity. This signal must be used with caution owing to the greater preservational potential of gonyaulacoid cysts (Zonneveld et al., 1997).

2.2.7 – Individual species / total gonyaulacoid cysts

In addition, key species of dinoflagellate cysts are plotted against total gonyaulacoid cysts, in order to obtain an indication of the paleoenvironment. Protoperidinioid cysts are excluded from the ratio total owing to preservational bias, and reworked cysts are not included because they contain no in-situ paleoecological information. The key species are as follows:

- *Bitectatodinium* cf. *raedwaldii*: as this is not a definitive identification, the ecological affinity is not conclusive. Nonetheless, this species likely represents an environment similar to that of *Bitectatodinium raedwaldii*, which is a warm water, neritic environment (De Schepper et al., 2011).
- *Capisocysta lyelli*: an extinct species with thermophilic neritic affinities judging from its presence in the Lower Pliocene of eastern England (Head, 1998), and its similarity with the extant tropical–warm-temperate species *Capisocysta lata* (Head, 1998).

- *Heteraulacacysta* sp. A of Costa & Downie (1979): an extinct species of goniodomoidean affinity, implying a restricted marine environment (De Schepper et al., 2009).
- *Lingulodinium machaerophorum*: an extant species known to tolerate a wide range of environments and salinities. High concentrations of this species are thought to indicate a neritic, temperate to tropical environment (De Schepper et al., 2011; Zonneveld et al., 2013).
- *Operculodinium israelianum*: this extant species is known to occur in and indicate mild temperate to tropical, neritic environments (De Schepper et al., 2011; Zonneveld et al., 2013).
- *Operculodinium tegillatum*: there are few reports of this extinct species outside the southern North Sea. Based on its abundance in the Lower Pliocene of eastern England (Head, 1997), it seems to indicate a temperate to warm neritic environment.
- Cysts of *Protoceratium reticulatum*: this extant theca-defined species, whose cysts are known in the literature as *Operculodinium centrocarpum* sensu Wall & Dale, is known to be cosmopolitan and wide ranging. Higher relative abundances of the cysts are found in cold to temperate regions (De Schepper et al., 2011).
- *Spiniferites*/*Achomosphaera* spp.: the grouping of all *Spiniferites* and *Achomosphaera* species is very wide ranging, and is thought to give an indication of a neritic environment (Quaijtaal et al., 2014).
- AIN: this grouping represents the total numbers of *Amiculosphaera umbraculum*, *Invertocysta lacrymosa* and *Nematosphaeropsis labyrinthus*. *A. umbraculum* is a typical outer neritic species (Verhoeven & Louwye, 2013), and *I. lacrymosa* and *N. labyrinthus*

are thought to be outer neritic to oceanic (Louwye et al., 2004; Louwye et al., 2008). This group is thought to indicate open ocean environments.

- Acritarch sp. 1: although not a formally defined species, this distinctive acritarch is plotted against the total marine palynomorphs to assess its paleoenvironmental significance.
- *Cymatiosphaera*? *invaginata*: the environmental significance of this acritarch is not well understood, although it can be the dominant marine palynomorph in some upper Neogene records of the North Atlantic. It is plotted against total marine palynomorphs in the present study to gain insights into its environmental significance.

2.3 – Constrained Cluster Analysis

Cluster analysis involves the agglomerating of individual objects into larger groups based on local similarities in their features, and displayed as hierarchical dendrograms (Dale & Dale, 2002). In this case, similarities in dinoflagellate cyst assemblages were the criteria for grouping. Constrained cluster analysis was chosen to show the similarities between samples while still maintaining stratigraphic order. By doing this, the samples can be divided into separate biozones based on their cyst associations. This analysis was performed with the statistical analysis program R, using the RIOJA package and the “coniss” similarity measure. The formulae and preferences used are outlined in Appendix IV.

Four dendrograms were produced: two based on the cyst counts including and excluding reworked cysts, and two based on the presence and absence of species including and excluding reworked cysts. These analyses were chosen to determine the effect of reworked species (taphonomic bias) and rare taxa (as well as taphonomic bias against protoperidinoid cysts) when analysing similarity.

2.4 – Multivariate Statistical Analysis

2.4.1 – Detrended Correspondence Analysis

Correspondence analysis is a form of statistical analysis that provides a graphical representation of cross tabulations. These arise whenever it is possible to place variables into separate categories, such as cyst assemblages and core depths. Detrended Correspondence Analysis (DCA) is a normalised form of correspondence analysis that produces plots that group samples depending on the relative proportions of their cyst assemblages. This allows for easier interpretation and understanding of the environmental factors that impact the distribution of the samples. Reworked specimens were excluded, as their concentrations do not rely on environmental factors.

Four plots were produced, one which includes all counted cysts, one that excludes reworked cysts, and one that excludes reworked cysts and *Spiniferites* spp. indet . The latter plot was made because the high proportions of *Spiniferites* spp. indet. in the samples may have grouped the samples too close together and obscured any discrete relationships between them. A final plot was produced based on the last plot, but more cleaned up and easier to read. DCA was performed using the VEGAN package in R.

2.4.2 – Canonical Correspondence Analysis

Canonical Correspondence Analysis (CCA) is a form of correspondence analysis, similar to DCA, that forces the samples to plot around a known environmental factor. The resulting plot more clearly displays the effect this environmental factor has on the samples. More than one factor can be used to visualize the effect the factors would have on each other in regards to sample distribution. Ideally, factors such as sea surface temperature, salinity or distality would be used. Since none of these data are available for the Rees borehole, plots were produced that use other proxies and factors, as follows:

- DP indices were used as a proxy for distality
- Gonyaulacoid against protoperidinioid indices were used as a proxy for the trophic signal
- Dinoflagellate concentrations
- Acritarch sp. 1 vs Total marine palynomorphs
- *Cymatiosphaera*? *invaginata* vs Total marine palynomorphs
- Richness

Six plots were produced using a combination of these factors to assess their impact on each other, as well as their effect on samples. CCA was performed using the VEGAN package in R.

3.0 – Results

Seventy-four in-situ dinoflagellate cyst taxa were recognized in the Diest, Kasterlee, Poederlee and Merksplas formations of the Rees borehole from a total of 55 productive samples analysed. All nine samples from the Mol Formation were found to be barren. In most samples, total *Spiniferites/Achomosphaera* spp. make up at least 20% of the assemblages. In addition to the dinoflagellate cysts, 12 acritarch taxa and six taxa of green algae were recorded. Because of the higher resolution of sampling for the Merksplas Formation, analysis results are plotted separately. Cyst concentrations, richness, Shannon Index values, evenness and pollen concentrations for the Diest, Kasterlee and Poederlee formations are shown in Figure 7, while those of the Merskplas Formation are shown in Figure 8. The results of individual species plotted against total gonyaulacoid cysts for the Diest, Kasterlee and Poederlee formations are shown in Figure 9, and the same analyses for the Merksplas Formation are shown in Figure 10. A list of recorded taxa of dinoflagellates, acritarchs and algae can be found in Appendix I. Descriptions of select inconclusively identified dinoflagellate cysts and acritarchs can be found in Appendix II. Raw counts of all palynomorphs, as well as calculated indices and ratios are found in Appendix V.

The DP (dinocyst against pollen) indices all show similar trends overall. DP indices of the Diest, Kasterlee and Poederlee are displayed in Figure 11, while the indices of the Merksplas are shown in Figure 12. DAp (dinocyst against all pollen types), DApF (dinocyst against all sporomorphs), and DBpNp (dinocyst against bisaccate and nonsaccate) are almost identical in values, and almost completely overlap each other on the graph. The DBp (dinocyst against bisaccate pollen) index exhibits the same trend, although at higher values, and the changes seem generally more pronounced. The same is true of the DNp (dinocyst against nonsaccate pollen) index, although with even higher values, and generally less pronounced changes than the other indices. BpNp (bisaccate against nonsaccate) indices follow the same trends as the DP indices, although there are some anomalous sections where DP values increase, and BpNp decrease.

The dinoflagellate cyst associations are described below. They are arranged by formation because constrained cluster analysis (Figures 13–16) does not show a clear segregation into biozones other than by formation, with the exception that the Kasterlee Formation is subdivided into informal assemblage biozones A and B. Constrained cluster analysis shows that the Merksplas Formation could be divided into two subdivisions, from 8.70–7.80 m and from 7.80–5.70 m, although it is difficult to understand what causes this division in similarity when examining the counts and statistical analysis graphs, and no difference is seen in sedimentology. The division may be caused by the sample at 7.80 m, which is particularly rich and has slightly different proportions from the remainder of the formation. Having a somewhat dissimilar sample in the middle of the productive interval in this formation may have forced a division in similarity, as constrained cluster analysis maintains stratigraphic order. When examining correspondence analysis results, the Merksplas samples are all seen to plot closely to each other. For this reason, the Merksplas Formation has not been subdivided into separate biozones.

3.1 – Diest Formation (40.00–33.25 m)

The flora of the Diest Formation comprises 52 dinoflagellate cyst taxa and 12 acritarch taxa based on a total of 9 samples analysed. Preservation of samples is moderate to poor, and there is evidence of strong oxidation, particularly in regions dominated by coarser sediment. Species richness ranges between 12 and 33, with an average of 22.44 taxa per sample. Shannon Index values are relatively wide ranging in comparison to the remainder of the borehole, and range between 1.07 and 2.13, with an average of 1.63. Evenness ranges between 0.448 and 0.638, with an average of 0.529, making species abundances moderately-well distributed. *Spiniferites/Achomosphaera* spp. comprise between 20 and 49% of the assemblage of each sample, with an average of 33.5%. Cyst concentrations are quite variable and fluctuate through the formation, and range between 27 and 2380 cysts/g, with an average of 734.55 cysts/g.

The Diest Formation is characterised by the highest abundances of *Gramocysta verricula, Habibtacysta tectata,* and *Trinovantedinium ferugnomatum*. Also present in relatively higher numbers are *Barssidinium pliocenicum*, *Bitectatodinium* cf. *raedwaldii*, *Brigantedinium* sp., *Heteraulacacysta* sp. A of Costa & Downie (1979), *Operculodinium israelianum* and *Operculodinium tegillatum*. The following taxa are also present: *Achomosphaera andalousiensis suttonensis, Dapsilidinium pastielsii*, cf. *Labyrinthodinium truncatum truncatum*, *Pyxidinopsis* sp., *Reticulatosphaera actinocoronata, Selenopemphix armageddonensis*, and *Trinovantedinium variabile*.

When considering the proportions of key species against total gonyaulacoid cysts, the lower half of the formation shows proportions of *Bitectatodinium* cf. *raedwaldii*, *Lingulodinium machaerophorum*, total *Achomosphaera*/*Spiniferites* spp., Acritarch sp. 1, and *Cymatiosphaera*? *invaginata* that begin slightly elevated and then decrease. Proportions of *Heteraulacacysta* sp. A of Costa & Downie (1979), *Operculodinium israelianum*, *Operculodinium tegillatum*, AIN and GP are lower. At around 35.98 m, a shift occurs that continues to the top of the formation. Proportions of *Heteraulacacysta* sp. A of Costa & Downie (1979), *Operculodinium israelianum*, *Operculodinium tegillatum*, AIN (ratio of total *A. umbraculum*, *I. lacrymosa* and *N. labyrinthus* against total marine palynomorphs) and GP (gonyaulacoid against protoperidinioid index) increase, while *Bitectatodinium* cf. *raedwaldii*, total *Achomosphaera*/*Spiniferites* spp., and

Acritarch sp. 1 decrease. *Lingulodinium machaerophorum* and *Cymatiosphaera*? *invaginata* proportions remain low.

Sporomorph concentrations in this formation are generally high, between 1601 and 178745 pollen grains/g, with an average of 56580.50 grains/g. Pollen counts are variable and fluctuate through the formation, displaying a similar trend to cyst concentration. Spore counts, both fungal and embryophyte, are quite low. DP indices show some variation. DAp ranges between 0.176 and 0.571, DApF from 0.172 to 0.557, and DBpNp from 0.177 to 0.571. The values of these indices are very close to each other, and display the same trends. The indices decrease up through the formation to 38.35 m, before increasing to 37.85 m, decreasing to 36.90 m, then overall increasing near the top of the formation to 34.35 m. Before the boundary with the Kasterlee Formation, values decrease once again. DBp values range from 0.289 to 0.865. This index displays the same trend as those previously mentioned, although with higher values and greater inflections. The DNp index ranges from 0.314 to 0.772, and displays a similar trend as the other indices but with minor differences. Between 36.90 m and 36.30 m and between 35.50 m and 34.35 m, DNp decreases whereas the other indices increase. Between 36.30 m and 35.98 m, DNp increases whereas the others decrease. The BpNp index ranges between 0.189 and 0.632 and exhibits a trend different from the other indices. BpNp increases to 36.90 m, decreases to 36.30 m, increases to 35.50 m, decreases to 34.35 m, and then increase towards the top of the formation.

One anomalous sample at the base of the borehole (39.50m depth) contains few dinoflagellate cysts, with a concentration of 27.26 cysts/g, but high numbers of the acritarch *Paralecaniella indentata*, with a concentration of 144.19 specimens/g. In this sample, species richness is low at 12. The Shannon Index value is 1.08, and evenness is 0.448. Total *Spiniferites/Achomosphaera* spp. indet. comprise 49% of all dinoflagellate cysts, though only 45 cysts were counted in the entire slide. Terrestrial palynomorphs are similarly low, with a pollen concentration of 1601.58. The DAp index is at 0.542, DBp at 0.865, DNp at 0.600, DBpNp at 0.549, DApF at 0.517 and BpNp at 0.189.

3.2 – Kasterlee Formation (33.25–25.30 m)

Based on the dinoflagellate cyst assemblages found in the samples of the Kasterlee Formation, two distinct assemblage biozones are recognized: Kasterlee Formation biozones A and B. The preservation of dinoflagellate cysts is good throughout the Kasterlee Formation.

3.2.1 – Kasterlee Formation Assemblage Biozone A (33.25–27.30 m)

Assemblage biozone A contains a total of 54 dinoflagellate cyst taxa, along with 12 acritarch species and 6 species of green algae, based on a total of 7 samples analysed. Palynomorphs show better preservation in this formation than in the Diest Formation. Species richness ranges between 25 and 34, with an average of 29.2 taxa per sample. Shannon Index values in this formation are more constrained than in the Diest Formation, and range between 1.56 and 1.95, with an average of 1.74. The values are slightly higher in general, making the individual samples slightly more diverse overall. Evenness ranges between 0.455 and 0.586, with an average of 0.530, making the species abundances moderately-well distributed, and slightly greater than the Diest Formation. Total *Spiniferites/Achomosphaera* spp. comprise 34 to 55% of each assemblage, with an average of 44.52%. The concentrations of cysts are between 548 and 4320 cysts/g, with an average of 2016.

Assemblage biozone A is characterized by the lowest occurrences of *Barssidinium graminosum*, *Batiacasphaera* cf. *minuta*, *Batiacasphaera sphaerica*, *Hystrichosphaeropsis obscura*?, and

Protoceratum reticulatum, and the highest occurrences of *Batiacasphaera sphaerica*, *Filisphaera filifera*, *Hystrichosphaeropsis obscura*?, *Hystrichosphaeropsis obscura*, cf. *Labyrinthodinium truncatum truncatum*, *Lingulodinium* sp., and *Tectatodinium* sp. The following occur in significant numbers throughout: *Barssidinium pliocenicum*, *Bitectatodinium* cf. *raedwaldii*, *Brigantedinium* sp., *Operculodinium israelianum*, *Operculodinium tegillatum*, *Operculodinium*? *eirikianum*, and *Reticulatosphaera actinocoronata*. Also present are *Achomosphaera andalousiensis andalousiensis*, *Achomosphaera andalousiensis suttonensis*, *Ataxiodinium choane*, *Heteraulacacysta* sp. A of Costa & Downie (1979), *Reticulatosphaera actinocoronata*, and *Selenopemphix armageddonensis*. The acritarch *Cymatiosphaera*? *invaginata* also appears in high quantities throughout the formation.

Individual cyst proportions against total gonyaulacoids show high *Operculodinium tegillatum*, total *Achomosphaera*/*Spiniferites* spp., Acritarch sp. 1, *Cymatiosphaera*? *invaginata* and G/P. AIN values fluctuate, but are high overall. *Heteraulacacysta* sp. A of Costa & Downie (1979) and *Lingulodinium machaerophorum* are low, and *Operculodinium israelianum* proportions decrease from the Diest Formation and are relatively low.

Sporomorph concentrations are much higher than for the Diest Formation, and range between 90567 and 226333 grains/g, with an average of 147771 grains/g. Embryophyte and fungal spores remain quite low. DAp values range between 0.142 to 0.465, DApF from 0.142 to 0.459, DBpNp from 0.143 to 0.465, DNp from 0.240 to 0.682, and DBp from 0.261 to 0.664. The different indices show some variability, but the overall trend is the same. Values decrease from the Diest boundary until 32.30 m, before increasing until 31.30 m. Values then decrease again until 29.33 m, then increase to 28.35 m, before decreasing to the top of the biozone. The BpNp values are between 0.421 and 0.608. This index exhibits a similar trend to the others until around 30.30 m.

The index then increases until 29.33 m, decreases until 28.35 m, then increases to the top of the biozone.

3.2.2 – Kasterlee Formation Assemblage Biozone B (26.79–25.30 m)

A total of 46 dinoflagellate cyst, 12 acritarch taxa and 4 green algae species are present in this biozone, based on a total of 4 samples analysed, representing the upper part of the Kasterlee Formation in the Rees borehole. Species richness is between 25 and 34, with an average of 29.5. The Shannon Index values are more constrained, ranging between 1.80 and 1.88, with an average of 1.86. Evenness values are between 0.530 and 0.594, with an average of 0.561. These values are slightly higher than those of the Lower Kasterlee, giving slightly higher diversity and distribution of species abundance. Total *Achomosphaera*/*Spiniferites* spp. comprise between 36 and 47% of the samples, with an average of 41.28%. Cyst concentrations range between 1602 and 1718 cysts/g, with an average of 1677 cysts/g.

Biozone B is characterized by the lowest occurrence of *Protoceratium reticulatum*, and the highest occurrences of *Apteodinium* sp., *Pyxidinopsis* sp. and *Reticulatosphaera actinocoronata.* It is also characterized by moderately high numbers of *Ataxiodinium choane, Barssidinium pliocenicum, Bitectatodinium* cf. *raedwaldii, Lingulodinium machaerophorum, Operculodinium israelianum* and *Protoceratum reticulatum. Operculodinium*? *tegillatum* is also present, although it decreases upwards through the zone. Conversely, *Heteraulacacysta* sp. A of Costa & Downie (1979) is also present, and increases upwards. Also present are *Achomosphaera andalousiensis suttonensis* and *Selenopemphix armageddonensis.* As in Biozone A, *Cymatiosphaera*? *invaginata* is present in large numbers.

Proportions of cysts against total gonyaulacoids show that *Heteraulacacysta* sp. A of Costa & Downie (1979), *Lingulodinium machaerophorum*, *Operculodinium israelianum*, and *Protoceratium reticulatum* increase in proportion upward through the formation. *Cymatiosphaera*? *invaginata* proportions decrease then increase, but remain high in this section. The GP index remains consistently high from Kasterlee biozone A. *Bitectatodinium* cf. *raedwaldii* and total *Achomosphaera*/*Spiniferites* spp. start relatively high at the base of the section, and decrease to the top of the Formation. *Operculodinium tegillatum*, AIN and Acritarch sp. 1 proportions are low.

Sporomorph concentrations in Biozone B are relatively consistent between 92340 and 164265 grains/g, averaging at 124567 grains/g. DAp values range from 0.279 and 0.410, DApF from 0.274 and 0.400, DBpNp from 0.281 and 0.410, DNp from 0.393 and 0.608, DBp from 0.496 to 0.561 and BpNp values from 0.395 to 0.608. These indices exhibit the same trends, decreasing upwards through the biozone to 26.56 m, increasing to 26.39 m, before decreasing to the boundary with the Poederlee Formation.

3.3 – Poederlee Formation (25.30–17.00 m)

A total of 47 dinoflagellate cyst taxa were found in the Poederlee Formation, along with 13 acritarch species and 6 green algae species, based on a total of 9 samples analysed. Palynomorphs are mostly well preserved in this formation. Dinoflagellate cyst richness is between 15 and 26 taxa per sample, with an average of 21.33 taxa. Shannon Index values are variable in comparison with the remainder of the borehole, ranging between 1.13 and 1.92, with an average of 1.48, making the Poederlee samples overall less diverse than the Diest and Kasterlee samples. Evenness is similarly variable, ranging between 0.404 and 0.603, with an average of 0.482, indicating a moderate distribution of species abundances overall. Total

Achomosphaera/*Spiniferites* spp. comprise about 35 to 65% of the assemblages, with an average of 53.33%. Cyst concentrations are 181 to 2180 cysts/g, with an average of 897. Concentrations distinctly decrease towards the top of the formation.

The Poederlee association is characterised by the lowest occurrence of *Spiniferites* sp. 1, and the highest occurrences of *Melitasphaeridium choanophorum*, *Selenopemphix brevispinosa*, *Selenopemphix dionaeacysta*, *Trinovantedinium glorianum*, *Trinovantedinium variabile* and *Trinovantedinium* sp. *Lingulodinium machaerophorum* is present in high numbers at the base of the formation, and decreases towards the top. On the other hand, *Heteraulocacysta* sp. A of Costa & Downie (1979) and *Cyclopsiella* sp. are found in increasing numbers higher in the formation. The association is also characterised by *Achomosphaera andalousiensis suttonensis*, *Invertocysta lacrymosa* and *Protoceratium reticulatum*.

Proportions of cysts against total gonyaulacoids show that *Protoceratium reticulatum* and total *Achomosphaera*/*Spiniferites* spp. are high in this formation. *Heteraulacacysta* sp. A of Costa & Downie (1979) and AIN increase upward through the formation. *Lingulodinium machaerophorum* proportions start quite high and decrease upsection. *Operculodinium tegillatum* is absent for almost the entire formation. Acritarch sp. 1, *Operculodinium israelianum* and *Cymatiosphaera*? *invaginata* are also low throughout the formation. *Bitectatodinium* cf. *raedwaldii* decreases from the base of the formation, then starts to increase around 22.58 m, but remains relatively low throughout the formation.

Sporomorph counts in the Poederlee Formation are generally very high. Concentrations range from 48882 to 201870 grains/g, with an average of 110168 grains/g. DAp values are between 0.174 and 0.390, DApF between 0.169 and 0.384, DBpNp between 0.175 and 0.392, DNp between 0.361 and 0.540, and DBp between 0.237 and 0.591. Although the values vary, the indices display the same trends. They decrease up the formation up to 23.80 m, increase to 22.58 m, generally decrease to 20.42 m, and then increase to the top of the formation. BpNp indices range between 0.446 and 0.696. Values increase from the base of the formation to 22.58 m, then decrease to 20.70 m, increase to 20.21 m, before decreasing towards the top of the formation.

3.4 – Mol Formation (17.00–9.00 m)

A total of nine samples of the Mol Formation were analysed, and all were found to be barren of dinoflagellate cysts and terrestrial palynomorphs.

3.5 – Merksplas Formation (9.00–3.00 m)

A total of 43 dinoflagellate cyst taxa were found in the Merksplas Formation, along with eight acritarch species and eight green algae species, based on a total of 29 samples analysed. The productive interval was found to be about 3.10 metres, between 5.60 and 8.70 m. All other samples were found to be barren. Preservation of palynomorphs is high in the productive part of this formation. Dinoflagellate cyst richness ranges between 15 and 25 taxa per sample, with an average of 19.16 taxa. Shannon Index values are variable in comparison to the other formations, ranging between 1.39 and 2.14, with an average of 1.87. Evenness is somewhat variable as well, ranging between 0.470 and 0.722, with an average of 0.661, indicating a lower distribution of species abundances overall. Total *Spiniferites/Achomosphaera* spp. comprise about 29 to 71% of the assemblages, with an average of 43.48%. Cyst concentrations are quite variable, between 20 and 1106 cysts/g, with an average of 326.76. Concentrations are higher in the bottom half of the formation than in the top.

The Merksplas association is characterised by the lowest occurrences of *Achomosphaera* sp. 1, *Capisocysta lyellii*, *Desotodinium wrennii*, *Geonettia waltonensis*, and *Pyxidinopsis* cf. *braboi*.

Occurring in high numbers are *Bitectatodinium* cf. *raedwaldii*, *Heteraulacacysta* sp. A of Costa & Downie (1979), *Operculodinium israelianum*, and *Protoceratium reticulatum*. It is also characterised by *Amiculosphaera umbraculum*, *Operculodinium centrocarpum*, *Spiniferites* sp. 1 and *Tuberculodinium vancampoae*.

Individual cyst proportions against total gonyaulacoids show that *Bitectatodinium* cf. *raedwaldii* proportions are generally high and relatively consistent, except at 8.00 m, rising to almost 32%. *Capisocysta lyellii* proportions are low and similarly consistent, except at 7.50 m, where abundance spikes to about 17%. *Heteraulacacysta* sp. A of Costa & Downie (1979) proportions are variable, but generally high until 7.20 m, where proportions decrease. When looking at *Lingulodinium machaerophorum*, proportions are quite low and usually less than 1%. *Operculodinium israelianum* proportions are low at the base, but start to increase upsection at around 6.80 m. *Protoceratium reticulatum* comprises 5–10% in the lower part of the formation, and at 6.80 m, proportions increase upsection until 6.50 m, and then decreases to the top of the formation. Total *Achomosphaera*/*Spiniferites* spp. proportions are generally consistent through the formation, although are high at the very bottom and the very top of the section. AIN values are very variable, but generally increase upsection until 7.20 m. At this point, proportions decrease until 6.30 m, before increasing, and then decreasing again after 5.80 m. GP proportions vary slightly, but are high overall throughout the section.

Sporomorph counts in the Merksplas Formation are variable, but somewhat low. Concentrations range from 60 to 657 grains/g, with an average of 333 grains/g. DP indices are also variable. DAp values range between 0.245 and 0.658, DApF between 0.238 and 0.653, DBpNp between 0.245 and 0.659, and DNp between 0.270 and 0.796. These indices exhibit the same trend, in that they increase from the base of the section to 8.60 m, then show an overall decrease to 8.00 m.

Values increase to 7.80 m before decreasing again to 7.70 m, then increasing until 7.40 m. The indices then decrease until 6.80 m, increase to 6.50 m, and then overall decrease to the top of the section. BpNp indices are much more variable, and range between 0.070 and 0.630. The trend exhibited by this index is similar to the others, with minor variations. DBp indices range between 0.619 and 0.929, and exhibits a less variable trend. Additionally, where this index increases to 8.50 m, then decrease until 7.70 m. Values overall increase until 7.40 m, then decrease to 6.70 m, before overall increasing to the top of the section.

3.6 – Constrained Cluster Analysis

3.6.1 – Presence/Absence Analysis

Samples from the Mol Formation, being barren, were excluded from the cluster analysis so as not to divide the dendrograms and obscure relationships between formations in the core.

When analysing the dendrograms that exclude (Figure 13) and include (Figure 14) reworked dinoflagellate cysts, little difference is evident. The similarities displayed by all samples between the two dendrograms are the same, with the exception being the four topmost samples in the Kasterlee Formation. The differences between these three are minor, however.

In both cases, samples within the same formation generally show a high degree of statistical similarity. The Diest samples all seem to be the most similar to each other. The same can be said about all but the topmost Kasterlee samples. The topmost Kasterlee is instead shown to be most similar to the lower half of the Poederlee Formation when excluding reworked cysts. Overall, the Diest and Kasterlee formations are found to be significantly statistically similar, with the exception of the topmost Kasterlee samples. As previously explained, the Merksplas Formation shows a possible division in similarity at 7.80 m, but this division seems not to be indicative of significant difference overall between the samples.

3.6.2 – Count-based Analysis

Little noticeable distinction can be found between the dendrograms that exclude (Figure 14) and include (Figure 15) reworked dinoflagellate cysts. The similarities displayed by the samples are remarkably different from the presence/absence dendrograms.

The Diest Formation samples are shown to be statistically similar to the lower four Kasterlee samples. The remainder of the Kasterlee samples are shown to be more similar to the lower three samples of the Poederlee Formation. The samples of the upper half of the Poederlee Formation show more similarity with the lower part of the Merksplas Formation. The Merksplas Formation displays higher degrees of intra-formational similarity between 8.50–7.30 m and 7.20–5.70 m.

3.7 – Correspondence Analysis

3.7.1 – Detrended Correspondence Analysis

When examining the different DCA plots, they all show that samples plot very closely together. Plots excluding (Figure 17) and including (Figure 18) reworked cysts are very similar, and the same relationships exist between samples in both plots. However, excluding reworked cysts seems to highlight these relationships by increasing the grouping. Removing *Spiniferites* spp. indet. (Figure 19) further highlights these relationships in the same way. Figure 20 shows the same plot, with species points removed and labels moved to clean up the plot. The results of this plot seem to show the same information as the cluster analysis, in that the Diest Formation and lower Kasterlee Formation plot together in the lower right quadrant, and the upper Kasterlee Formation and Poederlee Formation plot together towards the middle of the graph. Merksplas

Formation samples all plot very close to each other towards the middle left of the graph. A notable difference is that Diest sample 36.90 plots alone, in the top right corner.

3.7.2 – Canonical Correspondence Analysis

Although various proxies of environmental parameters were used and paired together for CCA, the resulting plots show little to no correlation (Figures 21, 22 & 23).

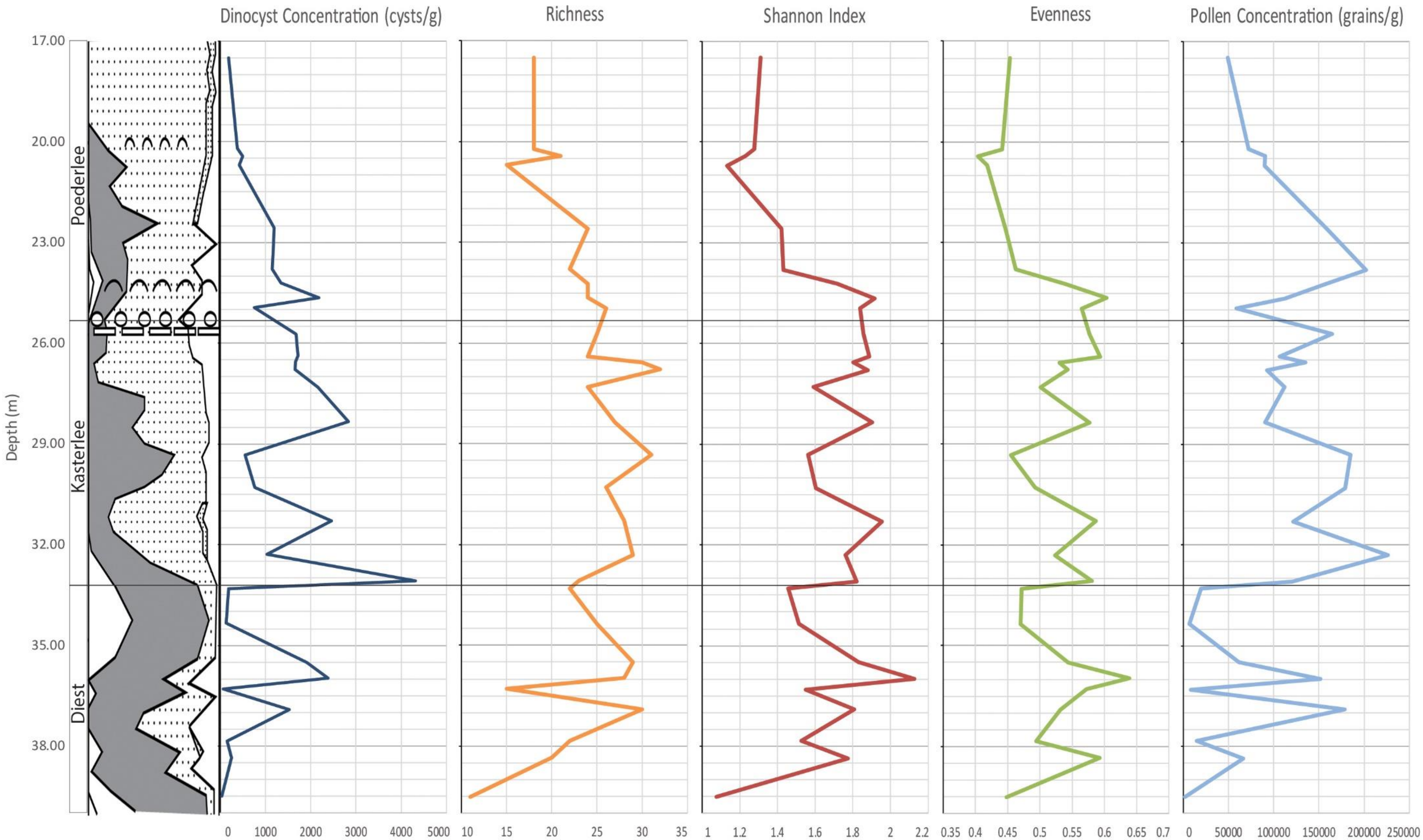

Figure 7 Various statistical analyses for dinoflagellate cysts (concentration, richness, Shannon, evenness) and pollen (concentration) plotted against depth for the Diest, Kasterlee and Poederlee formations.

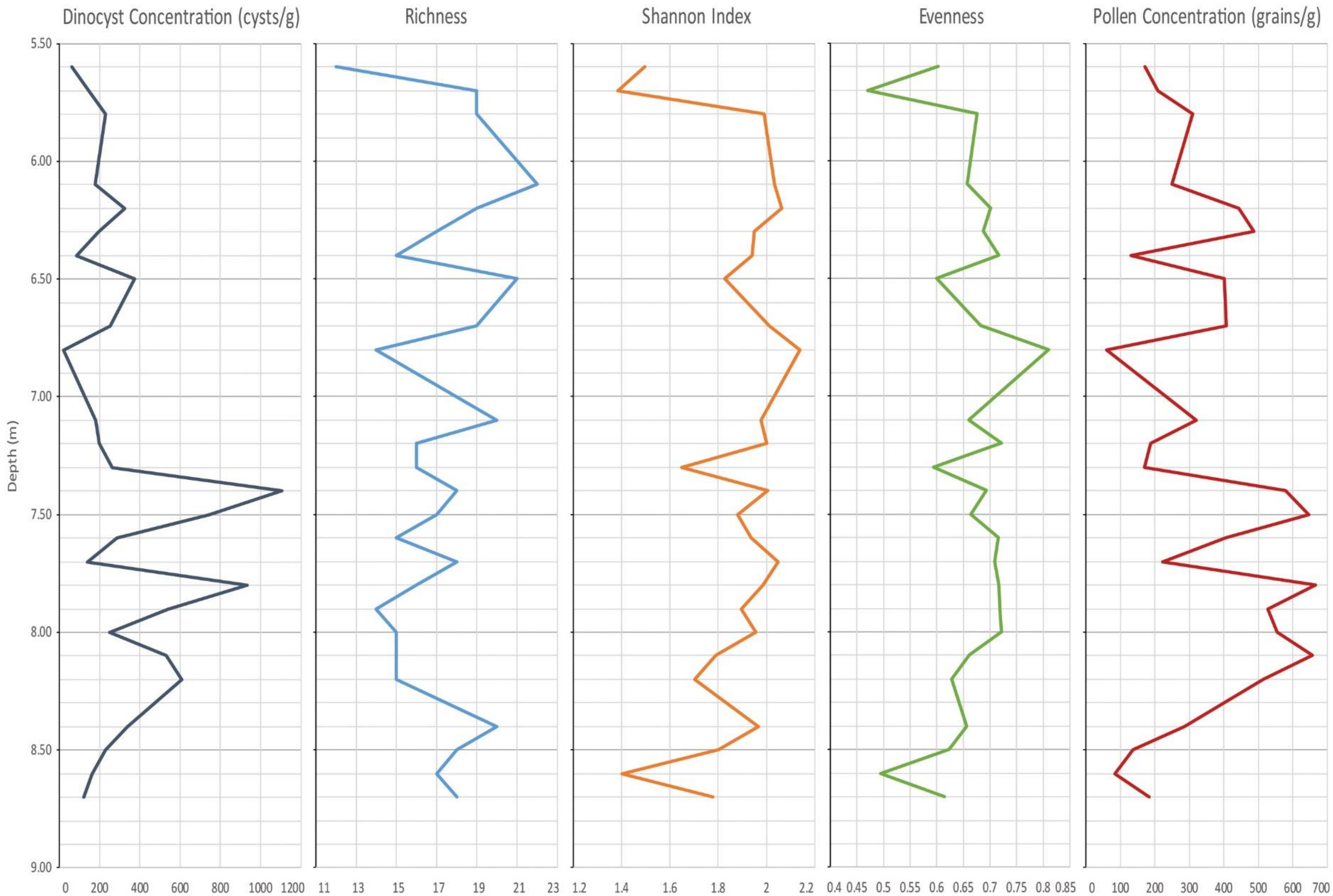

Figure 8 Various statistical analyses for dinoflagellate cysts (concentration, richness, Shannon, evenness) and pollen (concentration) plotted against depth for the Merksplas Formation.

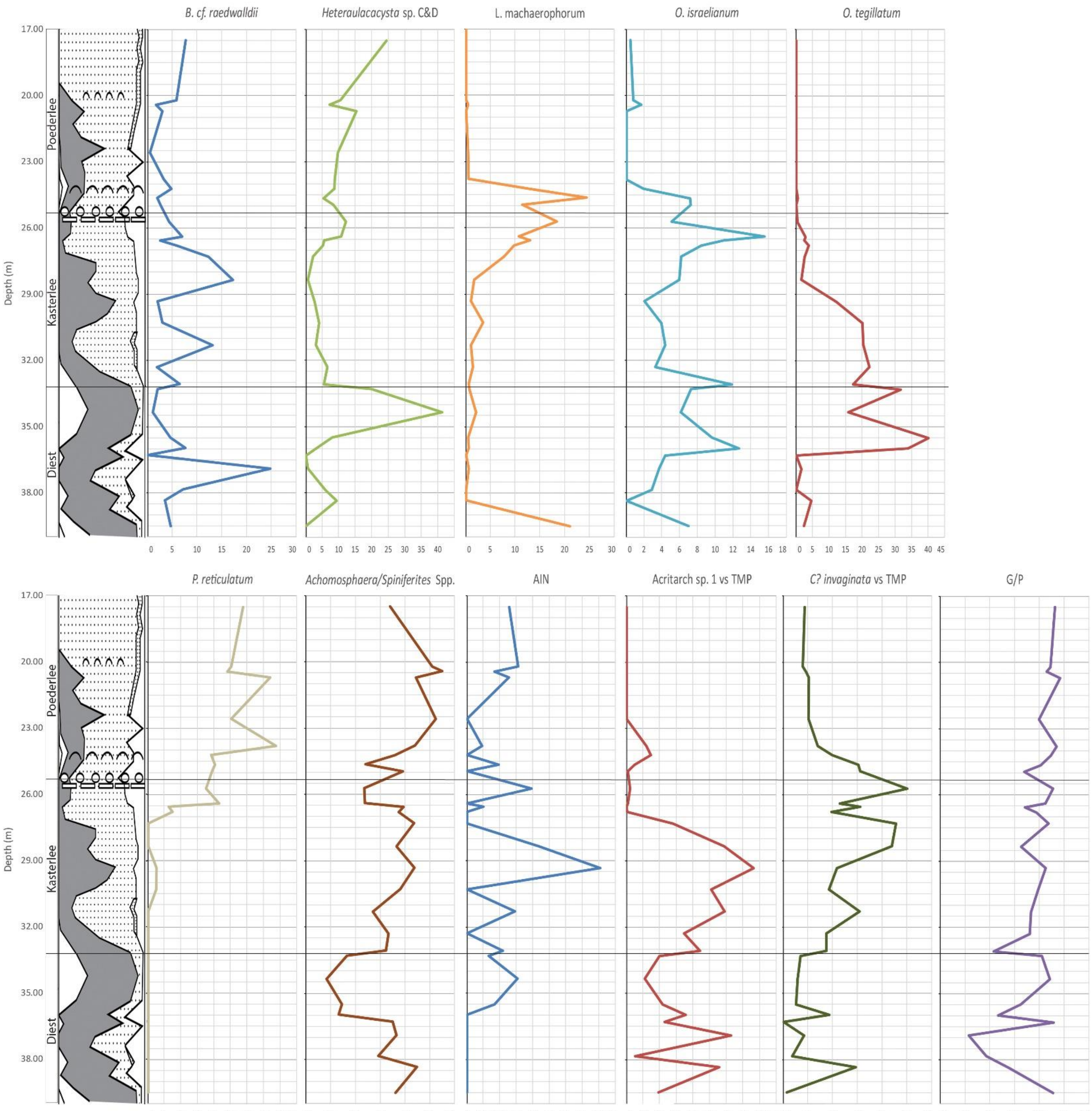

Figure 9 Individual species and the sum of A. umbraculum, I. lacrymosa *and* N. labrynthus *(AIN), plotted against total gonyaulacoid cysts, plotted against depth from the Diest, Kasterlee and Poederlee formations. Acritarch sp. 1 and* Cymatiosphaera? invaginata *are plotted against total marine palynomorphs (TMP).*

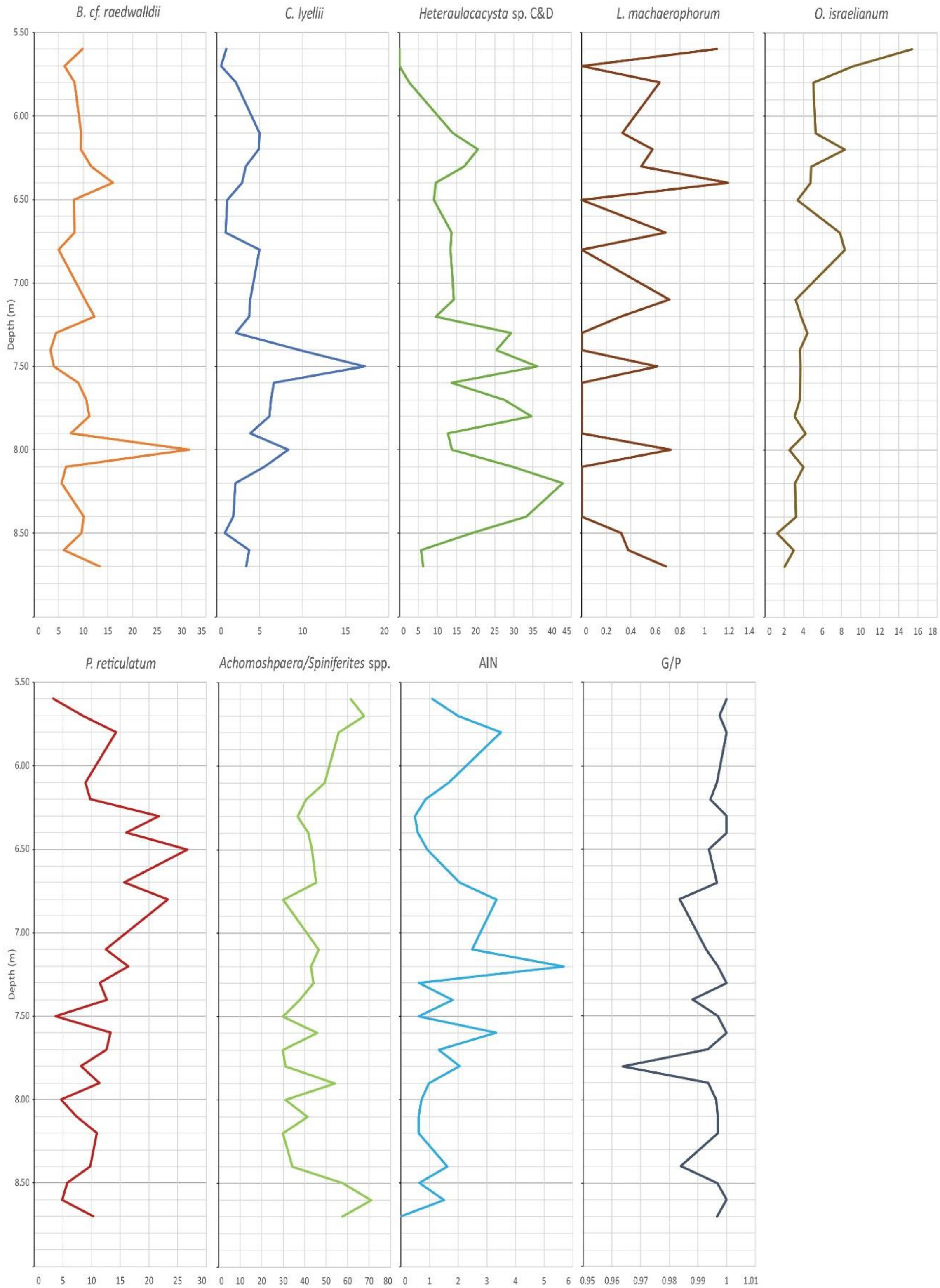

Figure 10 Individual species and the sum of A. umbraculum*,* I. lacrymosa *and* N. labrynthus *(AIN), plotted against total gonyaulacoid cysts, plotted against depth from the Merksplas Formation. Acritarch sp. 1 and* Cymatiosphaera*?* invaginata *are plotted against total marine palynomorphs (TMP).*

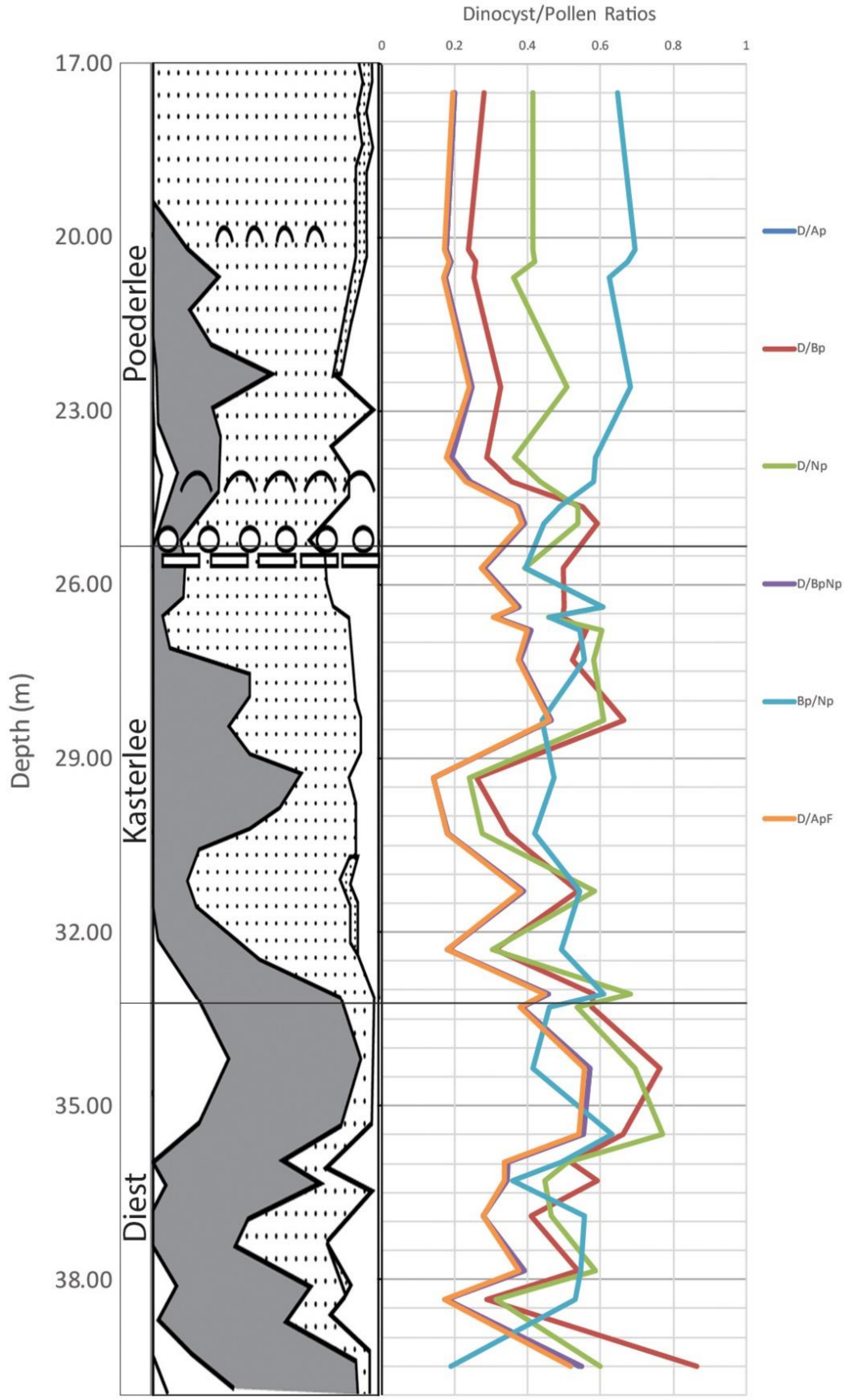

Figure 11 Graph showing the various dinoflagellate cyst against sporomorph indices, plotted against depth for the Diest, Kasterlee and Poederlee formations. DAp = dinocysts against all pollen types, DBp = dinocysts against bisaccate pollen, DNp = dinocysts against nonsaccate pollen, DBpNp = dinocysts against bisaccate and nonsaccate pollen, BpNp = bisaccate pollen against nonsaccate pollen, DApF = dinocysts against all sporomorphs.

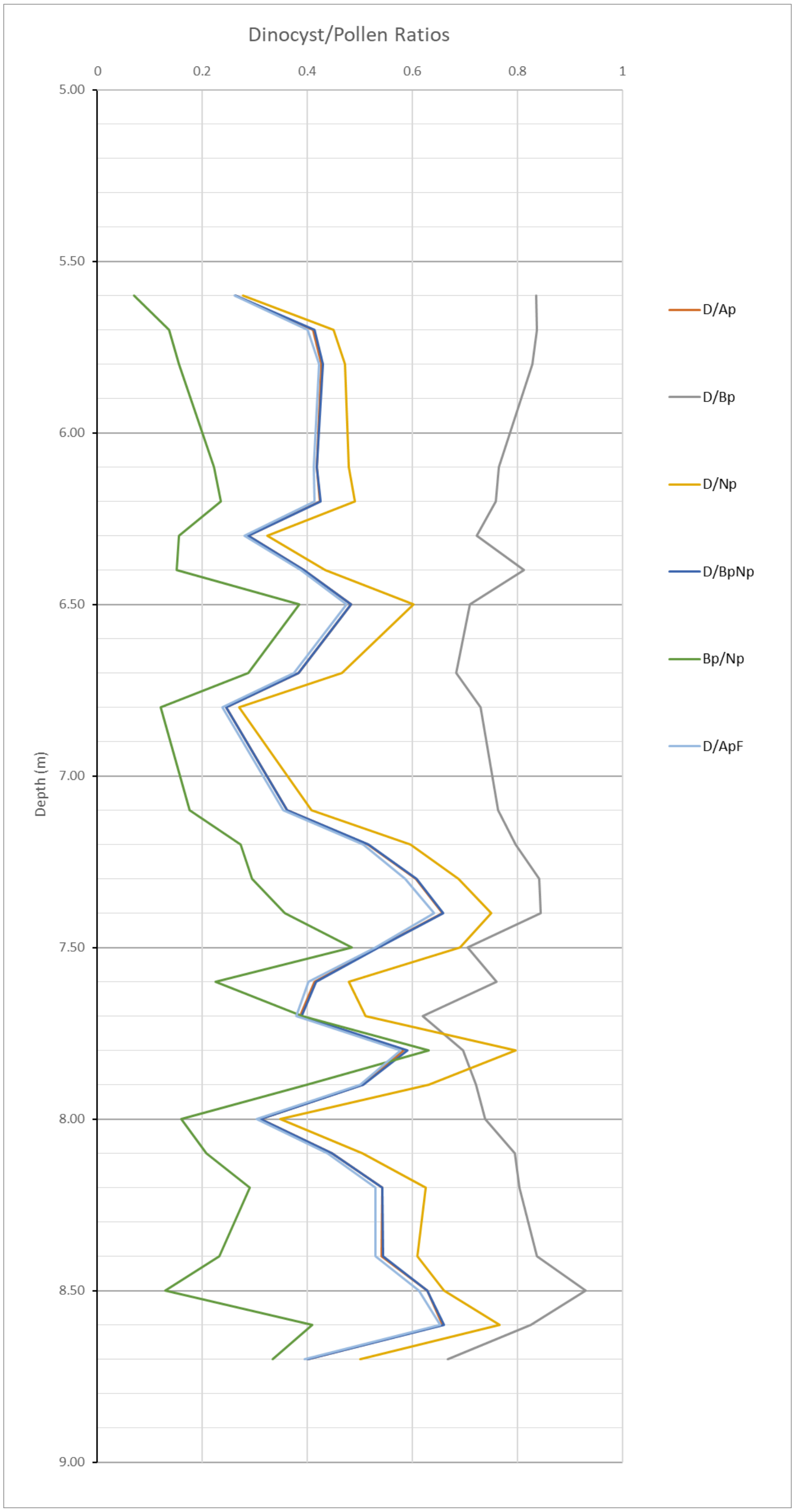

Figure 12 Graph showing the various dinoflagellate cyst against sporomorph indices, plotted against depth for the Merksplas Formation. DAp = dinocysts against all pollen types, DBp = dinocysts against bisaccate pollen, DNp = dinocysts against nonsaccate pollen, DBpNp = dinocysts against bisaccate and nonsaccate pollen, BpNp = bisaccate pollen against nonsaccate pollen, DApF = dinocysts against all sporomorphs.

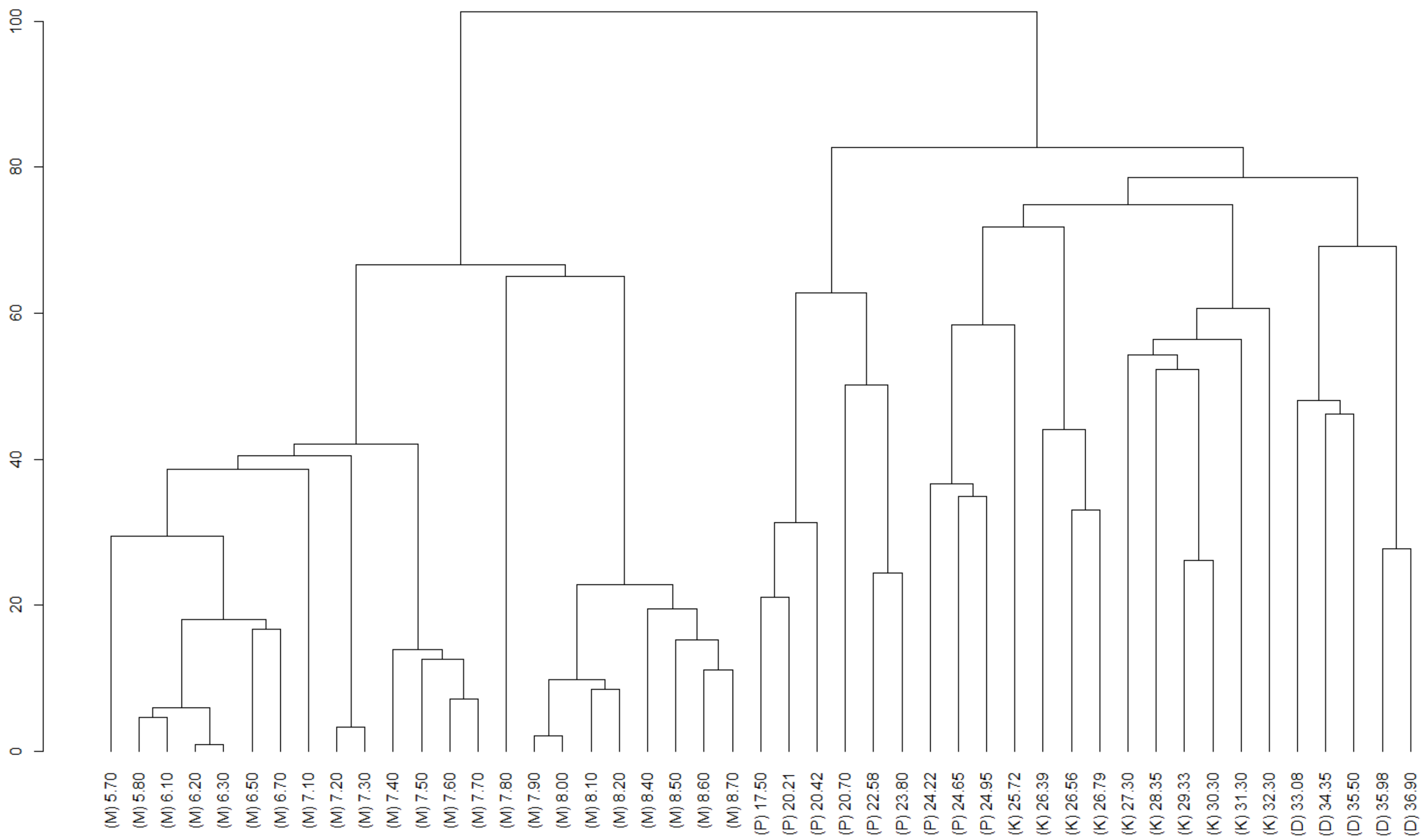

Figure 13 Constrained Cluster Analysis – Presence/absence of species, excluding reworked species. A letter preceding the sample depth indicates the formation from which the sample came: D = Diest, K = Kasterlee, P = Poederlee, M = Merkplas.

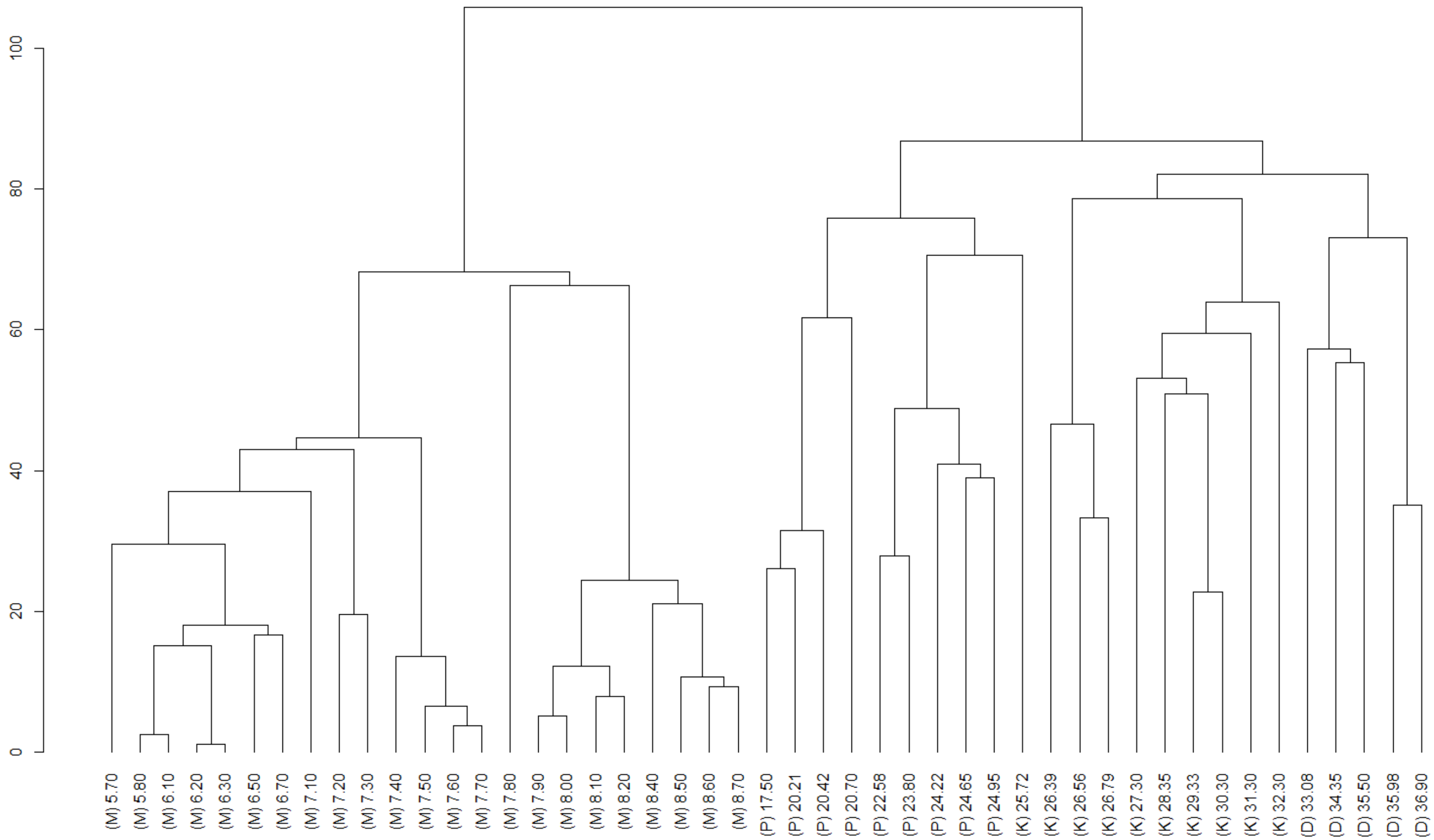

Figure 14 Constrained Cluster Analysis – Presence/absence of species, including reworked species. A letter preceding the sample depth indicates the formation from which the sample came: D = Diest, K = Kasterlee, P = Poederlee, M = Merkplas.

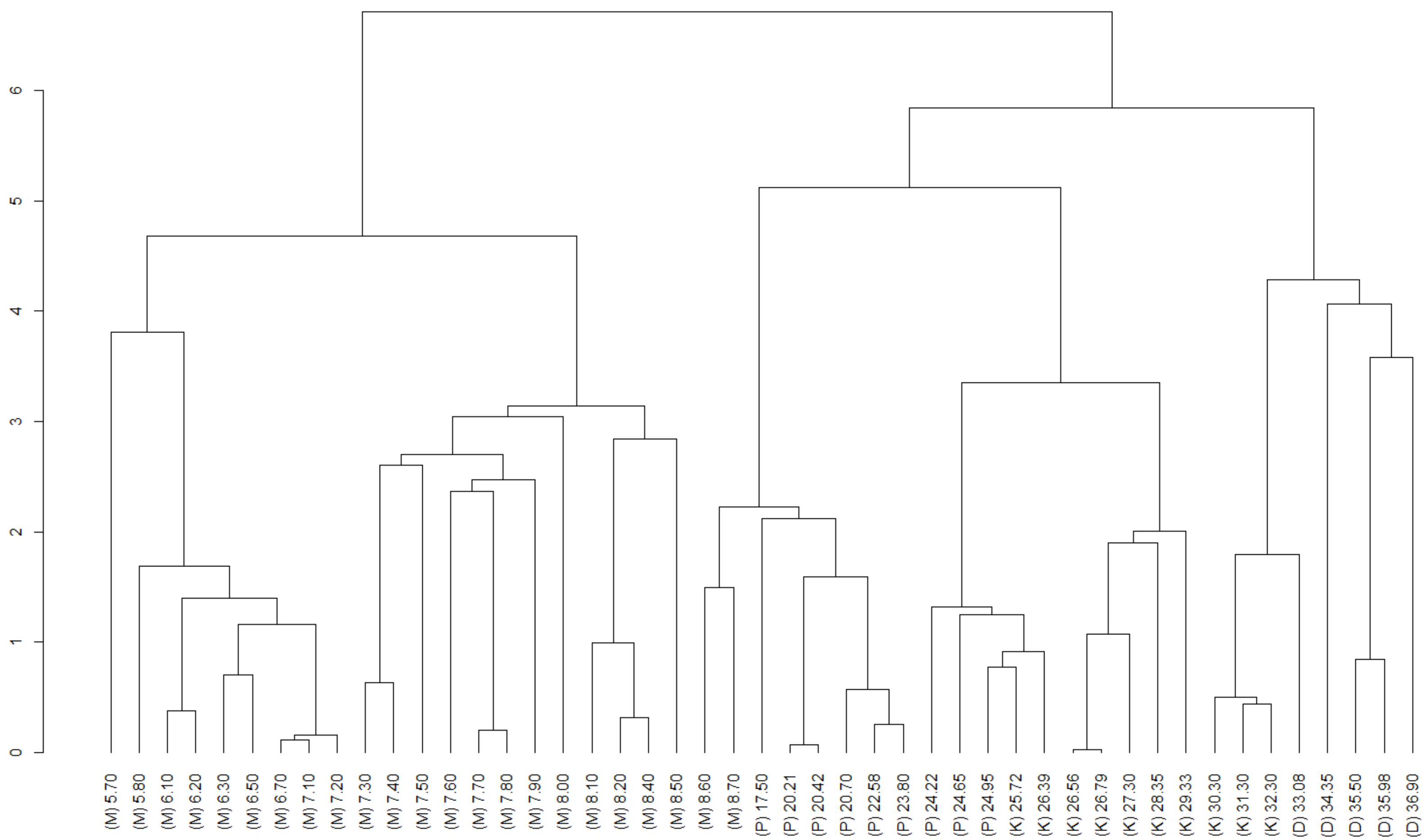

Figure 15 Constrained Cluster Analysis – Count-based analysis, excluding reworked species. A letter preceding the sample depth indicates the formation from which the sample came: D = Diest, K = Kasterlee, P = Poederlee, M = Merkplas.

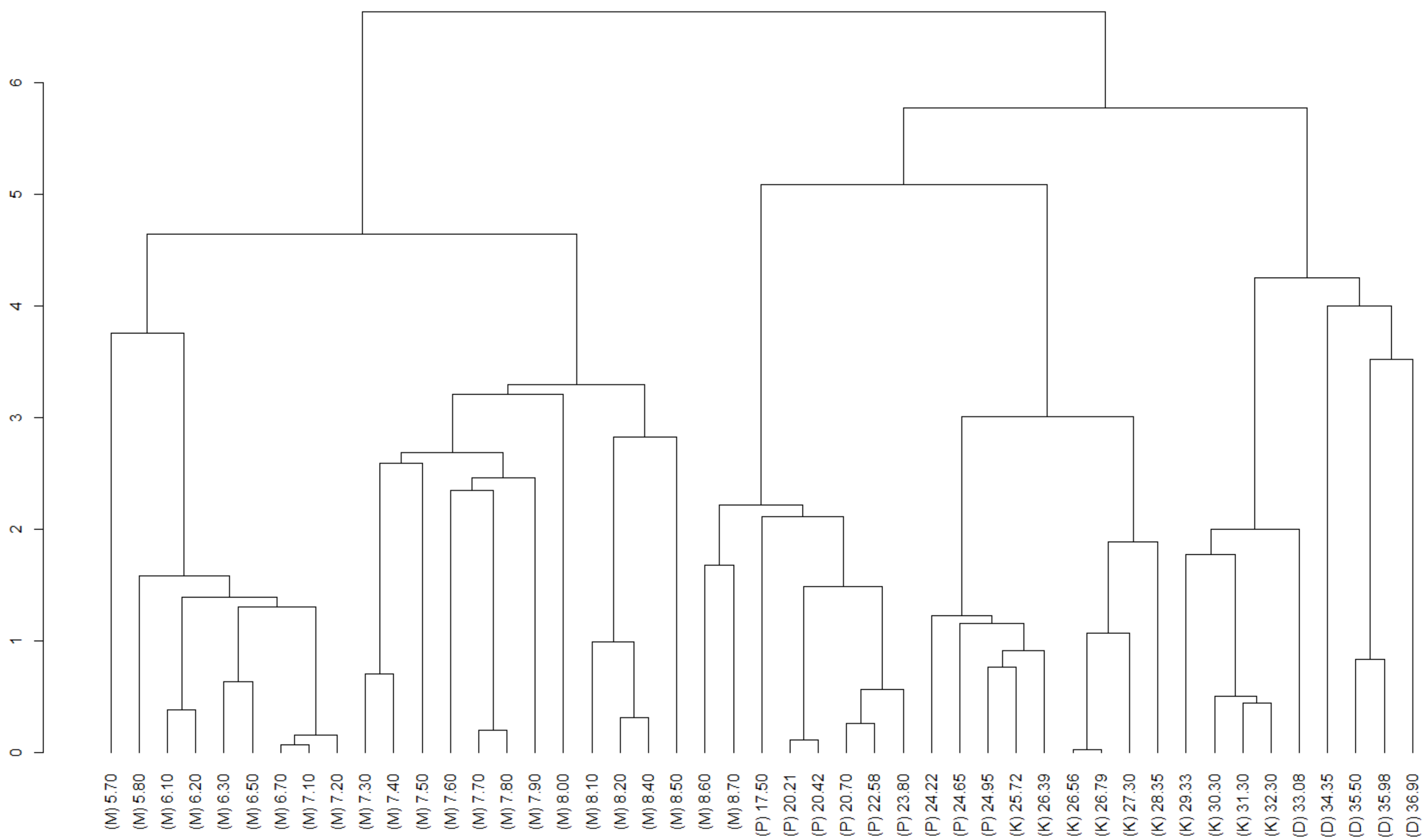

Figure 16 Constrained Cluster Analysis – Count based analysis, including reworked species. A letter preceding the sample depth indicates the formation from which the sample came: D = Diest, K = Kasterlee, P = Poederlee, M = Merkplas.

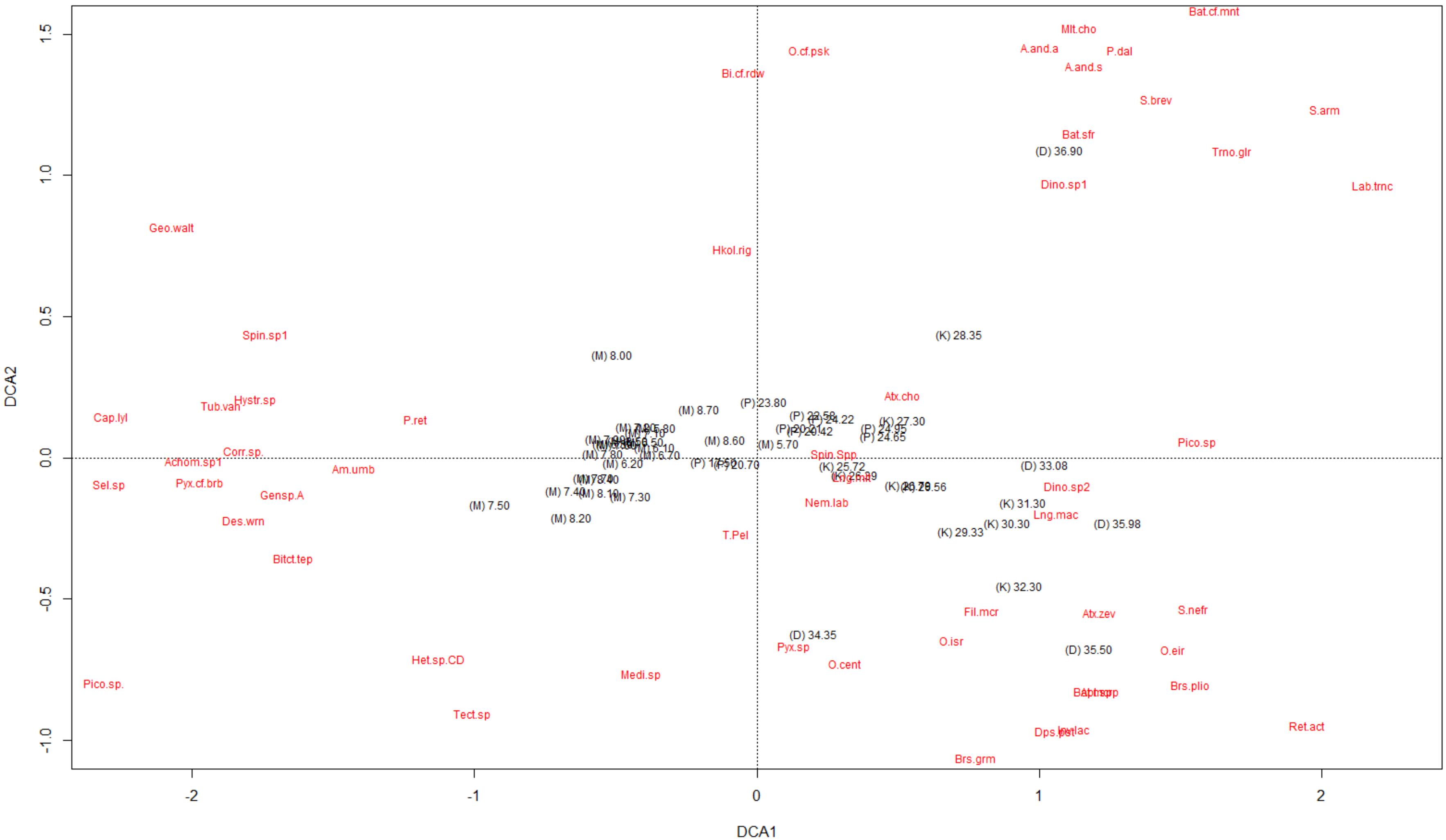

Figure 17 Detrended Correspondence Analysis – Reworked species excluded. A letter preceding the sample depth indicates the formation from which the sample came: D = Diest, K = Kasterlee, P = Poederlee, M = Merkslplas.

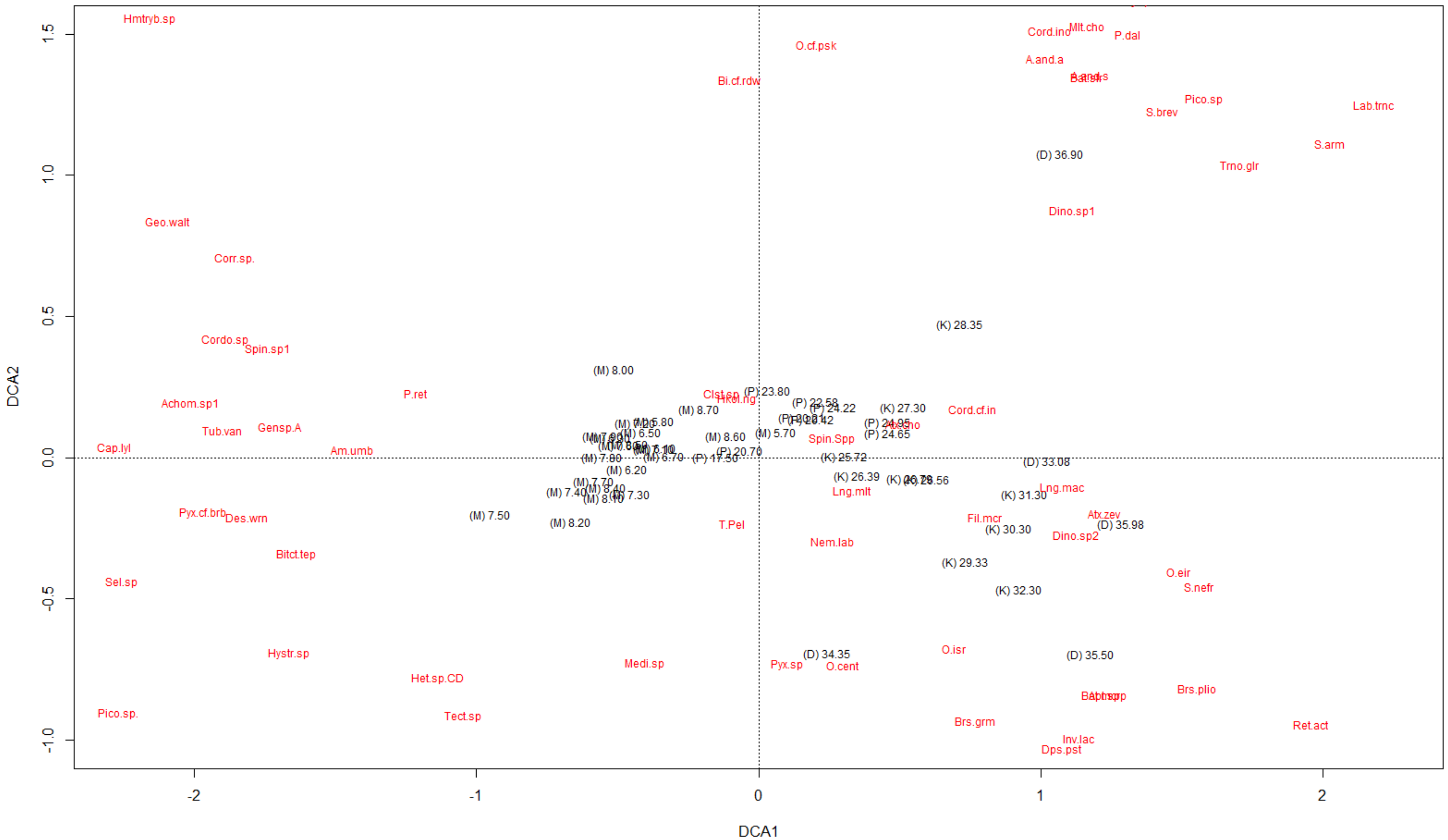

Figure 18 Detrended Correspondence Analysis – Reworked species included. A letter preceding the sample depth indicates the formation from which the sample came: D = Diest, K = Kasterlee, P = Poederlee, M = Merksplas.

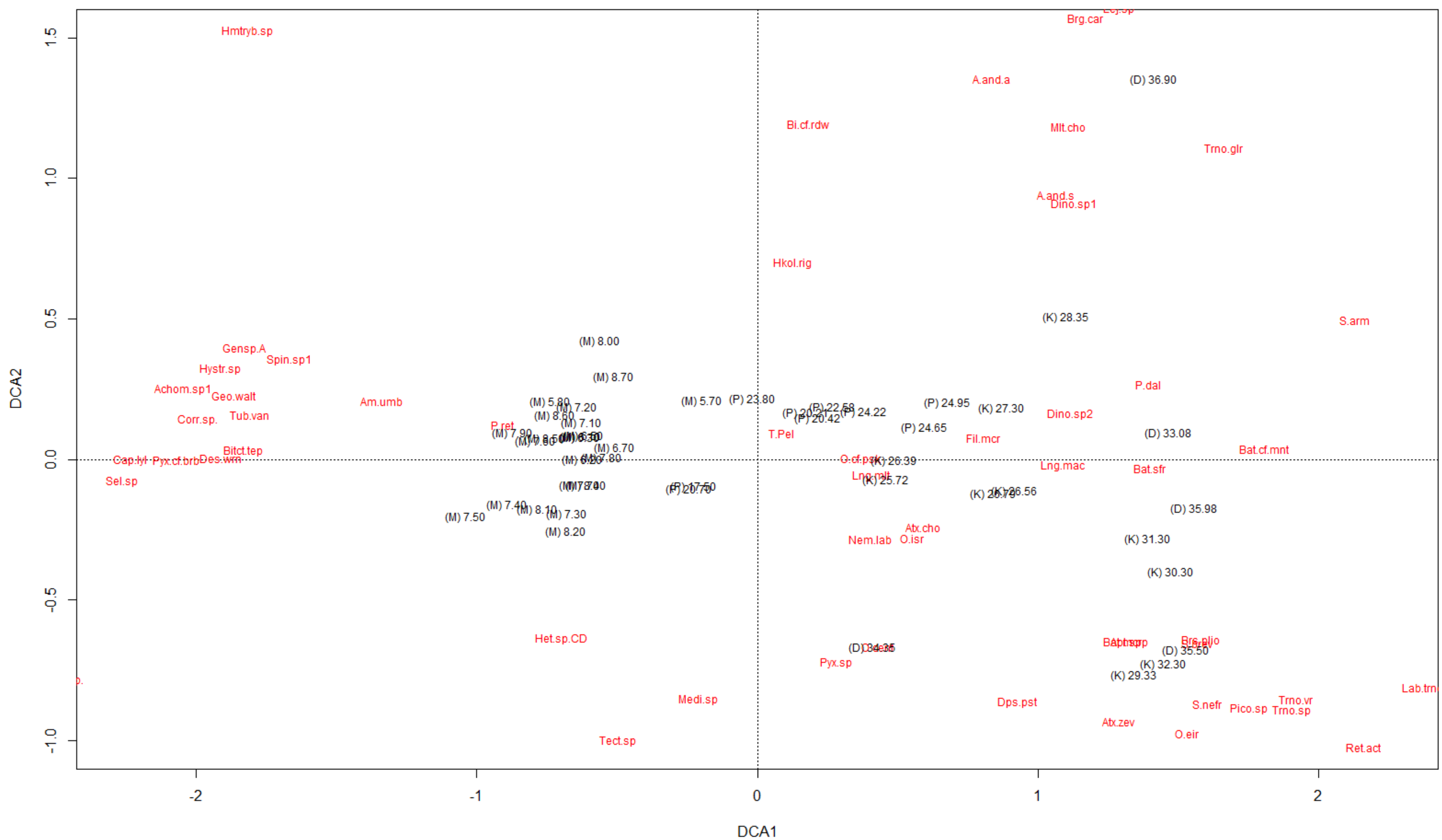

Figure 19 Detrended Correspondence Analysis – Reworked species and Spiniferites *spp. indet. excluded. A letter preceding the sample depth indicates the formation from which the sample came: D = Diest, K = Kasterlee, P = Poederlee, M = Merksplas.*

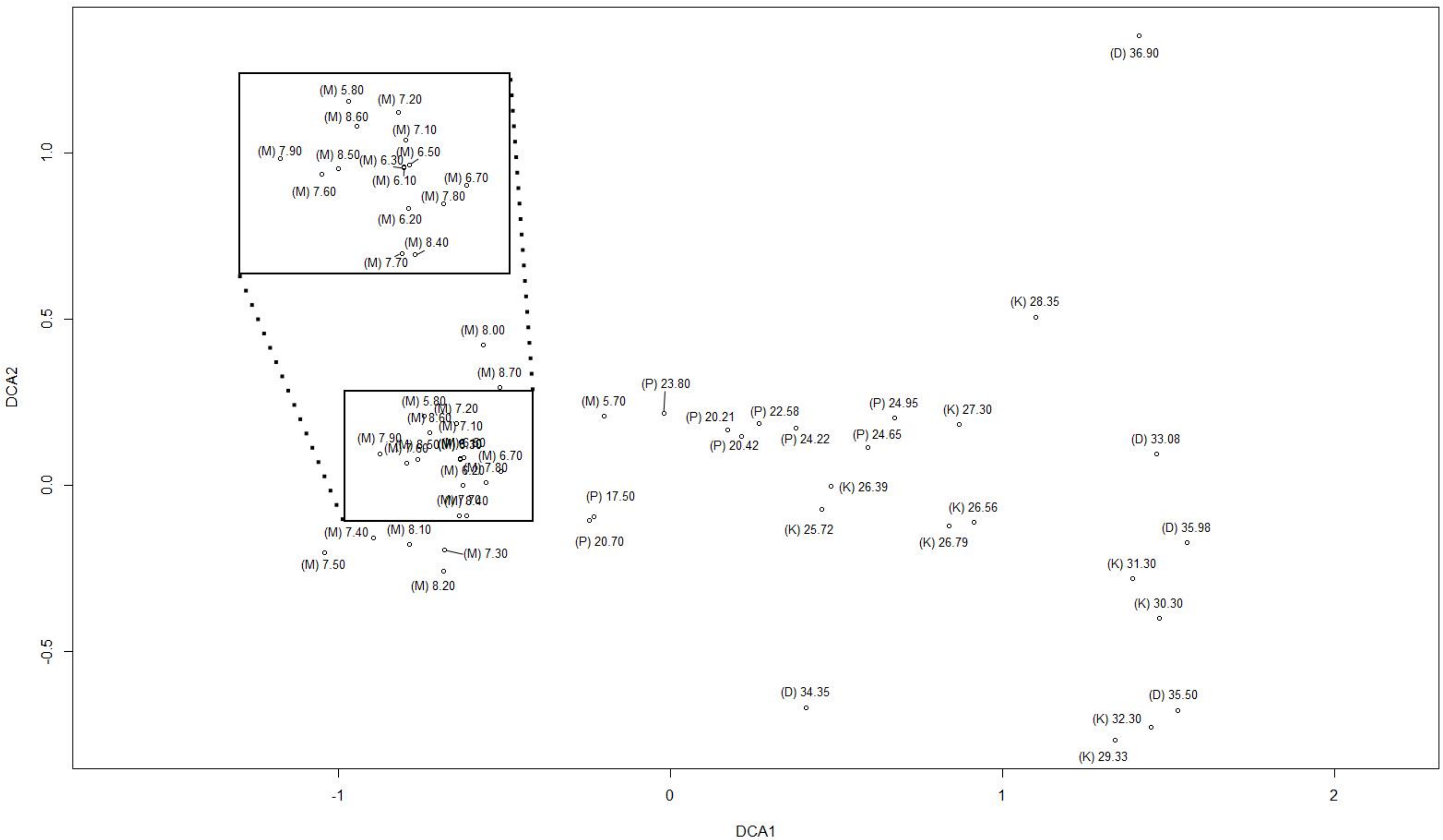

Figure 20 Detrended Correspondence Analysis – Reworked species and Spiniferites *spp. indet. excluded, species points removed and labels moved for visibility of samples. A letter preceding the sample depth indicates the formation from which the sample came: D = Diest, K = Kasterlee, P = Poederlee, M = Merksplas.*

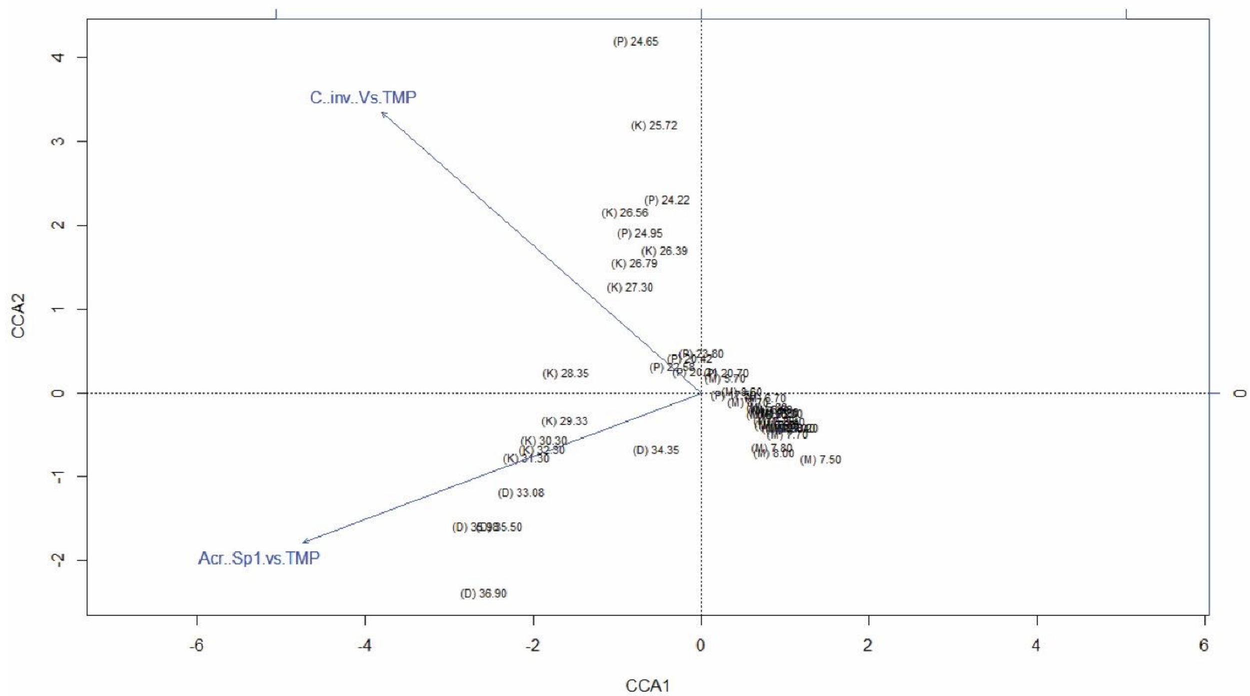

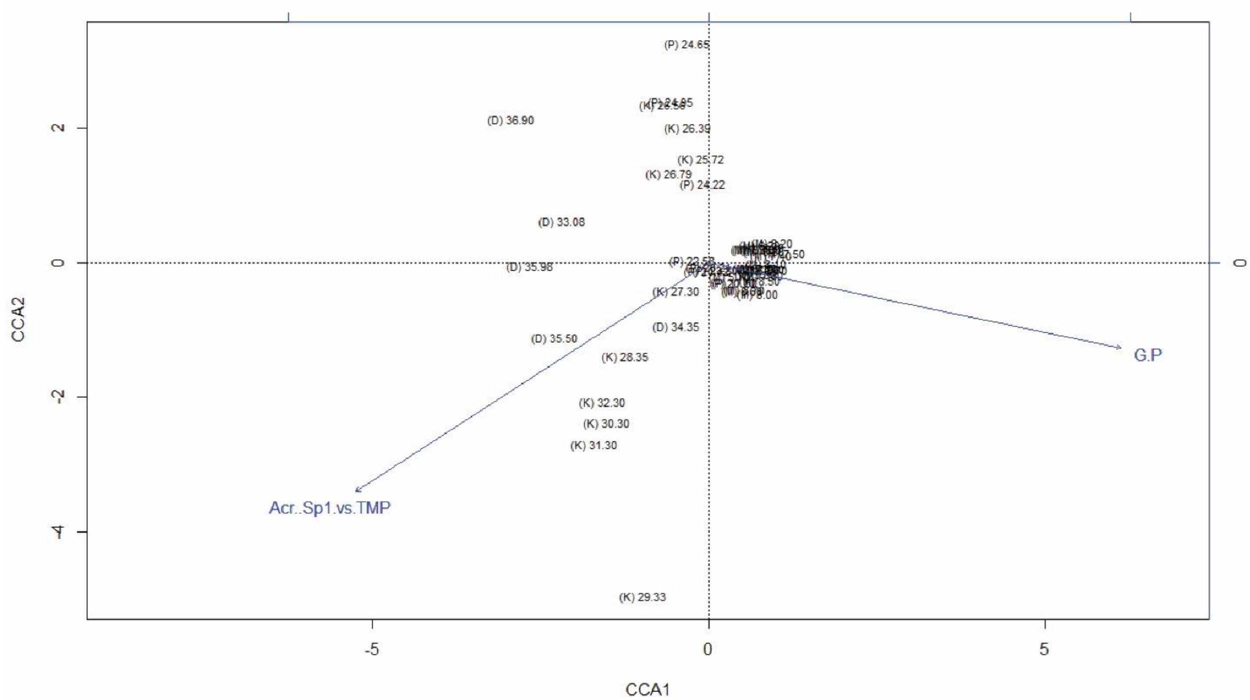

Figure 21 Canonical Correspondence Analysis – Top: Acritarch sp 1 vs Total Marine Palynomorphs (TMP) with Cymatiosphaera*?* invaginata *vs TMP; Bottom: Acritarch sp. 1 vs Total Marine Palynomorphs with GP index*

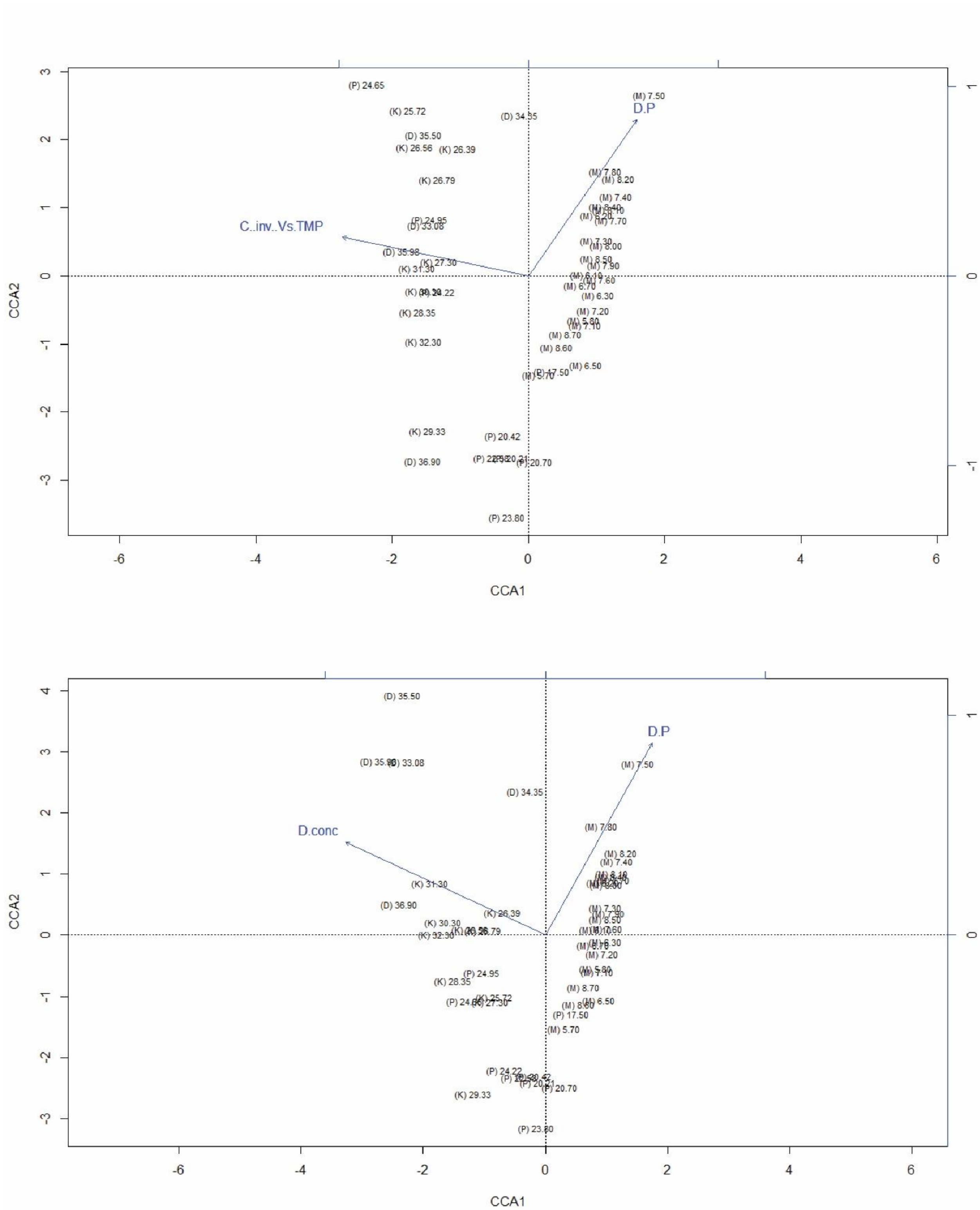

Figure 22 Canonical Correspondence Analysis – Top: Cymatiosphaera*?* invaginata *vs TMP with DApF; Bottom: Dinoflagellate concentrations with DApF.*

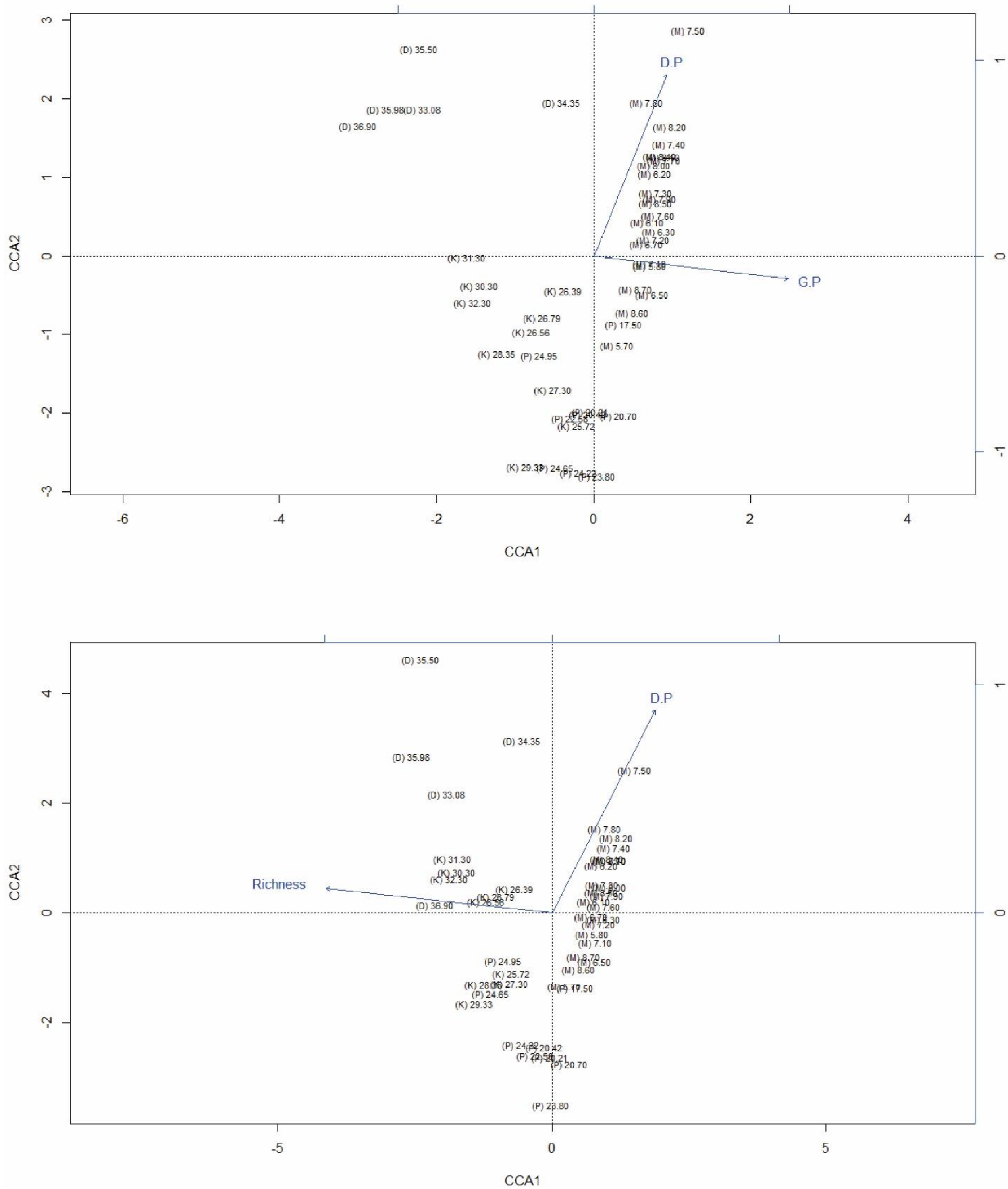

Figure 23 Canonical Correspondence Analysis – Top: DApF with GP index ; Bottom: DApF indices with Richness.

4.0 – Discussion

Statistical analyses followed by biostratigraphic and paleoenvironmental interpretations are discussed below for the Diest, Kasterlee (assemblage biozones A and B), Poederlee, and Merksplas formations. Published dinoflagellate cyst records for other areas are then compared with those from the Rees borehole, at the level of individual formations. Independent evidence from the sedimentology of the Rees borehole (Adriaens, 2016) suggests that the entire the Kasterlee Formation in the Rees borehole is reworked from the Diest Formation. Palynological evidence for this hypothesis is discussed. Nonetheless, biostratigraphic and paleoenvironmental interpretations presented below for the Kasterlee Formation make the prima facie assumption that the assemblages are largely in situ and carry a primary ecological signal. On balance, there does seem to be an in-situ ecological signal within the Kasterlee Formation, as discussed at the end of this chapter.

4.1 – Statistical Analysis

4.1.1 – Cluster Analysis

When considering excluding (Figures 13 and 15) or including (Figures 14 and 16) reworked cysts in the cluster analysis, little difference is seen between the graphs. This difference is mostly seen in the Kasterlee Formation in the presence/absence plot where reworked specimens are given as much statistical weight as in-situ specimens. It reflects taphonomic bias, given that the presence of reworked specimens in a sample is not controlled by environmental parameters. Accordingly, plots excluding reworked cysts are more indicative of such parameters.

The similarity displayed by the presence/absence and count-based cluster analysis varies. The differences between them are due to the statistical weight given to each cyst species. In the count-based analysis, species with higher counts are weighted more than those with lower counts, producing a representation of similarity that accounts for the paleoecological signals associated with species abundances. However, protoperidinioid taxa, which are susceptible to oxidation and loss of preservation (Zonneveld et al., 1997), and other rare taxa are not well represented in the count-based analysis, as their low numbers will be given less statistical weight. In presence/absence analysis, all samples are weighted equally, giving a more equitable representation of similarity.

The presence/absence analysis shows that the most restrained way to group the samples based on their dinoflagellate cyst content is by the formations themselves. The exception to this is the Kasterlee Formation, which can be separated into two distinct biozones. Biozone A (33.25–27.30 m) exhibits higher similarity with the Diest Formation, and Biozone B (26.79–25.30 m) exhibits higher similarity with the Poederlee Formation. When examining the graphs of abundances of key species, this division in the Kasterlee Formation is clearly seen, most notably as changes in *Bitectatodinium* cf. *raedwaldii*, *Heteraulocacysta* sp. A of Costa and Downie (1979), *Operculodinium israelianum*, *Operculodinium tegillatum* and *Protoceratium reticulatum*. The nature of these changes in described below. As previously explained, the Merksplas Formation could also be subdivided into two subdivisions based on the cluster analysis, but no clear difference can be seen in the assemblages or in the sedimentology. As such, the Merksplas Formation will not be divided into separate biozones. Given that the dinoflagellate cyst assemblages can be grouped by the formations themselves, with two biozones being recognised in the Kasterlee Formation, the depositional environment seems to have influenced the dinoflagellate cyst record in the Rees borehole.

4.1.2 – Correspondence Analysis

When examining the DCA plots, the relationships between samples is best displayed in the plot excluding *Spiniferites* spp. indet. and reworked cysts (Figure 17). The results of the plot support the results of the presence/absence cluster analysis in that samples from Kasterlee Biozone A plot nearer the Diest Formation samples, whereas Kasterlee Biozone B plots nearer to the Poederlee Formation. We also see that all Merksplas samples plot very close to each other, contradicting the separation seen in the cluster analysis. All samples plot relatively close together, reflecting the similarity in the environments exhibited by the borehole. The exception, sample 36.90 of the Diest Formation, plots separately, possibly due to high numbers of *Brigantedinium* spp., which would indicate higher nutrient levels. CCA plots show no significant correlation between the parameters used.

4.2 – Biostratigraphy

4.2.1 – Diest Formation (40.00–33.25 m)

The presence of *Achomosphaera andalousiensis* subsp. *andalousiensis*, *Barssidinium pliocenicum*, *Gramocysta verricula*, *Hystrichosphaeropsis obscura*, *Operculodinium*? *eirikianum*, *Operculodinium tegillatum*, *Reticulatosphaera actinocoronata*, *Selenopemphix armageddonensis*, and the acritarch *Nannobarbophora walldalei* are consistent with a Late Miocene age. The presence of cf. *Labyrinthodinium truncatum truncatum* would also point to a Late Miocene age if definitively identified. The top of the upper Tortonian DN9 biozone of de Verteuil and Norris (1996) is based on the highest occurrence of *Hystrichosphaeropsis obscura*, and the base of superjacent Tortonian to Messinian DN10 zone is defined by *Selenopemphix armageddonensis*. Since these two species do not overlap in the biostratigraphic scheme of

Verteuil & Norris (1996), as confirmed by a more recent study of the eastern U.S.A. (Edwards et al., 2005), whereas they co-occur throughout the Diest Formation in the present study, some discussion is warranted. Highest recorded occurrences of *Hystrichosphaeropsis obscura* in the North Atlantic region have been evaluated by Schreck et al. (2013) who found this species to have a consistent highest occurrence within the uppermost Tortonian, in conformity with the observations of de Verteuil and Norris (1996). The recorded lowest occurrences of *Selenopemphix armageddonensis* have been discussed by Louwye et al. (2007) and Louwye and De Schepper (2010) who noted an LO of 9.0 Ma (mid-Tortonian) in equatorial areas and an LO of 7.45 Ma in the mid-latitude Northern Hemisphere, based on a compilation by Williams et al. (2004). Given the apparently diachronous lowest occurrence of *Selenopemphix armageddonensis*, and assuming the specimens of *Hystrichosphaeropsis obscura* are not reworked, an assignment to the DN9 biozone of de Verteuil & Norris (1996) with age of late Tortonian is indicated for the Diest Formation of the Rees borehole. This assignment is supported by the presence of *Operculodinium*? *eirikianum* throughout the formation, which has a LO at the base of DN9 according to de Verteuil & Norris (1996), and of *Gramocysta verricula* which has not been recorded above the mid-Messinian (Louwye & De Schepper, 2010).

Dybkjær and Piasecki (2010) developed a Miocene and Pliocene biozonation for the eastern North Sea Basin based on deposits from onshore and offshore Denmark. Their Upper Miocene biozonation (*Hystrichosphaeropsis obscura* and *Selenopemphix armageddonensis* zones) is equivalent to the DN9 and DN10 zones of de Vertuil and Norris, and are defined by the same events. As such, the Diest Formation of the Rees borehole corresponds to the *Selenopemphix armageddonensis* zone of Dybkjær and Piasecki (2010).

It should be noted that *Achomosphaera andalousiensis suttonensis* is significantly represented within this formation and specimens appear to be in place, due to their robust appearance. The range of this species is not fully understood, although it has not been recorded outside of the Pliocene in the southern North Sea Basin (Louwye & Laga, 1998; Louwye et al., 2004; De Schepper et al., 2009; Louwye & De Schepper, 2010). Its presence in the Diest Formation, however, contradicts this. *Gramocysta verricula* (Louwye et al., 2007; Louwye & De Schepper, 2010) and *Hystrichosphaeropsis obscura* (Soliman et al., 2012) are specifically Miocene species. Their presence in the Diest Formation, their numbers and in-situ appearance along with the other previously mentioned species, place the formation unequivocally in the Miocene. As such, the range of *Achomosphaera andalousiensis suttonensis* must extend downwards into the Upper Miocene.

4.2.2 – Kasterlee Formation – Assemblage Biozone A (33.25–27.30 m)

The dinoflagellate cyst association of the Kasterlee Biozone A is similar to that of the underlying Diest Formation, and has the same biostratigraphically significant species: *Achomosphaera andalousiensis andalousiensis*, *Barssidinium pliocenicum*, *Hystrichosphaeropsis obscura*, *Operculodinium*? *eirikianum*, *Operculodinium tegillatum, Reticulatosphaera actinocoronata*, *Selenopemphix armageddonensis* and the acritarch *Nannobarbophora walldalei*. As with the Diest Formation, these taxa point to a late Tortonian age. Specimens of cf. *Labrynthodinium truncatum truncatum* also occur sporadically in this biozone.

As in the Diest Formation, *Achomosphaera andalousiensis suttonensis* occurs in significant numbers throughout Biozone A, indicating that this subspecies extends into the Upper Miocene.

4.2.3 – Kasterlee Formation – Assemblage Biozone B (26.79–25.30 m)

Operculodinium? *eirikianum, Operculodinium tegillatum, Reticulatosphaera actinocoronata,* and *Selenopemphix armageddonensis* are biostratigraphically significant components of Assemblage Zone B. The presence of *Operculodinium*? *eirikianum* and *Selenopemphix armageddonensis* indicates an age no greater than late Tortonian for Biozone B, as indicated above. The range top of *Selenopemphix armageddonensis* is open to interpretation. According to Louwye and De Schepper (2010), this species does not range above the Miocene, with Pliocene occurrences, including those within the North Sea Basin (Louwye et al., 2004; Piasecki et al., 2002) being sparse and presumably representing reworking. It should be noted that although *Selenopemphix armageddonensis* is recorded only in low abundances in Biozone B, similar abundances are recorded in Biozone A and in the Deist Formation. Biozone B is possibly therefore no younger than Late Miocene. Alternatively, if *Selenopemphix armageddonensis* is not considered, then *Reticulatosphaera actinocoronata* and *Operculodinium tegillatum* range as high as 5.0–4.4 Ma and ~3.7 Ma, respectively, in the Lower Pliocene (Zanclean) of the North Atlantic region (De Schepper et al., 2009). Assemblage Biozone B is therefore no older than late Tortonian and no younger than Messinian (HO of *Selenopemphix armageddonensis*) or early Zanclean (HO of *Reticulatosphaera actinocoronata*).

4.2.4 – Poederlee Formation (25.30–17.00 m)

Achomosphaera andalousiensis suttonensis, *Invertocysta lacrymosa* and *Operculodinium*? *eirikianum* are found throughout the Poederlee Formation, whereas *Reticulatosphaera actinocoronata* and *Batiacasphaera minuta*/*micropapilata* are absent. This points to a latest Zanclean to Piacenzian age. Specifically, *Invertocysta lacrymosa* has a highest occurrence of 2.72 Ma in the North Atlantic (Hennissen et al., 2014), indicating that the Poederlee Formation is no younger than 2.72 Ma. One poorly-preserved specimen of *Operculodinium tegillatum* found near the base of the formation is judged to be reworked. This species is known to range up to ca. 3.7 Ma in the North Atlantic (Louwye et al., 2004; De Schepper et al., 2009), as noted above. *Selenopemphix armageddonensis* is present in small numbers in one sample at the base of the formation. As previously mentioned, Pliocene occurrences of this species are thought to be due to reworking (Louwye et al., 2004; Piasecki et al., 2002). Its assumed absence therefore suggests that the Poederlee Formation is younger than 3.7 Ma.

The Poederlee of the Rees borehole could correspond to the *Melitasphaeridium choanophorum* zone of Dybkjær and Piasecki (2010), which is defined by the highest occurrence of *Barssidinium evangelineae* (5.0 Ma) to the highest occurrence of *Melitasphaeridium choanophorum* at 3.6 Ma in the eastern North Sea basin. *Melitasphaeridium choanophorum* does occur in the Poederlee Formation of the Rees borehole, so its age is presumably no younger than 3.6 Ma. *Melitasphaeridium choanophorum* is, however, an extant species known to occur in the Gulf of Mexico (Limoges et al., 2013). Its highest occurrence in the North Sea Basin is likely environmentally controlled, so any age assignment based on this species alone must be tentative.

As such, the age of this formation in the Rees borehole is considered to be between 3.7 and 2.7 Ma (latest Zanclean–late Piacenzian), and tentatively between 3.7 and 3.6 Ma, based on the apparent highest occurrence of *Melitasphaeridium choanophorum* in the North Sea Basin.

4.2.5 – Merksplas Formation (9.00–3.00 m)

The presence of *Capisocysta lyelli*, *Desotodinium wrennii*, *Geonettia waltonensis*, *Invertocysta lacrymosa*, and *Pyxidinopsis* cf. *braboi* point towards a mid- to late Pliocene age for the Merksplas Formation. *Geonettia waltonensis* has a lowest known occurrence in the lower

Pliocene in Eastern England, dated at around 3.8–3.6 Ma, (Head, 2000), although its full range is not well documented. *Desotodinium wrennii* and *Pyxidinopsis braboi* have been reported from the upper lower Pliocene to lower upper Pliocene of Belgium (De Schepper et al., 2004). Specifically, *Pyxidinopsis braboi* is thought to have a range between 3.15-2.57 Ma in the North Atlantic (De Schepper et al., 2009), although its identification in the Merksplas Formation is inconclusive. The presence of *Invertocysta lacrymosa* indicates an age no younger than 2.72 Ma and the absence of *Operculodinium tegillatum* which has a highest range of 3.7 Ma in the North Atlantic (Louwye et al., 2004; De Schepper et al., 2009) suggests an age no older than 3.7 Ma, as for the Poederlee Formation.

When considering the biozonation of Dybkjær and Piasecki (2010), the Merksplas Formation may lie within the *Barssidinium pliocenicum* zone, which is based on the last occurrence of *Melitasphaeridium choanophorum* (3.6 Ma) to the first occurrence of *Impagidinium multiplexum* (2.4 Ma). The absence of *Melitasphaeridium choanophorum* and the presence of *Barssidinium pliocenicum* and *Invertocysta lacrymosa* would put the Merksplas in the lower part of this biozone, and no older than 3.6 Ma. As previously explained, *Melitasphaeridium choanophorum* is an extant species, so this age assignment is tentative.

The age of the Merksplas Formation is therefore between 3.7 and 2.72 Ma, and possibly no older than 3.15 Ma depending on the identification of *Pyxidinopsis braboi*, or 3.6 Ma depending on the highest occurrence of *Melitasphaeridium choanophorum*.

4.3 – Paleoecology

Assemblage compositions throughout the Rees Borehole, which are characterised by an absence of the oceanic genus *Impagidinium* (Dale, 1996) and scarcity of other open-ocean taxa including

Invertocysta lacrymosa (Hennissen et al., 2017) reflect neritic deposition within a restricted marine basin under temperate to warm climates.

4.3.1 – Diest Formation (40.00–33.25 m)

The lower part of the cored interval of the Diest Formation has high numbers of *Brigantedinium* spp. (up to 28%), *Bitectatodinium* cf. *raedwaldii* (up to 15%) and total *Spiniferites*/*Achomosphaera* spp. (up to 49%), and low AIN. This indicates a nearshore, somewhat restricted, warm-temperate environment, with relatively high nutrient levels judging from relatively common heterotrophs including *Brigantedinium* spp. (Dale, 1996). The sample at 36.90 m contains moderate numbers of *Gramocysta verricula*, a species with an affinity for shallow marine conditions (Warny & Wrenn, 2002). The lowest sample investigated, at 39.50 m, is uniquely dominated by the extinct acritarch *Paralecaniella indentata*, presumably indicating restricted marine conditions of a particular kind, although the autecology of this species is not known. In the upper part of the Diest Formation, *Bitectatodinium* cf. *raedwaldii* and *Spiniferites* spp. decrease whereas *Heteraulocacysta* sp. A of Costa and Downie (1979) increases to up to 42%. This species when occurring in abundance has been associated with restricted marine conditions in an inner neritic setting in the Pliocene of Belgium (De Schepper et al., 2009; Louwye & De Schepper, 2010). *Operculodinium israelianum* and *Operculodinium tegillatum* increase significantly. The autecology of the extinct *Operculodinium tegillatum* is not well known, but *Operculodinium israelianum* is an extant species common today in very shallow depths, especially in estuaries (Head, 1996b). Its increase in the upper part of the Diest Formation suggests a shallowing upwards trend. AIN values generally increase at this point, but remain low overall. This shows a shift to more temperate conditions. *Cyclopsiella* sp., which is speculated to have exhibited an epilithic or encrusting mode of life and to have lived in the photic zone (Matsuoka & Head, 1992), and *Paralecaniella indentata* which is considered to be typical of restricted marine conditions (Brinkhuis & Schiøler, 1996), are also present throughout the formation. Although these acritarchs indicate a shallow marine, warm-water environment, the low numbers would indicate an environment at the limit of their tolerance. Relatively high numbers of green algae indicate freshwater influence. Evenness values indicate moderately-well distributed species abundances.

Pollen concentrations fluctuate up the formation. DP trends are generally the same, in that they decrease from the base, overall increase, then decrease at the top of the formation. This suggests changes in the distance from shore, and an overall decrease in distality from the base to the top of the formation. BpNp show a slightly different result. This index increases from the base towards the middle of the formation, before decreasing again. Overall, there's an increase in the index, which points towards an increase in distality, which would contradict the DP results. This may reflect unreliable BpNp index due to preservational or counting bias, or perhaps climate-driven changes in the terrestrial vegetation. In this formation, oxidation is evidently quite high. In these sections, the degraded pollen would cause underrepresentation in counting. As such, the DP index is thought to be a more reliable indicator of relative distance from shore for the Diest Formation.

Overall, the palynological record of the Diest Formation indicates warm to temperate, inner neritic conditions. A reduction in water depth seems to have occurred over time, perhaps due to the loss of accommodation space.

4.3.2 – Kasterlee Formation – Biozone A (33.25–27.30 m)

Kasterlee Biozone A is distinguished from the Diest Formation by higher numbers of *Spiniferites* spp. and lower numbers of *Operculodinium israelianum* and, apart from the lowest sample, lower numbers of *Heteraulacacysta* sp. A of Costa and Downie (1979). These trends suggest more open-water conditions relative to the Diest Formation. *Operculodinium tegillatum* is abundant in the lowest part of the Kasterlee Formation, but declines up through Biozone A, suggesting a change in paleoenvironments over time. AIN values increase upsection, but remain low. In general, a warm, neritic environment is indicated. Evenness values point towards moderate species abundance distribution.

The trends exhibited by the DP indices suggest varying degrees of distality upsection, beginning with low values relative to the Diest Formation, then an increase then a slight decrease near the top of the biozone. The BpNp trends are slightly different, showing an overall decrease, then a slight increase near the top of the section. This discrepancy could be explained by the same possible preservation bias seen in the Diest Formation, where pollen counts are underrepresented due to high oxidation. Again, the DP indices is probably more robust in representing distality. Overall pollen concentrations exhibit similar trends to the DP indices, indicating a deepening towards the middle of the section, before beginning to shallow upwards.

The Kastelee Biozone A overall represents a temperate to warm water, neritic, shallow marine environment, where distality shifts back and forth. This is a similar environment to the subjacent Diest Formation. This is further supported by the similar species and similar quantities of *Cyclopsiella* sp. in the section. Green algae are fewer than for the Diest Formation, however, suggesting a reduced freshwater influence.

<u>4.3.3 – Kasterlee Formation – Biozone B (26.79–25.30 m)</u>

Kasterlee Biozone B is characterised by the decline of *Brigantedinium* spp. to low values (with a maximum of 2.5%), a progressive increase in *Heteraulacacysta* sp. A of Costa and Downie (1979) through the zone and reaching a maximum abundance of 11.5%, significant increases in *Lingulodinium machaerophorum* especially towards the top of the zone (up to a maximum of 17%), and increases in *Operculodinium israelianum* (up to 14%) and *Protoceratium reticulatum* (maximum of 8%). In addition, *Operculodinium tegillatum* numbers decline up-section. *Spiniferites*/*Achomosphaera* spp. remains high. Acritarch sp. 1 declines substantially in Biozone B although its autecology is not known. AIN values overall increase up-section, but remain low. The increases in *Heteraulacacysta* sp. A of Costa and Downie (1979), *Lingulodinium machaerophorum*, and *Operculodinium israelianum* all suggest the encroachment of nearshore conditions. *Lingulodinium machaerophorum* is an extant euryhaline species particularly associated today with estuarine environments and somewhat elevated nutrient levels (Dale, 1996; Zonneveld et al., 2013). The cosmopolitan extant species *Protoceratium reticulatum* (usually reported in the literature as *Operculodinium centrocarpum* sensu Wall and Dale, 1966) is regarded as a pioneer species able to thrive in unstable conditions, although elevated numbers are more usually associated with the neritic–oceanic transition than with nearshore conditions (Dale, 1996). Nevertheless, *Protoceratium reticulatum* can be found in high abundances in coastal environments (Zonneveld et al., 2013) and in neritic environments where salinities are somewhat reduced (e.g. Head et al., 2005; Head, 2007). On balance the assemblage changes seem to reflect a shallowing of the water column through Biozone B.

DP index values overall decrease towards the top of this section and likewise suggest a shallowing upward trend, and this is further confirmed by a similar trend in the BpNp index and an upsection increase in pollen concentration. Evenness values are similar to Biozone A, indicating similarly moderate species abundance distribution. Green algae concentrations are also similar to those of the Biozone A, and indicate similar levels of freshwater influence.

Overall, the Kasterlee Biozone B points towards a temperate, increasingly restricted, shallowing-upwards environment.

4.3.4 – Poederlee Formation (25.30–17.00 m)

The Poederlee Formation contains elevated numbers of *Heteraulacacysta* sp. A of Costa and Downie (1979) to a maximum of 23% in the highest sample and moderately abundant (6–15%) *Protoceratium reticulatum* throughout the formation. *Spiniferites* spp. remain abundant (35–65%) throughout the formation. *Lingulodinium machaerophorum* and *Operculodinium israelianum* have relatively high values (up to 22% and 6%, respectively) near the base of the formation, and decrease to very low numbers higher in the formation. AIN shows an overall increase up-section, although the numbers remain low, but nonetheless indicate an open marine influence. The assemblages of the Poederlee Formation represent a warm-water restricted marine environment, with conditions perhaps becoming more restricted up-section. Green algae numbers increase up through the formation, indicating an increasing freshwater influence, while consistently high *Cyclopsiella* sp. further indicate a shallow-marine, warm water environment.

DP indices show similar trends, and generally decrease up the formation, indicating decreasing distallity. Pollen concentrations increase near the base, and then decrease up the formation, but remain very high. These indicators point towards a shallowing-upwards, near shore trend. Evenness similarly decreases slightly up-section, consistent with a more restricted environment.

Overall, the Poederlee Formation reflects a warm water, shallow marine environment that shallows upwards and become more restricted.

4.3.5 – Merksplas Formation (9.00–3.00 m)

The samples from the Merksplas Formation contain high numbers of *Heteraulocacysta* sp. A of Costa and Downie (1979) and *Protoceratium reticulatum*, and relatively abundant *Capisocysta lyellii*. *Spiniferites*/*Achomosphaera* spp ind. and *Operculodinium israelianum* proportions are relatively lower. These species indicate a warm-water, restricted, nearshore environment. This is further demonstrated by the presence of *Geonettia waltonensis*, athough it is a rare species, which may indicate the limits of its environmental tolerance. Evenness values are relatively high, indicating lower species abundance distribution. The DP and BpNp indices values are relatively high, pointing towards an offshore environment, although the species present suggest a more lagoonal setting.

4.4 – Comparison with other studies in Belgium

4.4.1 – Diest Formation

The Rees borehole penetrated only the upper part of the Diest Formation, this being the Diest Sands member. The dinoflagellate cyst record here compares well with those of the upper part of the Diest Sands documented from the Kalmthout, Oostmalle, Poederlee, Retie, Mol, Dessel-2 and Wijshagen wells, the Borgerhout Rivierenhof XIV, Borgerhout Rivierenhof VII, Berchem, Deurne and Olen outcrops near the city of Antwerp. Previous studies of these localities (Louwye & Laga, 1998; Louwye et al., 1999; Louwye, 2002; Louwye et al., 2007; Louwye & Laga, 2008) have placed the upper part of the formation in the DN9 and DN10 biozones. An important taxon in the Diest Formation is *Labrynthodinium truncatum truncatum.* While common in the greater part of the formation, it is mostly absent in the Rees borehole, with a few possible specimens found (as cf. *Labrynthodinium truncatum truncatum*). This is consistent with uppermost parts of the formation, where the species is absent in the upper Diest of the Oostmalle, Poederlee, Retie, and Mol wells, and completely absent in the Kalmthout well (Louwye & Laga, 1998; Louwye et al., 1999).

The lowermost sample studied in the Rees borehole, at 39.50 m, is dominated by the acritarch *Paralecaniella indentata*. This was also reported from the upper part of the Diest Formation in the Wijshagen borehole by Louwye & Laga (2008), but attributed by these authors to partial post-depositional oxidation such that only the resistant *Paralecaniella indentata* survived (Louwye & Laga, 2008). Oxidation is evident throughout the Diest Formation in the Rees borehole, as cyst preservation is lower than in the remainder of the borehole, and specimens tend to be more degraded. This may reflect the coarser grain size of the Diest Sands, which will have allowed oxidizing meteoric waters to circulate more freely through the formation. The higher glauconite content also implies low sedimentation rates and therefore prolonged exposure of cysts to degradation on the sea floor (Louwye & Laga, 2008). The Rees sample does not, however, seem consistent with this explanation because the few dinoflagellate cysts present are as well preserved as elsewhere in the formation, and the presence of the oxidation-susceptible heterotrophs *Lejeunecysta* sp. and *Selenopemphix dioneaecysta* do not imply excessive oxidation of this sample. Nor is the assemblage dominated by more robust cyst morphotypes. As such, oxidation and degradation of cysts does not appear to account for the anomalous dominance of *Paralecaniella indentata*. Instead, this sample appears to represent a very specific shallow-marine environment in which *Paralecaniella indentata* thrives.

4.4.2 – Kasterlee Formation

Previous studies from around northern Belgium place the Kasterlee Formation in the Messinian (upper Upper Miocene). Given that Kasterlee Biozone A immediately overlies the Diest Formation, the closest direct comparison is with the study by Louwye et al. (2007) of the Kasterlee Formation in the Dessel-2 well and Olen outcrop, where it too overlies the Diest Formation. Similarly, Kasterlee Biozone B is subjacent to the Poederlee Formation, and is here compared to the study by Louwye and De Schepper (2010) of the Kasterlee Formation from the Oud-Turnhout borehole where it directly underlies the Poederlee Formation.

4.4.2.1 – Kasterlee Biozone A (33.25–27.30 m)

Louwye et al. (2007) found that although there are some similarities between the assemblages of the Kasterlee and the Diest formation, there were also distinct differences, namely that the Kasterlee contained large numbers of *Gramocysta verricula* near the boundary with the Diest Formation. The presence of *Gramocysta verricula*, along with *Selenopemphix armageddonensis*, were used to constrain the age range of the formation at between 7.5 and 5.3 Ma.

The Kasterlee Formation in the Rees borehole shows a distinct absence of *Gramocysta verricula* in both biozones. In addition, the Rees Kasterlee Biozone A has numbers of *Bitectatodinium* cf. *raedwaldii* that are significantly higher than the *B. raedwaldii* values recorded by Louwye et al. (2007), and also significantly higher values of *Heteraulocacysta* sp. A of Costa and Downie (1979), *Operculodinium israelianum* and *Selenopemphix armageddonensis. Labrynthodinium truncatum truncatum* and *Apteodinium* sp. are not generally found in the Kasterlee Formation, but are recorded rarely in the Kasterlee Biozone A, whereas *Apteodinium* sp. and cf. *Labrynthodinium truncatum truncatum* occur rarely in the Rees borehole. Given particularly the absence of *Gramocysta verricula*, the Kasterlee Biozone A of the Rees borehole shows significant differences with the Kasterlee Formation of other areas.

<u>4.4.2.2 – Kasterlee Biozone B (26.79–25.3 m)</u>

Louwye and De Schepper (2010) found that the Kasterlee Formation in the Oud-Turnhout well correlated well with the Kasterlee Formation analysed from the Dessel-2 borehole and the Olen outcrop (Louwye et al., 2007). The Oud-Turnhout association is characterised by *Bitectatodinium raedwaldii*, *Lingulodinium machaerophorum*, low values of *Barssidinium taxandrianum*, *Gramocysta verricula, Operculodinium israelianum*, *Selenopemphix armageddonensis* and *Trinovantedinium ferugnomatum,* and an upsection decrease in *Barssidinium pliocenicum* and *Operculodinium tegillatum*. *Heteraulocacysta* sp. A of Costa and Downie (1979) and *Protoceratium reticulatum* (as *Operculodinium centrocarpum* sensu Wall and Dale (1966)) counts are high at the boundary with the Poederlee Formation. The age of the section was attributed to the Messinian, due to the presence of *Barssidinium taxandrianum*, *Gramocysta verricula*, *Selenopemphix armageddonensis* and *Trinovantedinium ferugnomtum* and the absence of *Labrynthodinium truncatum truncatum.*

Kasterlee Biozone B of the Rees borehole is similarly characterised by *Lingulodinium machaerophorum* and low *Selenopemphix armageddonensi*s, and has moderate numbers of *Bitectatodinium* cf. *raedwaldii* (perhaps corresponding to *Bitectatodinium raedwaldii* of Louwye and De Schepper, 2010). There is also a decrease in *Barssidinium pliocenicum* and *Operculodinium tegillatum* up-section, and an increase in *Heteraulocacysta* sp. A of Costa and Downie (1979) and *Protoceratium reticulatum*. Conversely, Biozone B shows higher numbers of *Operculodinium israelianum* than the Kasterlee Formation in the Oud-Turnhout well, and also contains *Achomosphaera andalousiensis suttonensis,* although this could be due to local environmental differences in the Rees borehole area. Biozone B also lacks *Barssidinium taxandrianum*, *Gramocysta verricula* and *Trinovantedinium ferugnomatum*, although these taxa are rare in the Oud-Turnhout section.

The Oud-Turnhout Kasterlee Formation and the Rees Biozone B share many of the same species and show some of the same trends. Kasterlee Biozone B section may therefore represent the same interval of the Kasterlee Formation as seen in the Oud-Turnhout well. Given the lack of the important species in the Rees borehole, however, a similar age restriction cannot be made for Kasterlee Biozone B in the Rees borehole. As such, a definitive correlation cannot be made.

4.4.3 – Poederlee Formation (25.30–17.00 m)

Only Louwye and De Schepper (2010) have previously studied the palynology of the Poederlee Formation, which they undertook during their analysis of the Oud-Turnhout well. A mid-Pliocene age between 3.7 Ma and 2.7 Ma was proposed, based on the presence of *Achomosphaera andalousiensis* subsp. *suttonensis*, *Invertocysta lacrymosa*, *Operculodinium*? *eirikianum* and the absence of *Reticulatosphaera actinocoronata*, *Operculodinium tegillatum* and *Batiacasphaera minuta/micropapilata*. Based on this, the dinoflagellate cyst association of Poederlee Formation in the Rees borehole compares closely to the association of the Oud-Turnhout well.

4.4.4 – Merksplas Formation (9.00–3.00 m)

This study marks the first palynological analysis of the Merksplas Formation, so correlation to the Merksplas Formation in other areas based on dinoflagellate cyst biostratigraphy is not possible. Comparison can, however, be made with the Merksem Sands of the Pliocene Lillo Formation, analysed by De Schepper et al. (2009). The ages of both the Merksem sands and the

Merksplas Formation are approximately the same, and share many of the same cysts. Notably, both have high numbers of *Heteraulocacysta* sp. A of Costa and Downie (1979) and *Protoceratium reticulatum* (as *Operculodinium centrocarpum* sensu Wall and Dale, 1966). *Desotodinium wrennii* is present, albeit rarely, in both sections.

Although environments seem similar, the Merksplas Formation contains higher numbers of *Achomosphaera andalousiensis andalousiensis*/*suttonensis*, *Amiculosphaera umbraculum*, *Capisocysta lyellii* and *Tuberculodinium vancampoae*. While the associations in both sections indicate a warm, restricted environment, the other species in the Merksplas Formation may indicate a more offshore environment.

4.5 – Depositional environment

With the exception of the Kasterlee Formation, the dinoflagellate cyst assemblages divide according to the formations in the Rees borehole. This implies that changes in depositional environment occurred from one formation to another, notwithstanding any possible changes to the flora due to evolutionary and extinction processes with passing geological time. These environmental changes were likely not dramatic, as paleoenvironmental interpretations indicate similar neritic, warm to temperate environments throughout the Rees succession.

The Diest Sands member was thought to have been deposited in a large erosional gulley, after the shifting of the depocentre towards the Antwerp region, as a series of sand bars in marginal marine conditions (Wouters & Vandenberghe, 1994). This is represented in the Rees borehole as coarse packed, rusty coloured, poorly sorted sand containing glauconite (Buffel et al., 2001). Dinoflagellate analysis supports the sedimentological analysis, pointing towards a warm water, inner neritic environment that shallows upwards. The rusty colour indicates heavy oxidation and the coarse grain size likely the flow of meteoric water through the section. This is seen in the poorer preservation of the dinoflagellate cysts in comparison to the remainder of the borehole. The overlying Kasterlee Formation of the Rees borehole is described as being identical to the Diest Formation, but with finer grain size and better sorting, and pointing towards a similar shallow marine deposit (Buffel et al., 2001). The environment interpreted from the dinoflagellate assemblages is also similar to the underlying Diest. The finer grain size of the Kasterlee would account for the better preservation of palynological material compared to the Diest.

The Poederlee Formation is thought to have been deposited during a transgression to highstand phase, in a shallow marine environment, with fresh water input (Louwye & De Schepper, 2010). The Poederlee of the Rees borehole is represented as fine grained, glauconitic sands. This is supported by palynological analysis, which indicates a warm water, shallow marine environment. The shallowing upwards trend is reflected in the sedimentology, as sorting increases up the formation, and in the palynological analysis, as a decrease in DP index and an increase in green algae concentrations.

The Mol Formation is considered to represent continental to estuarine deposition (National Commission for Stratigraphy Belgium), and forms coarse, white, very high quartz sands in the Rees borehole. The lack of palynomorphs may be explained by the coarse grain size, implying a high energy depositional environment that would not favour the accumulation of palynomorphs, and post-depositional circulation of meteoric water, causing enhanced oxidation.

The Merksplas Formation has been considered continental to estuarine in origin, deposited in sandy tidal flats (National Commission for Stratigraphy Belgium; Buffel et al., 2001). The formation is represented in the Rees borehole as fine, slightly glauconitic, light-brown quartz sands. The presence of dinoflagellate cysts in the productive interval (8.70–5.60 m) indicates marine conditions. The barren sections of the formation are coarser grained and lighter in colour, which would explain the lack of palynomorphs. Dinoflagellate concentrations increase from the base of the productive interval, peak at 7.40 m, and then decrease to the top. Pollen concentrations remain high at the top of the interval, with an increase in nonsaccate pollen in relation to bisaccate pollen. This points towards an increase in distality and marine conditions from the base to 7.40 m, followed by a decrease in distality. It implies that the productive interval in the Merksplas Formation corresponds to a sea-level high stand, which is supported by the lithological change from coarse white sand, to light brown finer sand, and back to coarse white sand.

4.6 – Diest and Kasterlee issue

The palynology of the Diest Formation has been analysed quite thoroughly over the last few decades, and cyst assemblages of the Diest in the Rees borehole compare well with previous studies. On the other hand, the Kasterlee Formation in the Rees borehole differs from other sites. Two informal assemblage biozones, A and B, are recognised in the Kasterlee Formation of the Rees borehole. Louwye et al (2007) found a distinct difference between the associations of the Diest and Kasterlee formations in the Dessel-2 borehole and outcrops in the Olen area. Diest Formation contained specimens of *Labrynthodinium truncatum* subsp. *truncatum*, albeit in small numbers, and the base of the Kasterlee Formation had a markedly higher concentration of *Gramocysta verricula*. No *Gramocysta verricula* is found in the Kasterlee of the Rees borehole. Instead, the association of Kasterlee Biozone A is very similar to the Diest association, with the exception that *Labrynthodinium truncatum* subsp. *truncatum* was not recorded definitively (although sparse specimens of cf. *Labrynthodinium truncatum* subsp. *truncatum* were registered in the Rees borehole). The presence of *Apteodinium* sp. in the Kasterlee Formation is potentially significant. This genus is present in the Diest Formation in the Kalmthout well (as *Apteodinium australiense* and *Apteodinium spiridoides*; Louwye & Laga, 1998), but has not been recorded in the Kasterlee Formation from any location. These similarities raise the possibility that Diest sediment has been reworked into the Kasterlee Formation. The presence/absence cluster dendrogram and DCA plots show a strong statistical similarity between the Diest Formation and Kasterlee Biozone A in the Rees borehole. This is to be expected, as they share many of the same species, although in different concentrations. Kasterlee Biozone B shows some similarity with the Kasterlee Formation of the Out-Turnhout well. Nonethless, while they share many species and trends, they lack important rare cyst taxa that were used to date the Out-Turnhout Kasterlee, and a direct correlation between them is therefore tentative.

Adriaens (2016) suggested that the Kasterlee Formation of the Rees borehole entirely comprises sediment reworked from the underlying Diest Formation. This was based on the differences in the mineralogy and clay content of the Kasterlee Formation in the Rees compared to the Kasterlee in other areas, as well as the similarity of the mineralogy and clay content of the Kasterlee and Diest formations in the Rees borehole. This reworked section has been seen previously in the Dessel-2 and Dessel-3 boreholes, although its maximum recorded thickness has only ever been about 2 m, as compared with 8 m for the Kasterlee Formation in the Rees borehole. Results of the palynological analysis of the Rees borehole show that the dinoflagellate cyst associations of the Diest and Kasterlee formations are very similar, and key species typically found in the Kasterlee Formation are absent. This would support the hypothesis that the Kasterlee Formation in the Rees borehole comprises reworked sediment from the underlying Diest Formation, at least for the Kasterlee Biozone A. Although the superjancent Biozone B does share many species and trends with the Kasterlee Formation of Oud-Turnhout, the lack of important species, in conjunction with the difference in mineralogy found by Adriaens, raises the possibility that Biozone B is also made up largely of reworked Diest material. This would make the reworked section in the Rees borehole much thicker than seen anywhere else.

If the Kasterlee Formation does comprise reworked sediment from the underlying Diest, it would be difficult to ascertain which species of the Kasterlee Formation are in situ and which are reworked. A direct comparison of the cysts in these two formations in the Rees borehole exposes some difference in the cyst assemblages. This difference can be explained in part by the reworking of some species, and by environmental exclusion of others. Moving up from the Diest Formation to the Kasterlee Formation, conditions change to be less optimal for some species. This would explain the lack of *Batiacasphaera* species and *Apteodinium* sp. in the Diest, and the presence of *Filisphaera filifera* and *Habibacysta tectata*. Another difference between the two formations is an abrupt rise in concentrations of the acritarch *Cymatiosphaera*? *invaginata*, though the ecological significance of this is unclear. These differences suggest that an in-situ ecological signal has been preserved within the Kasterlee Formation.

4.7 – Merksplas Formation

The presence of dinoflagellate cysts in the Merksplas Formation indicates that at least the interval from 8.70 m to 5.60 m depth consists of marine sediments. *Geonettia waltonensis* and *Capisocysta lyelli* are present throughout the section, and are delicate species that would not easily survive reworking. Their presence points towards the assemblage being in place.

In their study of the Oud-Turnhout well, Louwye et al. (2010) sampled the Brasschaat Member and found it to be barren. With the reclassification of the Brasschaat Member by the National Commission for Stratigraphy Belgium, the Brasschaat Member is incorporated into the

Merksplas Formation where both are present (National Commission for Stratigraphy, Belgium). This would make the Brasschaat Member of the Oud-Turnhout well part of the same Merksplas Formation of the Rees borehole. The productive interval in the Rees Merksplas Formation was found to be about 3.10 metres, between 8.70 and 5.60 m, and all other samples were found to be barren. The cyst concentrations for this interval were also very variable. It is possible that a similar productive interval in the Oud-Turnhout Brasschaat Member could lie in a different section than that sampled by Louwye et al. (2010), possibly higher in the member.

4.8 – Eastern North Sea Basin correlation

Correlation has been attempted between the Rees borehole formations and the eastern North Sea Basin biozonation of Dybkjær and Piasecki (2010), which is based on onshore and offshore data from Denmark. The Upper Miocene formations of the Rees (Diest Formation and Kasterlee Biozone A) correlate well with the eastern North Sea biozonation, which is equivalent to the DN9 zone of de Verteuil and Norris (1996). Correlation with the Pliocene deposits (Poederlee and Merksplas formations) are less straightforward. Age assignment of these formations based on the eastern North Sea biozonation rely mostly on the occurrence of *Melitasphaeridium choanophorum*, which is thought to have a highest occurrence at 3.6 Ma in the North Sea Basin (Dybkjær and Piasecki, 2010). As this is now considered an extant species (Limoges et al., 2013), any past Quaternary records of this species in other areas may have been incorrectly dismissed as reworked. Its occurrence is likely controlled by environmental factors, and as such, its last occurrence in the southern North Sea Basin may be different than in the eastern North Sea Basin, as the eastern North Sea Basin is a different sub basin of the North Sea that existed under different conditions. Correlation between the Pliocene deposits of the Rees borehole and the eastern North Sea Basin biozonation is therefore tentative.

5.0 – Summary and Conclusions

5.1 – Relevance

The dinoflagellate cyst analysis of the Rees borehole based on 58 productive samples has yielded much information on the biostratigraphy and depositional history of the southern North Sea Basin in the Campine area. Although only the upper part of the Diest Formation was penetrated by the Rees borehole, the dinoflagellate cyst record compares well to the upper part of the Diest Formation in other areas. The Poederlee Formation similarly compares closely to the Poederlee Formation seen in the Oud-Turnhout well about 10 km to the north. With respect to these two formations, the Rees borehole fits well within the established regional stratigraphy of the southern North Sea Basin. The continental/estuarine Mol Formation was found to be barren of palynomorphs. The significant differences within the Rees borehole are found in the Kasterlee and Merksplas formations.

The Kasterlee Formation in the Rees borehole has been reported to consist predominantly of reworked material from the underlying Diest Formation (Adriaens, 2016, unpublished thesis). Although accumulations of reworked Diest Formation have been found elsewhere, the Rees borehole appears to contain the thickest section (8 m) yet recorded, effectively comprising the entire Kasterlee Formation. Fobe (1995) suggested that the rivers in the area had eroded the Diest Formation and that it was in relief prior to the deposition of the Kasterlee Formation. Distribution of this eroded sediment must have covered a large portion of the Campine area, given the presence of the reworked Diest in other boreholes in the area. Expansion of river systems and regional subsidence are known to have occurred in the southern North Sea Basin at this time (Gibbard & Lewin, 2016), which would have facilitated erosion and reworking on this scale.

During the Late Pliocene, glaciation was an important factor in the North Sea Basin. At the southern margin, the shore was thought to have been prograding at this time due to increased sedimentation from fluvial input and from uplift of the area (Gibbard & Lewin, 2016). The Campine area would therefore have occupied a marginal setting near the coast, with sedimentation controlled in part by eustasy. The Merksplas Formation has been interpreted as continental to estuarine in nature (National Commission for Stratigraphy Belgium; Buffel et al., 2001), but the presence of in-situ marine dinoflagellate cysts (this study) in the middle of the Merksplas Formation indicates neritic conditions. The Merksplas Formation presumably therefore corresponds to a sea-level high stand during the Late Pliocene. It is not clear how much time is represented by the productive interval within the Merksplas Formation, or whether a single or multiple climate cycles are involved. Nor is it possible to elucidate the depositional environment before or after the establishment of marine conditions because the remainder of the Merksplas Formation is barren of palynomorphs. However, it is likely that such conditions were largely restricted to the productive interval, given the palynological indications of increasing and then decreasing distality, and the fact that the productive interval is bounded by coarser grained, white quartz sand indicating higher energy depositional environments.

5.1 – Summary

Samples from the Rees borehole of the Campine area were analysed for dinoflagellate cysts, in order to understand more fully the biostratigraphy and paleoecology of the Diest, Kasterlee, Poederlee, Mol and Merksplas formations. In particular, dinoflagellate cyst analysis was used to investigate the anomalous nature of the Kasterlee Formation in the Rees borehole. The Mol

Formation was found to be barren of palynomorphs, likely due to it being a coarse grained continental deposit. Otherwise, the dinoflagellate cyst associations reflect fluctuating environments within a temperate to warm climatic setting in a variably restricted marine basin.

The dinoflagellate cyst record of the Diest Formation compare well to those of the upper Diest Formation found in other areas, namely in the Kalmthout (Louwye & Laga, 1998), Mol, Retie and Poederlee wells (Louwye et al., 1999). The assemblages represent a warm-water, shallow marine, nearshore environment of late Tortonian age in the Rees borehole.

The Kasterlee Formation of the Rees borehole can be divided into two informal dinoflagellate cyst assemblage biozones. Kasterlee Biozone A is distinctly different from Kasterlee Formation assemblages seen in other locations, lacking key species normally found in the Kasterlee, especially at the boundary with the Diest Formation. This biozone ostensibly appears to represent a temperate to warm-water, shallow marine environment, where distality shifts back and forth. A late Tortonian age is indicated. Kasterlee Biozone B displays some similarity with the Kasterlee Formation seen in the Oud-Turnhout well (Louwye & De Schepper, 2010) but lacks key species used to date this formation at Oud-Turnhout. The assemblages characterising Biozone B point towards a temperate, increasingly restricted, shallowing upwards, neritic environment, with a late Tortonian to early Zanclean age. This is consistent with Late Miocene age assignments for the Kasterlee Formation as reported in other boreholes in the southern North Sea Basin.

It has been suggested that the Kasterlee Formation in the Rees borehole consists of reworked underlying Diest sediment, based on the clay and glauconite composition. This is a plausible explanation, at least for Kasterlee Biozone A. Although Biozone B displays some similarity with the Kasterlee of the Oud-Turnhout well, its lack of key species and difference in mineralogy also suggest a reworked Diest component. It isn't completely clear which cysts are reworked and which are in situ, however, as there are cyst species present in the Kasterlee Formation that are not in the Diest. Moreover, the cyst record through the Kasterlee Formation is not homogenous, but appears to show stratigraphic trends, and of course there is a clear separation between Biozones A and B. This all suggests that in spite of sedimentological evidence for reworking, and clear discrepancies in the dinoflagellate cyst record, a primary signal of environmental change has been preserved in the Kasterlee Formation of the Rees borehole. Nonetheless, the scale of Diest reworking in the Rees borehole, up to 8 m in thickness, is unusual for the this part of the Campine area. Additional data, such as a seismic section, would be needed to determine whether this is a very localized or more widespread accumulation.

The Poederlee Formation dinoflagellate cyst assemblages compare well to those reported from the Oud-Turnhout well (Louwye & De Schepper, 2010). A warm-water, shallow marine, shallowing upwards environment is represented, that is between 3.7 and 2.7 Ma in age (latest Zanclean–late Piacenzian; mid- to late Pliocene).

Samples from the Mol Formation were found to be completely barren of palynomorphs. Marine palynomorphs were not particularly expected, given the continental to estuarine nature of the deposit (National Commission for Stratigraphy Belgium). The absence of terrestrial palynomorphs probably reflects the coarse grain size, reflecting a high-energy depositional environment and attendant winnowing, and postdepositional circulation of water causing enhanced oxidation. No biostratigraphic age could therefore be suggested for the Mol Formation.

Dinoflagellate cysts have been recorded from the Merksplas Formation for the first time. This formation was previously considered to be estuarine (National Commission for Stratigraphy Belgium; Buffel et al., 2001). The productive interval was found to be at about 3.10 m. The presence of delicate cysts, namely *Capisocysta lyellii* and *Geonettia waltonensis*, and a distinctive cyst association dominated by *Heteraulacacysta* sp. A of Costa & Downie (1979) and accompanying *Capisocysta lyelii*, all imply that these dinoflagellate cysts are in place. This interval is clearly marine, indicating a warm-water, restricted, lagoonal environment that is between 3.7 Ma and 2.7 Ma in age. The presence of marine cysts indicates an undocumented, short-lived transgression. In-depth palynological analysis has not been conducted on the Merksplas Formation in other areas, but a productive interval with similar cyst association has been recorded from the Merksem Sands (Lillo Formation) in the Antwerp area, which is of similar age (De Schepper et al., 2009).

The Upper Miocene Rees formations correlate well with the eastern North Sea Basin biozonation of Dybkjær and Piasecki (2010), which is based on data from onshore and offshore Denmark. Correlation of Pliocene formations is tentative, however, as the key event in the correlation is the highest occurrence of *Melitasphaeridium choanophorum*. This species is now known to be extant, and occurs in the present day Gulf of Mexico (Limoges et al., 2013). It is no longer possible to dismiss specimens recorded in the Quaternary as reworked. The disappearance of this species in the North Sea Basin is likely due to environmental factors, and as such, its range top may not be a reliable indicator of age. While it is important to consider the full extent of the North Sea basin, nearshore sedimentary facies show strong lateral variability and discontinuity. As such, long-distance correlation within the North Sea Basin is challenging, with difficulties reflecting the complex development of the basin and its restricted marine nature.

The analysis of the Rees borehole represents a continuation of the ongoing process of understanding the Neogene stratigraphy and paleoenvironments of Belgium, and their basin-wide relevance. New information gathered in the present study offers a more detailed understanding both of the complex development of the North Sea Basin, and the paleoecology of cyst-forming dinoflagellates living along the southern margin of this restricted marine basin.

References

Balson, P., Butcher, A., Holmes, R., Johnson, H., Lewis, M., & Musson, R. (2002). *North Sea Geology*. British Geological Survey.

Bogemans, F. (1999). The Campine clays and sands in northern Belgium: a depositional model related to sea level fluctuations. *Contr. Tert. Quatern. Geol.*, *36*(1-4), 59–72.

Brinkhuis, H., & Schiøler, P. (1996). Palynology of the Geulhemmerberg Cretaceous/Tertiary boundary section (Limburg, SE Netherlands). In J. Brinkhuis (Ed.), *Palynology of the Geulhemmerberg Cretaceous/Tertiary boundary section (Limburg, SE Netherlands)* (pp. 193–213). Geologie en Munbouw.

Buffel, P., Vandenberghe, N., & Laga, P. (2001). The Pliocene sediments in 4 boreholes in the Turnhout area (North-Belgium): the relationship with the Lillo and Mol Formations. *Aardkundige Mededelingen*, *11*, 1–9.

Dale, B. (1996). Dinoflagellate cyst ecology: modeling and geological applications. In J. Jansonius, & D. C. McGregor (Eds.), *Palynology: Principles and Applications* (Vol. 3, pp. 1249–1275). Dallas, TX: American Association of Stratigraphic Palynologists Foundation.

Dale, B., & Dale, A. (2002). Application of ecologically based statistical treatments to micropaplaeontology. In S. Haslett (Ed.), *Quaternary Environmental Micropalaeontology* (pp. 259–286). London: Edward Arnold.

De Heinzelin, J. (1955). Considerations nouvelles sur le Neogene de l'Ouest de l'Europe. *Bulletin de la Societe belge de Geologie, de Paleontologie et d'Hydrologie, 64*(3), 463–476.

De Meuter, F., & Laga, P. (1976). Lithostratigraphy and biostratigraphy based on benthic Foraminifera of the Neogene deposits of northern Belgium. *Bulletin Belgische Vereniging voor Geologie*, *85*(4), 133–152.

De Schepper, S., Fischer, E. I., Groeneveld, J., Head, M. J., & Matthiessen, J. (2011). Deciphering the palaeoecology of Late Pliocene and Early Pleistocene dinoflagellate cysts. *Palaeogeography, Palaeoclimatology, Palaeoecology, 309*, 17–32.

De Schepper, S., Head, M. J., & Louwye, S. (2004). New dinoflagellate cyst and incertae sedis taxa from the Pliocene of northern Belgium, southern North Sea Basin. *Journal of Paleontology*, *78*(4), 635–644.

De Schepper, S., Head, M. J., & Louwye, S. (2009). Pliocene dinoflagellate cyst stratigraphy, palaeoecology and sequence stratigraphy of the Tunnel-Canal Dock, Belgium. *Geological Magazine, 146*(1), 92–112.

De Verteuil, L., & Norris, G. (1996). Miocene dinoflagellate stratigraphy and systematics of Maryland and Virginia. *Micropaleontology, 42*, 1–172.

Doppert, J. W., Laga, P. G., & De Meuter, F. J. (1979). Correlation of the biostratigraphy of marine Neogene deposits, based on benthonic Foraminifera, established in Belgium and The Netherlands. *Mededelingen Rijks Geologische Dienst, 31*, 1–8.

Dumont, A. (1839). Rapport sur les travaux de la Carte geologique. *Bulletin de l'Academie Royale de Belgique, 6*(2), 479–481.

Dybkjær, K., & Piasecki, S. (2010). Neogene dinocyst zonation for the eastern North Sea Basin, Denmark. *Review of Palaeobotany and Palynology* 161, 1–29.

Edwards, L. E., Barron, J. A., Bukry, D., Bybell, L. M., Cronin, T. M., Poag, C. W., . . . Wingard, G. L. (2016). Paleontology of the Upper Eocene to Quaternary Postimpact Section in the USGS–NASA Langley Core, Hampton, Virginia. U.S. Geological Survey.

Fobe, B. (1995). Litologie en litostratigrafie van de Formatie van Kasterlee (Plioceen van de Kempen). *Natuurwetenschappelijk Tijdschri, 75*, 35–45.

Gibbard, P. L., & Lewin, J. (2016). Filling the North Sea Basin: Cenozoic sediment sources and river styles. *Geologica Belgica, 19*.

Gilbert, M., & De Heinzelin, J. (1955). La faune et l'age Miocene Superieur des Sables de Deurne. *Bulletin de l'Institut royal des Sciences naturelles de Belgique, XXXI*(71), 1–27.

Glennie, K. W. (1998). *Petroleum Geology of the North Sea: Basic Concepts and Recent Advances.* Blackwell Science.

Graham, A. G., Stoker, M. S., Lonergan, L., Bradwell, T., & Stewart, M. A. (2010). The Pleistocene Glaciations of the North Sea basin. In J. Ehlers, & P. L. Gibbard (Eds.), *Quaternary Glaciations – Extent and Chronology.* Elsevier.

Gulinck, M. (1962). Essaie d'une carte geologique de la Campine. Etat de nos connaissances sur la nature des terrains neogenes recoupes par sondages. *Memoires de la Societe belge de Geologie, Paleontologie et Hydrologie, 6*, 30–36.

Gulinck, M. (1963). Symposium sur la Stratigraphie du Neogene nordique, Gand 1961. Essai d'une carte geologique de la Campine. Etat de nos connaissances sur la nature des terrains neogenes recoupes par sondages. *Memoires de la Societe belge de Geologie, 6*, 30–39.

Halet, F. (1935). Nouvelles observations sur la stratigraphie du Bolderberg. *Bulletin de la Societe Geologique de la Belgique, XLV*, 94–103.

Hardenbol, J., Thierry, J., Farley, M. B., Jacquin, T., De Graciansky, P. C., & Vail, P. R. (1998). Mesozoic and Cenozoic sequence chronostratigraphic framework of European basins. *Mesozoic and Cenozoic Sequence Stratigraphy of European Basins, Special Publication*(60), 3–29.

Head, M. J. (1996b). Late Cenozoic dinoflagellates from the Royal Society borehole at Ludham, Norfolk, eastern England. *Journal of Paleontology, 70*(4), 543–570.

Head, M. J. (1998). New Goniodomacean Dinoflagellates with a Compound Hypotractal Archeopyle from the Late Cenozoic: *Capisocysta Warny* and Wrenn, Emend. *Journal of Paleontology*, *72*(5), 797–809.

Head, M. J. (2000). *Geonettia waltonensis*, a new Goniodomacean dinoflagellate from the Pliocene of the North Atlantic region, and its evolutionary implications. *Journal of Paleontology*, *74*(5), 812–827.

Head, M. J. (2007). Last Interglacial (Eemian) hydrographic conditions in the southwestern Baltic Sea based on dinoflagellate cysts from Ristinge Klint, Denmark. *Geological Magazine*, *144*(6), 987–1013.

Head, M. J., Seidenkrantz, M. S., Janczyk-Kopikowa, Z., Marks, L., & Gibbard, {. L. (2005). Last Interglacial (Eemian) hydrographic conditions in the southeastern Baltic Sea, NE Europe, based on dinoflagellate cysts. *Quaternary International*, *130*, 3–30.

Hennissen, J. A., Head, M. J., De Schepper, S., & Groenevel, J. (2014). Palynological evidence for a southward shift of the North Atlantic Current at ~2.6 Ma during the intensification of late Cenozoic Northern Hemisphere glaciation. *Paleoceanography*, *29*(6).

Hennissen, J. A., Head, M. J., De Schepper, S., & Groeneveld, J. (2017). Dinoflagellate cyst paleoecology during the Pliocene–Pleistocene climatic transition in the North Atlantic. *Palaeogeography, Palaeoclimatology, Palaeoecology*, *470*, 81–108.

Hooeyberghs, H. (1996). Planktonic foraminifera from the Zonderschot Sands, Member of the Berchem Formation (Miocene) at Zonderschot, Belgium. *Tertiary Research*, *17*, 15–25.

Jarsve, E. M. (2014). *Mesozoic and Cenozoic basin development and sediment infill in the North Sea region – shifting depocenters associated with regional structural development.* Oslo: Faculty of Mathematics and Natural Sciences, University of Oslo.

Krebs, C. J. (1998). *Ecological Methodology* (2nd ed.). Menlo Park, USA, CA: Benjamin-Cummings.

Laga, P., & De Meuter, F. J. (1972). A foraminiferal fauna found in the lower member of the Diest Formation of borings of the Antwerp Kempen. *Bull. Soc. Belge Géol., Pal. Hydrol.*, *81*, 211–220.

Limoges, A., Londeix, L., & de Vernal, A. (2013). Organic-walled dinoflagellate cyst distribution in the Gulf of Mexico. *Marine Micropaleontology*, *102*, 51–68.

Louwye, S. (2002). Dinoflagellate cyst biostratigraphy of the Upper Miocene Deurne Sands (Diest Formation) of northern Belgium, southern North Sea Basin. *Geological Journal*, *37*, 55–67.

Louwye, S., & De Schepper, S. (2010). The Miocene–Pliocene hiatus in the southern North Sea Basin (northern Belgium) revealed by dinoflagellate cysts. *Geological Magazine, 147*(5), 760–776.

Louwye, S., & Laga, P. (1998). Dinoflagellate cysts of the shallow marine Neogene succession in the Kalmthout well, northern Belgium. *Bulletin of the Geological Society of Denmark, 45,* 73–86.

Louwye, S., & Laga, P. (2008). Dinoflagellate cyst stratigraphy and palaeoenvironment of the marginal marine Middle and Upper Miocene of the eastern Campine area, northern Belgium (southern North Sea Basin). *Geological Journal, 43,* 75–94.

Louwye, S., De Coninck, J., & Verniers, J. (1999). Dinoflagellate cyst stratigraphy and depositional history of Miocene and Lower Pliocene formations in northern Belhium (southern North Sea Basin). *Geologie en Mijnbouw, 78,* 31–46.

Louwye, S., De Coninck, J., & Verniers, J. (2000). Shallow marine Lower and Middle Miocene deposits at the southern margin of the North Sea Basin (northern Belgium): dinoflagellate cyst biostratigraphy and depositional history. *Geological Magazine*, *137*(4), 381–394.

Louwye, S., De Schepper, S., Laga, P., & Vandenberghe, N. (2007). The Upper Miocene of the southern North Sea Basin (northern Belgium): a palaeoenvironmental and stratigraphical reconstruction using dinoflagellate cysts. *Geological Magazine, 144*(1), 33–52.

Louwye, S., Foubert, A., Mertens, K., Van Rooij, D., & The IODP Expedition 307 Scientific Party. (2008). Integrated stratigraphy and palaeoecology of the Lower and Middle Miocene of the Porcupine Basin. *Geol. Mag., 145*(3), 321–344.

Louwye, S., Head, M. J., & De Schepper, S. (2004). Dinoflagellate cyst stratigraphy and palaeoecology of the Pliocene in northern Belgium, southern North Sea Basin. *Geol. Mag., 141*(3), 353–378.

Magurran, A. (2004). *Measuring biological diversity.* Oxford, UK: Blackwell Publishing.

Maher, L. J. (1981). Statistics for microfossil concentration measurements emplying samples spiked with marker grains. *Review of Palaeobotany and Palynology, 32*, 153–191.

Matsuoka, K., & Head, M. J. (1992). Taxonomic revision of the Neogene marine palynomorphs Cyclopsiella granosa (Matsuoka) and Batiacasphaera minuta (Matsuoka) and a new species of Pyxidinopsis Habib (Dinophyceae) from the Miocene of the Labrador Sea. *Neogene and Quaternary Dinoflagellate Cysts and Acritarchs*, 165–180.

McCarthy, F. M., Katz, M. E., Kotthoff, U., Browning, J. V., Miller, K. G., Zanatta, R., . . . Mountain, G. S. (2013). Sea-level control of New Jersey margin architecture: Palynological evidence from Integrated Ocean Drilling Program Expedition 313. *Geosphere, 9*(6), 1457-1487.

Mourlon, M. (1882). *Memoires sur les terrains Cretaces et Tertiaire prepares par feu Andre Dumont, IV*(Bruxelles, 702 pp).

Mourlon, M. (1896). Les mers quaternaires en Belgique d'apres l'etude stratigraphique des depots flandriens et campiniens et leurs relations avec les couches tertiaires pliocenes. *Bull. Acad. Roy. Belg., 32*(3), 671-711.

Nadin, P. A., & Kusznir, N. J. (1995). Palaeocene uplift and Eocene subsidence in the northern North Sea Basin from 2D forward and reverse stratigraphic modelling. *Journal of the Geological Society, 152*, 833-848.

NGSB. (n.d.). *National Commission for Stratigraphy Belgium – 2.10 Merksplas Formation*. (F. Bogemans, & T. Lanckacker, Editors) Retrieved August 2016, from http://ncs.drupalgardens.com/paleogene-neogene/210-merksplas-formation

NGSB. (n.d.). *National Commission for Stratigraphy Belgium – 2.8 Mol Formation*. Retrieved August 2016, from http://ncs.drupalgardens.com/paleogene-neogene/28-mol-formation-ml

Nuyts, H. (1990). Note on the biostratigraphy (benthic foraminifera) and lithostratigraphy of Pliocene deposits at Kallo (Oost-Vlaanderen, Belgium). *Contributions Tertiary and Quaternary Geology, 27*, 17-24.

Piasecki, S., Gregersen, U., & Johannessen, P. N. (2002). Lower Pliocene dinoflagellate cysts from cored Utsira Formation in the Viking Graben, northern North Sea. *Marine Petroleum Geology, 19,* 55-67.

Quaijtaal, W., Donders, T. H., Persico, D., & Louwye, S. (2014). Characterising the middle Miocene Mi-events in the Eastern North Atlantic realm: A first high-resolution marine palynological record from the Porcupine Basin. *Palaeogeography, Palaeoclimatology, Palaeoecology, 399*, 140-159.

Scalter, J. G., & Christie, P. A. (1980). Continental stretching: An explanation of the Post-Mid-Cretaceous subsidence of the central North Sea Basin. *Journal of Geophysical Research, 85*(87), 3711–3739 .

Schreck, M., Meheust, M., Stein, R., & Matthiessen, J. (2013). Response of marine palynomorphs to Neogene climate cooling in the Iceland Sea (ODP Hole 907A). *Marine Micropaleontology, 101*, 49-67.

Soliman, A., Coric, S., Head, M. J., Piller, W., & El Beialy, S. Y. (2012). Lower and Middle Miocene biostratigraphy, Gulf of Suez, Egypt, based on dinoflagellate cysts and calcareous nannofossils. *Palynology, 36*(1), 1-42.

Tavernier, R., & De Heinzelin, J. (1962). Introduction au Neogene de la Belgique. *Memoires de la Societe belge de Gelogie, Paleontologie et Hydrologie, 6*, 7-28.

Thomas, D. J., & Via, R. K. (2007). Neogene evolution of Atlantic thermohaline circulation: Perspective from Walvis Ridge, southeastern Atlantic Ocean. *Paleoceanography, 22*.

Van Ertborn, O. (1902). Un desideratum stratigraphique au sujet des couches de Lenham par rapport au Pliocene belge. *Bulletin de la Societe belge de Geologie, 16*, 160-161.

Vanden Broeck, E. (1882). Diestien, Casterlien et Scaldisien. *Societe malacologique de Belgique, 17*, 103-108.

Vanden Broeck, E. (1902). Le Diestien et les sables de Lenham, le Mioc`ene d´emantel´e et les Box Stones en Angleterre. *Bulletin de la Societe belge de Geologie, 16*, 170-173.

Vandenberghe, N., Laga, P., Steurbaut, E., Hardenbol, J., & Vail, P. R. (1998). Tertiary sequence stratigraphy at the southern border of the North Sea Basin in Belgium. *Mesozoic and Cenozoic Sequence Stratigraphy of European Basins, Society for Sedimentary Geology (SEPM) Special Publication no. 60*, 119-154.

Vandenberghe, N., Van Simaey, S., Steurbaut, E., Jagt, J. W., & Felder, P. J. (2004). Stratigraphic architecture of the Upper Cretaceous and Cenozoic along the southern border of the North Sea Basin in Belgium. *Netherlands Journal of Geosciences, 83*(3), 155-171.

Verhoeven, K., & Louwye, S. (2013). Palaeoenvironmental reconstruction and biostratigraphy with marine palynomorphs of the Plio–Pleistocene in Tjörnes, Northern Iceland. *Palaeogeography, Palaeoclimatology, Palaeoecology, 376*, 224-243.

Versteegh, G. J. (1994). Recognition of cyclic and non-cyclic environmental changes in the Mediterranean Pliocene: A palynological approach. *Marine Micropaleontology 23, 23*, 147-183.

Warny, S. A., & Wrenn, J. H. (2002). Upper Neogene dinoflagellate cyst ecostratigraphy of the Atlantic coast of Morocco. *Micropaleontology, 48*(3), 257-272.

Williams, G. L., Brinkhuis, H., Pearce, M. A., Fensome, R. A., & Weegink, J. W. (2004). Southern Ocean and glocal dinoflagellate cyst events compared. Index events for the Late Cretaceous-Neogene. *Proceedings of the Ocean Drilling Program, Scientific Results, vol. 189, eds N. F. Exon, J.P. Kennett & M.J. Malone*, 1-98.

Williams, G. L., Fensome, R. A., & MacRae, R. A. (2017). The Lentin and Williams Index of Fossil Dinoflagellate 2017 Edition. In *AASP Contributions Series Number 48.*

Wouters, L., & Vandenberghe, N. (1994). Geologie van de Kampen - Niras, Brussels.

Zachos, J. C., Dickens, G. R., & Zeebe, R. E. (2008). An early Cenozoic perspective on greenhouse warming and carbon-cycle dynamics. *Nature, 451*, 279-283.

Zachos, J., Pagani, M., Sloan, L., Ellen, T., & Billups, K. (2001). Trends, Rhythms, and Aberrations in Global Climate 65 Ma to Present. *Science, 292*, 686-693.

Ziegler, P. A. (1975). The Geological Evolution of the North Sea Area in the Tectonic Framework of North Western Europe. *Norges Geologiske Undersokelse, 316*(1-27).

Ziegler, P. A. (1978). North-Western Europe: Tectonics and Basin Development. *Geologie en Mijnbouw, 57*(4).

Zonneveld, K. A., Marret, F., Versteegh, G., Bogus, K., Bonnet, S., Bouimetarhan, I., . . . Young, M. (2013). Atlas of modern dinoflagellate cyst distribution based on 2405 data points. *Review of Palaeobotany and Palynology*, *191*, 1-197.

Zonneveld, K. A., Versteegh, G. J., & de Lange, G. J. (1997). Preservation of organic-walled dinoflagellate cysts in different oxygen regimes: a 10,000 year natural experiment. *Marine Micropaleontology*, *29*(3-4), 393-405.

Appendix I – Species List

The following is a list of all taxa recorded from the Rees borehole in the present study. Authorial citations of dinoflagellate cysts follow the Lentin and Williams Index of Fossil Dinoflagellates 2017 edition (Williams et al., 2017).

In-situ dinoflagellate cysts

Achomosphaera andalousiensis subsp. *andalousiensis* Jan du Chêne, 1977

Achomosphaera andalousiensis subsp. *suttonensis* Head, 1997

Achomosphaera sp. 1

Amiculosphaera umbraculum Harland, 1979

Apteodinium sp.

Ataxiodinum choane Reid, 1974

Ataxiodinum zevenboomii Head, 1997

Barssidinium graminosum Lentin et al., 1994

Barssidinium pliocenicum Head, 1993

Batiacasphaera sp. cf. *B. minuta* (Matsuoka, 1983) Matsuoka and Head, 1992

Batiacasphaera micropapillata Stover, 1977

Batiacasphaera sphaerica Stover, 1977

Bitectatodinium sp. cf. *B. raedwaldii* Head, 1997

Bitectatodinium sp.

Bitectatodinium tepikiense? Wilson, 1973

Brigantedinium cariacoense (Wall, 1967) Lentin and Williams, 1993

Brigantedinium sp.

Capisocysta lyellii Head, 1998

Corrudinium? sp.

Dapsilidinium pastielsii Bujak et al., 1980

Desotodinium wrennii De Schepper et al., 2004

Dinocyst sp. 1

Dinocyst sp. 2

Filisphaera filifera Bujak, 1984

Filisphaera microornata (Head et al., 1989) Head, 1994

Gen. et sp. indet. A

Geonettia waltonensis Head, 2000

Gramocysta verricula (Piasecki, 1980) Lund and Lund-Christensen in Daniels et al., 1990

Habibacysta tectata Head et al., 1989

Heteraulacacysta sp. A of Costa and Downie, 1979

Homotryblium sp.

Hystrichokolpoma rigaudiae Deflandre and Cookson, 1955

Hystrichosphaeropsis obscura Habib, 1972

Hystrichosphaeropsis obscura?

Hystrichosphaeropsis sp.

Invertocysta lacrymosa Edwards, 1984

cf. *Labyrinthodinium truncatum* subsp. *truncatum* Piasecki, 1980

Lejunecysta sp.

Lingulodinium machaerophorum (Deflandre and Cookson, 1955) Wall, 1967

Lingulodinium multivirgatum de Verteuil and Norris, 1996

Lingulodinium sp.

Medicodinium sp.

Melitasphaeridium choanophorum (Deflandre and Cookson, 1955) Harland and Hill, 1979

Nematosphaeropsis labyrinthus (Ostenfeld, 1903) Reid, 1974

Operculodinium centrocarpum (Deflandre and Cookson, 1955) Wall, 1967

Operculodinium sp. cf. *O. piaseckii* Strauss and Lund, 1992

Operculodinium israelianum (Rossignol, 1962) Wall, 1967

Operculodinium tegillatum Head, 1997

Operculodinium? *eirikianum* Head et al., 1989

Piccoladinium sp.

Piccoladinium sp.?

Polysphaeridium zoharyi (Rossignol, 1962) Bujak et al., 1980

Cyst of *Protoceratium reticulatum* (Claparède and Lachmann, 1859) Bütschli, 1885

Pyxidinopsis sp. cf. *P. braboi* De Schepper et al., 2004

Pyxidinopsis sp.

Pyxidinopsis? sp.

Reticulatosphaera actinocoronata (Benedek, 1972) Bujak and Matsuoka, 1986

Selenopemphix armageddonensis de Verteuil and Norris, 1992

Selenopemphix brevispinosa Head et al., 1989

Selenopemphix dionaeacysta Head et al., 1989

Selenopemphix nephroides Benedek, 1972

Selenopemphix quanta (Bradford, 1975) Matsuoka, 1985

Selenopemphix sp.

Spiniferites falcipedius Warny and Wrenn, 1997

Spiniferites mirabilis (Rossignol, 1964) Sarjeant, 1970

Spiniferites sp. 1

Spiniferites / Achomosphaera spp. indet.

Tectatodinium pellitum Wall, 1967

Tectatodinium sp.

Trinovantedinium ferugnomatum de Verteuil and Norris, 1992

Trinovantedinium glorianum (Head et al., 1989) de Verteuil and Norris, 1992

Trinovantedinium sp.

Trinovantedinium variabile (Bujak, 1984) de Verteuil and Norris, 1992

Tuberculodinium vancampoae (Rossignol, 1962) Wall, 1967

Reworked dinoflagellate cysts

Cleistosphaeridium sp.

Cordosphaeridium inodes (Klumpp, 1953) Eisenack, 1963

Cordosphaeridium sp. cf. *C. inodes* (Klumpp, 1953) Eisenack, 1963

Cordosphaeridium sp.

Glaphyrocysta sp.

Acritarchs

Acritarch sp. 1

Acritarch sp. 2

Acritarch sp. 3

Acritarch sp. 4

Cyclopsiella sp.

Cymatiosphaera sp.

Cymatiosphaera? *invaginata* Head et al., 1989

Halodinium sp.

Lavradosphaera sp.

Nanobarbophora walldalei Head, 1998

Paralecaniella indentata (Deflandre and Cookson, 1955) Fensome et al., 1990

Quadrina? *Condita* de Verteuil and Norris, 1992

Green Algae

Botryococcus sp.

Gelasinicysta vangeelii Head, 1992

Pediastrum spp. indet.

Sigmopollis sp.

Tasmanites sp.

Appendix II – Taxonomy

The following is a list with brief descriptions of selected dinoflagellate cyst and acritarch taxa that were encountered but inconclusively identified in the present study.

Dinoflagellate cyst species:

Batiacasphaera cf. *minuta*

Plate 2, Figures 1, 2

Cysts are proximate, small and spherical. Central body diameter 25–30 µm, (3 specimens measured). Surface is distinctly microreticulate, although reticulation is incomplete. Archeopyle is apical, but principal suture less angular than normally seen in *Batiacasphaera minuta*. The incomplete microreticulation distinguishes specimens from *Batiacasphaera minuta.*

Bitectatodinium cf. *raedwaldii*

Plate 2, Figures 7–9

Cysts are originally proximate and spherical. Central body diameter 30–38 µm, including luxuria (6 specimens measured). Granular surface appearance results from short pilli that arise from the pedium and fuse distally to form luxuria. Similar specimens with short pilli were included in *Bitectatodinium raedwaldii* by Head (1997) but are treated separately in the present study. The holotype, from the lower Pliocene of eastern England, has long pilli that fuse distally to form ropey ridges that drape over the surface of the luxuria (Head, 1997).

Corrudinium sp.

Plate 2, Figures 14–16

Cysts are proximate and spherical to subspherical. Central body diameter 36–40 µm, including luxuria (3 specimens measured). Precingular archeopyle with sharp angles. Surface distinctly microreticulate. Wall thickness including ornament around 2 µm.

Dinocyst sp. 1

Plate 3, Figure 1

Cysts are proximate and spherical to subspherical, although usually crumpled. Central body diameter 38–42 µm (3 specimens measured). Smooth surface, light brown color.

Dinocyst sp. 2

Plate 3, Figure 2

Cysts are proximate, spherical to subspherical, though usually crumpled. Central body diameter 47–55 µm (3 specimens measured). Smooth surface, dark brown color. Some specimens appear to show broken plates.

Hystrichosphaeropsis obscura?

Plate 3, Figure 11

Cysts bicavate, with subspherical to ovoid central body. Central body diameter 58 µm (2 specimens measured). Specimens are possibly damaged individuals of *H. obcura*, as appearance is very similar, although the epitract and hypotract are usually damaged or compressed, and no archeopyle is visible.

cf. *Labyrinthodinium truncatum* subsp. *truncatum*

Plate 3, Figures 14–16

Cysts very small, spherical, and proximochorate. Central body diameter 15–18 µm (3 specimens measured). Processes are of variable thickness, and expand distally to form the appearance of a thin, incomplete outer wall. Similar to *Labyrinthodinium truncatum truncatum* as seen in the southern North Sea Basin (Louwye, et al., 2007; Figure 7, a–c), although considerably smaller. Type specimens from the Middle Miocene of the Gram borehole of Denmark have a central body diameter of 23 (29) 40 µm, based on 30 specimens (Piasecki, 1980). The small size of the Rees borehole specimens and uncertain nature of the archeopyle (or pylome?) account for the tentative assignment.

Pyxidinopsis cf. *braboi*

Plate 5, Figures 1–3

Cysts are spherical and proximate. Central body diameter 32–38 µm (3 specimens measured). Distinctly microreticulate surface. Archeopyle is precingular, with a distinctive re-entrant on left adapical margin (side 1 of de Verteuil and Norris, 1996) of the 3” plate. Very similar to *Pyxidinopsis braboi* from the Pliocene of Belgium (De Schepper et al., 2008) except the microreticulation is less complete.

Pyxidinopsis sp.

Plate 5, Figures 4–6

Cysts are spherical and proximate. Central body diameter 25–30 µm (3 specimens measured). Finely microreticulate surface. Archeopyle is precingular with sharp angles.

Pyxidinopsis? sp.

Plate 5, Figures 7, 8

Cysts are small and proximate. Central body diameter 20–22 µm (2 specimens measured). Very pronounced reticulation. Always crumpled, and no archeopyle recognised.

Spiniferites sp. 1

Plate 6, Figures 1–3

Cysts are ovoid spiniferate cysts, with distinctly granular surface. Central body diameter 45–60 µm (8 specimens measured). Tabulation expressed by crests that are more pronounced in large specimens, and sometimes not seen in smaller specimens. Processes are gonal, with wide and hollow bases, with usually trifurcate endings that are much more pronounced and long in larger specimens. Secondary bifurcation is usually present, and also longer in larger specimens. Species seemingly restricted to the Pliocene of the Rees borehole.

Tectatodinium? sp.

Plate 6, Figures 4–7

Cysts spherical to subspherical, proximate and with a granular surface. Central body diameter 44–48 µm including luxuria (2 specimens measured). Walls are spongey, with a thickness is about 1.5-2 um. Archeopyle is precingular. A distinctive apical protrusion is always present. May be part of the *Tectatodinium* genus, but distally open luxuria is not clear.

Acritarch species:

Acritarch sp. 1

Plate 7, Figures 1, 2

Central body is spherical with a distinctly tectate wall. Central body diameter 15–35 µm (9 specimens measured). Always dark brown in colour. No evidence of tabulation or definitive archeopyle. Specimens are seemingly confined to the Miocene of the Rees borehole.

Acritarch sp. 2

Plate 7, Figures 3, 4

Irregularly shaped and small body. Maximum diameter 17-21 µm (5 measured specimens). Distinct horn-shaped, irregular protrusions all over body, with irregular striations that don't appear to follow any tabulation. No archeopyle evident.

Acritarch sp. 3

Plate 7, Figure 5

Small central body with relatively regular outer wall that links to central body through invaginations. Central body diameter 10–17 µm excluding outer wall (6 specimens measured). When examining a specimen through cross section, there are usually five invaginations, and outer walls may have points at their highest points.

Acritarch sp. 4

Plate 7, Figures 6, 7

Small central body with very thin, irregular, solid processes. Central body diameter 13–18 µm (4 specimens measured). Similar to *Pentapharsodinium dalei*, but specimens always have some processes with bi- or trifurcate endings.

Appendix III – Photoplates

Slide number and England Finder (in parentheses) coordinates given sequentially for each specimen. CBD = maximum central body diameter. MD = maximum diameter. WT = wall thickness.

Plate 1:
Figures 1,2. *Achomosphaera andalousiensis andalousiensis*. Ventral view (1) at upper focus, and (2) at mid-focus; note large fenestrations on distal platforms of processes; CBD = 39 µm. Sample 568 (R27/0).

Figures 3,4. *Achomosphaera andalousiensis suttonensis*. Right lateral view (3) at upper focus, and (4) at mid-focus; note finer and greater number fenestrations on distal platforms of processes; CBD = 42 µm. Sample 1160 (A49/4).

Figures 5, 6. *Achomosphaera* sp. 1. Orientation uncertain (5) at upper focus, and (6) at mid-focus; note thick, hollow, branching processes; CBD = 83 µm. Sample 1160 (V42/0).

Figure 7. *Amiculosphaera umbraculum*. Dorsal surface (7) at upper mid-focus; CBD = 40 µm. Sample 1159 (A39/2).

Figures 8 – 10. *Apteodinium* sp. Orientation uncertain (8) at upper focus, (9) at mid-focus, and (10) at lower focus; note thick, spongy wall and granular surface appearance; CBD = 61 µm, WT = 3 µm. Sample 531 (J19/0).

Figure 11, 12. *Ataxiodinium choane*. Antapical view (11) of antapical surface, and (12) at lower mid-focus; CBD = 31 µm. Sample 568 (F29/2).

Figure 13, 14. *Ataxiodinium zevenboomii*. Left lateral view (13) at upper focus, and (14) at mid-focus; CBD = 30 µm. Sample 924 (Q53/0).

Figure 15, 16. *Barssidinium graminosum*. Orientation uncertain (15) of mid-focus, and (16) of lower focus; note constrictions within long processes; CBD = 36 µm. Sample 568 (K56/2).

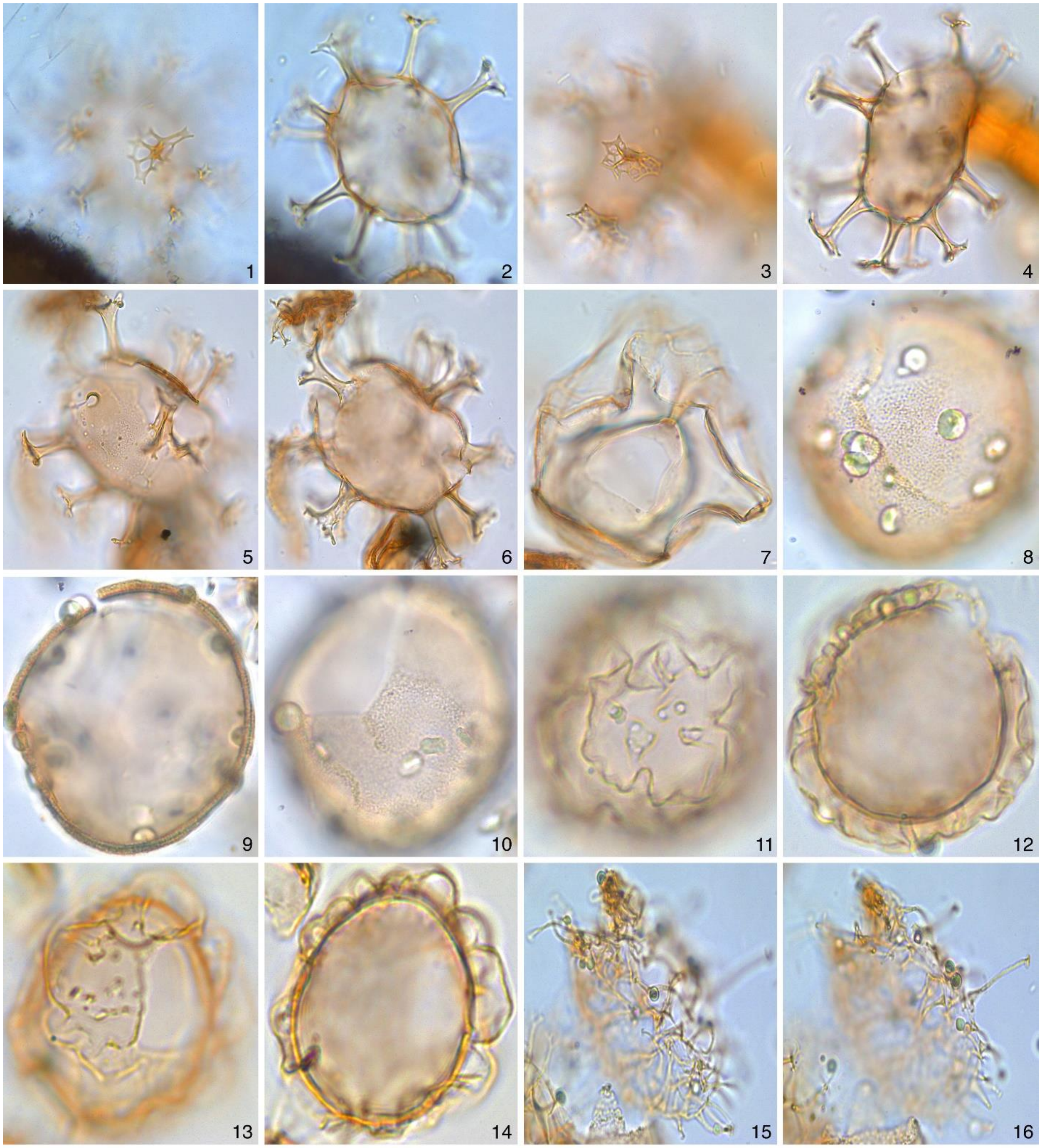
1
2
3
4
5
6
7
8
9
10
11
12
13
14
15
16

Plate 2:
Figures 1, 2. *Batiacasphaera* cf. *minuta*. Dorsal view (1) at upper surface, and (2) mid-focus; CBD = 28 µm. Sample 921 (Q47/0). Microreticulation less complete than B. minuta, and archeopyle less angular.

Figures 3, 4. *Batiacasphaera micropapillata*. Antapical view (3) or antapical surface, and (4) mid-focus; note thin wall and microreticulate surface texture; CBD = 33 µm, WT = 1 µm. Sample 532 (E47/1).

Figures 5, 6. *Batiacasphaera sphaerica*. Apical view (5) of apical surface, and (6) mid-focus; CBD = 35 µm. Sample 920 (M34/2).

Figures 7–9. *Bitectatodinium* cf. *raedwaldii*. Dorsal view (7) of dorsal surface, (8) mid-focus, and (9) ventral surface; note archeopyle formed by release of plates 3'' and 4''; and distribution of pilli that result in a granular surface appearance; CBD = 36 µm. Sample 1161 (Q46/4).

Figures 10, 11. *Bitectatodinium* sp. Antapical view (10) of mid-focus, and (11) apical surface; CBD = 45 µm. Sample 1161 (Q45/3).

Figures 12, 13. *Capisocysta lyellii*. Ventral view (12) of ventral surface, and (13) dorsal surface; note strongly granulate surface and broad sulcal tab; MD = 52 µm. Sample 568, (O31/2).

Figures 14–16. *Corrudinium* sp. Ventral view (14) of ventral surface, (15) mid-focus, and (16) dorsal surface; CBD = 40 µm, WT = 2 µm. Sample 568 (J29/0).

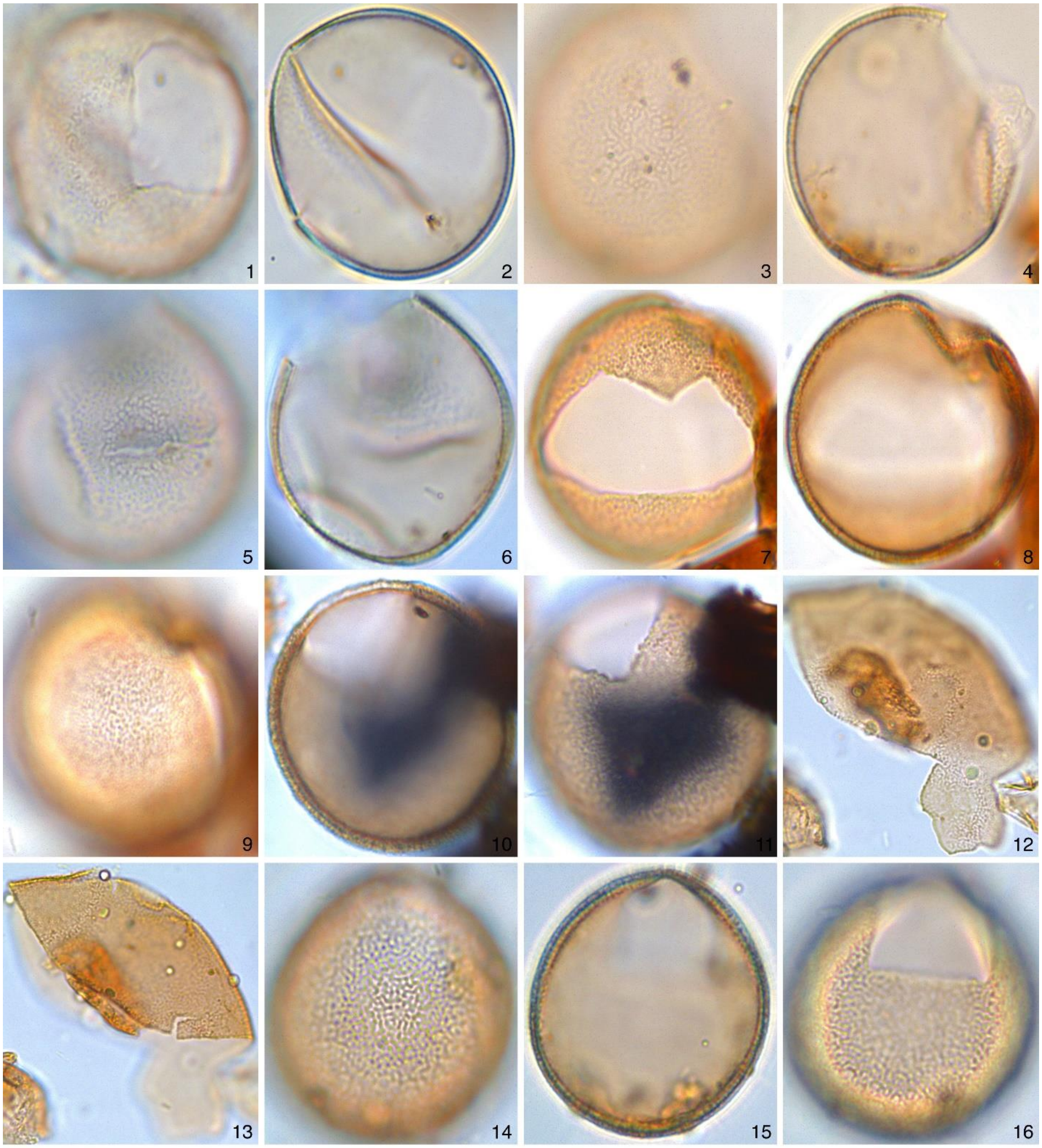
1
2
3
4
5
6
7
8
9
10
11
12
13
14
15
16

Plate 3:
Figure 1. Dinocyst sp. 1. Orientation uncertain, upper focus; CBD = 42 µm. Sample 543 (D63/4).

Figure 2. Dinocyst sp. 2. Orientation uncertain, upper focus; CBD = 65 µm. Sample 535, (L55/4).

Figures 3, 4. Gen et sp. A. Orientation uncertain (3) upper focus, and (4) mid-focus; note pilli that make up wall; CBD = 42 µm. Sample 1160 (B56/3).

Figure 5. *Geonettia waltonensis*. Upper focus; note smooth wall surface and presence of discrete cingular plates; central plate maximum diameter = 14 µm. Sample 568 (P24/2).

Figures 6–9. *Gramocysta verricula*. Orientation uncertain, (6) upper focus, (7) high focus on precingular plates, (8) mid-focus, and (9) lower focus; MD = 68 µm. Sample 932 (T30/1).

Figure 10. *Heteraulacacysta* sp. of Costa & Downie (1979). Apical view; MD = 78 µm. Sample 534 (F24/3).

Figure 11. *Hystrichosphaeropsis obscura*?. Orientation uncertain, upper mid-focus; note damaged epitract and hypotract, preventing a conclusive identification; MD = 59 µm. Sample 930 (W32/2)

Figure 12. *Hystrichosphaeropsis obscura*. Orientation uncertain, upper mid-focus; CBD = 52 µm. Sample 929 (U40/1).

Figure 13. *Invertocysta lacrymosa*. Orientation uncertain, middle focus, CBD = 32 µm. Sample 574 (L32/4).

Figures 14–16. cf. *Labyrinthodinium truncatum truncatum*. Left lateral view, (14) upper focus, (15) upper mid-focus, and (16) mid-focus; note small size and uncertain archeopyle; CBD = 18 µm. Sample 925 (O47/1).

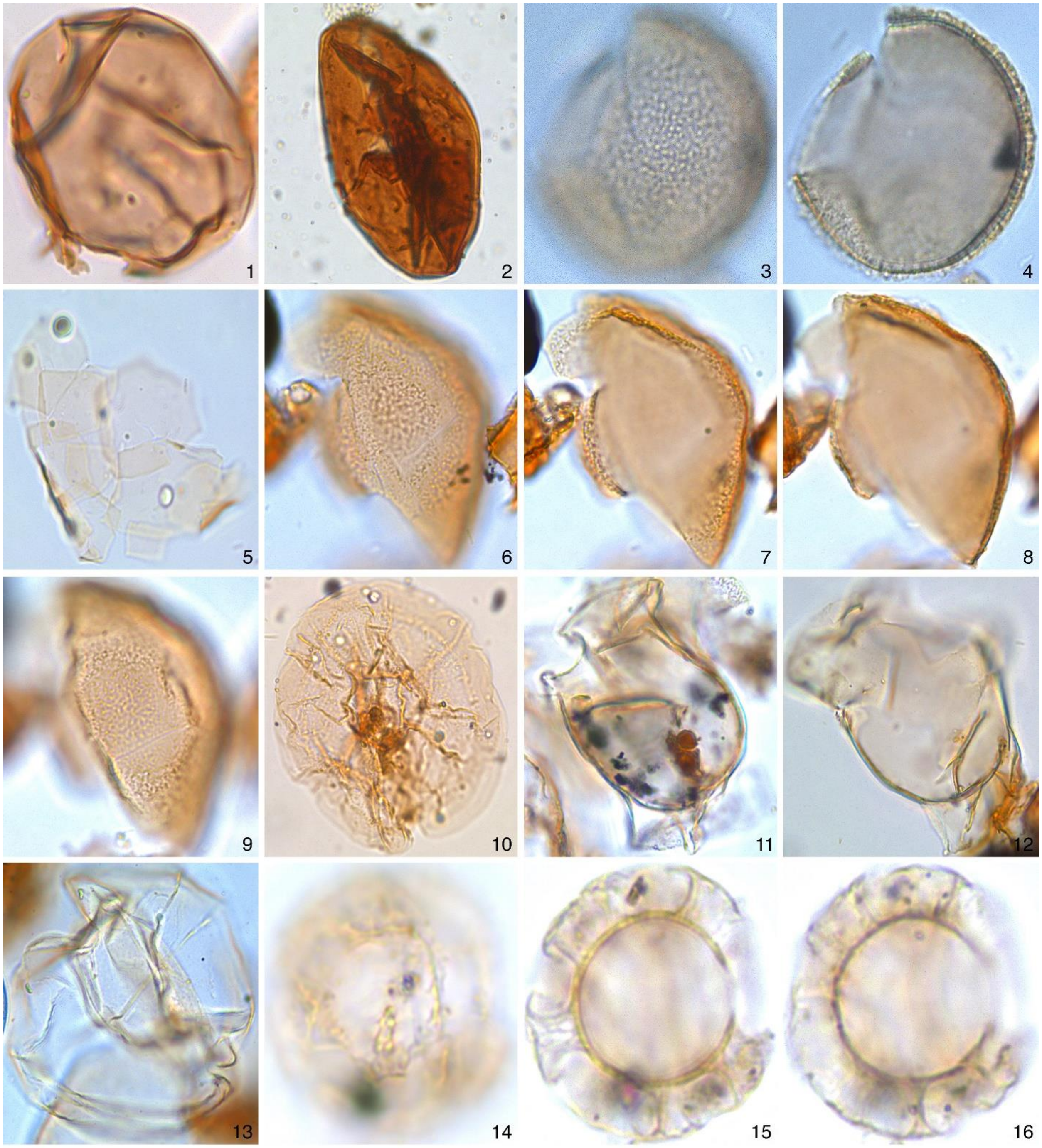
1
2
3
4
5
6
7
8
9
10
11
12
13
14
15
16

Plate 4:
Figures 1, 2. *Lingulodinium multivirgatum*. Orientation uncertain, (1) upper focus, and (2) mid-focus; CBD = 52 µm. Sample 935 (E55/2).

Figure 3. *Mendicodinium* sp. Orientation uncertain, upper focus; note reticulated surface texture, MD = 90 µm. Sample 574 (M36/3).

Figure 4–6. *Operculodinium* cf. *piaseckii*. Antapical view, (4) of antapical surface, (5) mid-focus, and (6) apical surface; CBD = 36 µm, WT = 2 µm. Sample 537 (L26/0).

Figure 7–9. *Operculodinium tegillatum*. Ventral view (7) of ventral surface, (8) mid-focus, and (9) dorsal surface; note tegillate central body wall, CBD = 34 µm. Sample 925 (L43/1).

Figure 10, 11. Cyst of *Pentapharsodinium dalei*. Orientation uncertain (10) at upper surface, and (11) mid-focus; CBD = 19 µm. Sample 924 (Q53/0).

Figure 12–14. *Piccoladinium* sp. Orientation uncertain (12) at upper surface, (13) mid-focus, and (14) lower focus; CBD = 43 µm. Sample 530 (Y32/0).

Figure 15, 16. Cyst of *Protoceratium reticulatum*. Orientation uncertain (15) at upper focus, and (16) mid focus; note hollow processes, CBD = 30 µm. Sample 574 (P36/1).


1
2
3
4
5
6
7
8
9
10
11
12
13
14
15
16

Plate 5:
Figures 1–3. *Pyxidinopsis* cf. *braboi*. Left lateral view (1) at upper focus, (2) focusing on protrusion (re-entrant) at apical margin of archeopyle, and (3) mid-focus; note discontinuous microreticulation, CBD = 33 μm. Sample 1162. R45/3.

Figures 4–6. *Pyxidinopsis* sp. Ventral view (4) of ventral surface, (5) mid-focus, and (6) dorsal surface; note sharp archeopyle angles, CBD = 34 μm. Sample 1159 (A50/0).

Figures 7, 8. *Pyxidinopsis*? sp. Orientation uncertain (7) at upper focus, and (8) midfocus; MD = 21 μm. Sample 924 (H46/4). Sample 924 (H46/4).

Figures 9, 10. *Reticulatosphaera actinocoronata*. Orientation uncertain (9) at upper focus, and (10) mid-focus; note branching or process endings, CBD = 29 μm. Sample 532 (N50/3).

Figure 11. *Selenopemphix armageddonensis*. Apical view of upper surface; CBD = 34 μm. Sample 531 (J43/2).

Figure 12. *Selenopemphix brevispinosa*. Antapical view of upper surface; note hair-like cingular processes, CBD = 39 μm. Sample 934 (N50/4).

Figure 13. *Selenopemphix dionaecysta*. Apical view of upper surface; note thick, branching processes, CBD = 40 μm. Sample 932 (S44/1)

Figure 14. *Selenopemphix*? sp. Apical view of upper mid-focus; CBD = 53 μm. Sample 1161 (V41/2)

Figure 15, 16. *Spiniferites falcipedius*. Dorsal view (15) at upper focus, and (16) mid-focus; CBD = 61 μm. Sample 932 (R38/0).

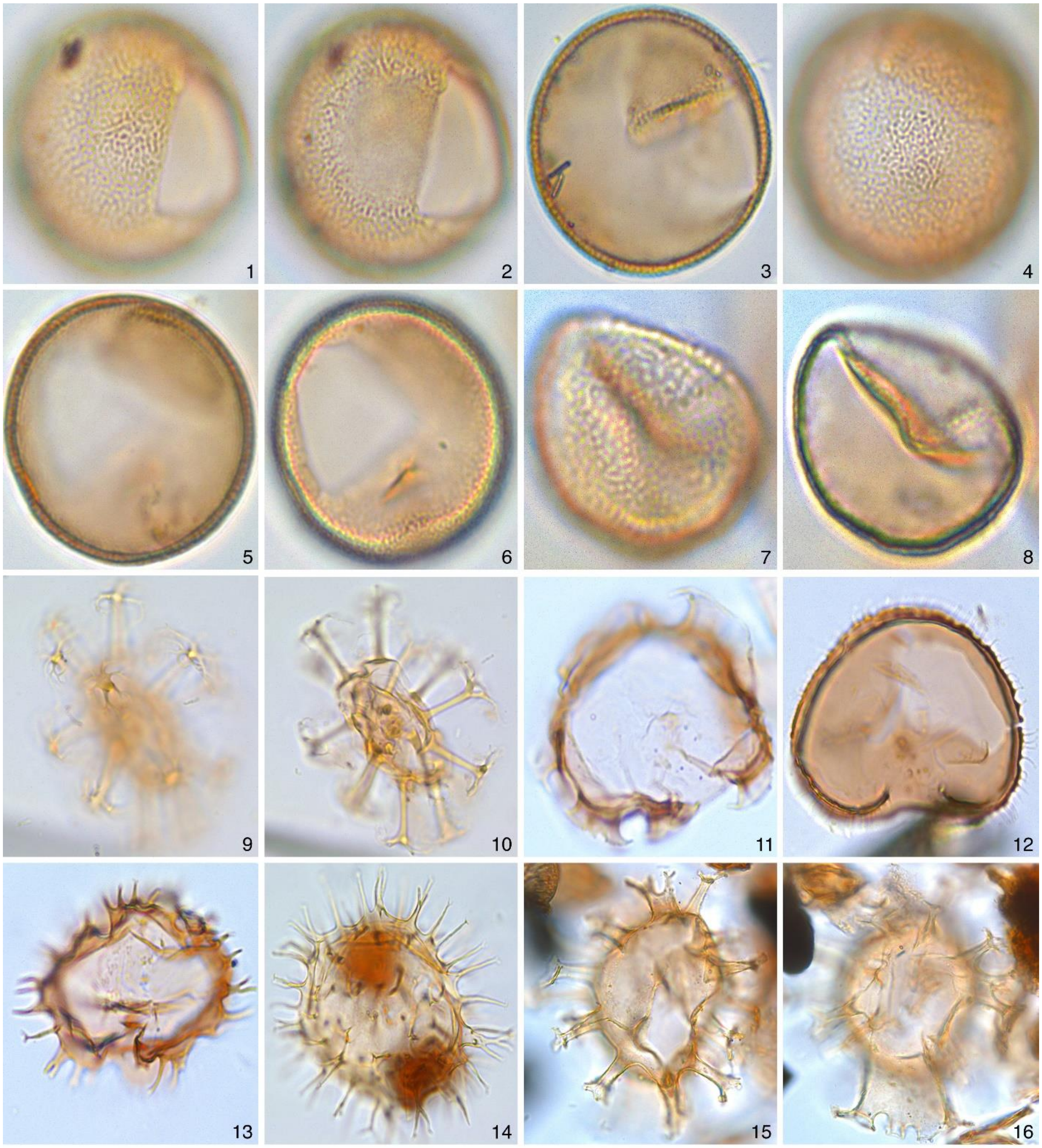
1
2
3
4
5
6
7
8
9
10
11
12
13
14
15
16

Plate 6:

Figure 1–3. *Spiniferites* sp. 1. Right lateral view (1) at upper focus, (2) upper surface, and (3) mid-focus; note granular surface texture and long branches at process endings, CBD = 52 µm, WT = 2 µm. Sample 1161 (R53/3).

Figure 4–7. *Tectatodinium*? sp. Ventral view (4) of ventral surface, (5) at mid-focus, (6) focusing on apical protrusion, and (7) dorsal surface; WT = 1.5 µm, CBD = 44 µm. Sample 1165 (E58/2).

Figure 8. *Trinovantedinium ferugnomatum*. Orientation uncertain at upper mid-focus; CBD = 44 µm. Sample 932 (S47/3).

Figure 9, 10. *Trinovantidinium glorianum*. Apical view (9) at upper focus, and (10) mid-focus; CBD = 52 µm. Sample 932 (V40/4).

Figure 11. *Trinoventidinium variabile*. Orientation uncertain at upper mid-focus; note long, solid processes with aculeate (star-shaped) endings, CBD = 49 µm. Sample 574 (S40/0).

Figure 12. *Tuberculodinium vancampoae*. Orientation uncertain at upper focus; CBD = 92 µm. Sample 1158 (Z41/0).


1
2
3
4
5
6
7
8
9
10
11
12

Plate 7:
Figure 1, 2. Acritarch sp. 1. (1) Upper focus, and (2) mid-focus; note tectate wall, CBD = 14 µm. Sample 932 (L49/3).

Figure 3, 4. Acritarch sp. 2. (3) Upper focus, and (4) mid-focus; note thin processes, some of which exhibit branching, CBD = 14 µm. Sample 533 (B31/2).

Figure 5. Acritarch sp. 3. Upper mid-focus; MD = 21 µm. Sample 531 (M48/1).

Figure 6, 7. Acritarch sp. 4. (6) Upper focus, and (7) mid-focus. CBD = 11 µm. Sample 536 (T43/1).

Figure 8, 9. *Cymatiosphaera*? *invaginata*. (8) Upper focus, and (9) mid-focus; note distinctive cresting, CBD = 15 µm. Sample 574 (D46/3).

Figure 10. *Cymatiosphaera* sp. Upper focus; CBD = 11 µm. Sample 533 (B32/3).

Figure 11. *Cyclopsiella* sp. Upper focus; MD = 31 µm. Sample 543 (O47/1).

Figure 12. *Nanobarbophora walldalei*. Upper mid-focus; CBD = 24 µm. Sample 574 (E50/1)

Figure 13. *Paralecaniella indentata*. Upper focus; MD = 68 µm. Sample 574 (L53/3)

Figure 14. *Pediastrum* sp. Upper focus; MD = 64 µm (excluding projecting segments). Sample 537 (F49/2).

Figure 15, 16. *Quadrina condita*. (15) Upper focus, and (16) lower focus; CBD = 31 µm. Sample 932 (S45/4).

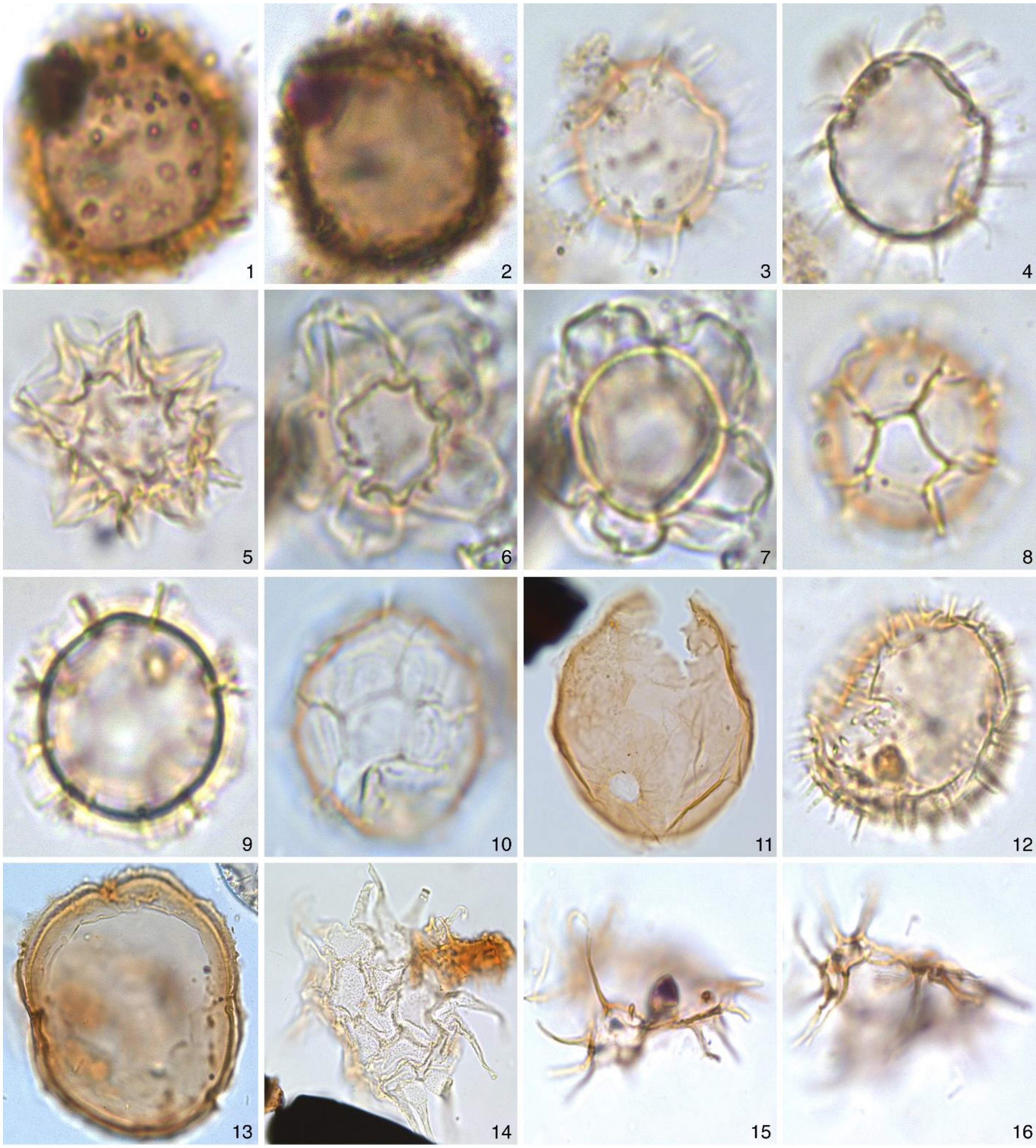
1
2
3
4
5
6
7
8
9
10
11
12
13
14
15
16

Appendix IV: R documentation

The following section details the processes and formulae used with the statistical program R to produce the analysis used in this study. The use of the GUI package RStudio is recommended, as it helps with visualisation and display of data and steps. Commands are in italics. R version used is 3.3.1, and RStudio version used is 0.99.903. Any future versions of the software may require slight changes to commands and processing. Copying commands into R from this document may not work due to text formatting.

Constrained Cluster Analysis

- Data to be used should be in .csv format (e.g. data1.csv)
- Package to be used is rioja. After installing the package, launch package with the following command:

    Library(rioja)

- Import data.csv from "Import Dataset" in top right pane. The following settings should be used:
    - Encoding: Automatic
    - Heading: Yes
    - Row names: Use first column
    - Separator: Comma
    - Decimal: Period
    - Quote: Double Quote (")
    - Comment: None
    - Na.strings: NA
    - Strings as factors checked
- If dataset is not in proportions, convert to proportions using the following command:

    "data1" <- sweep("data", 1, rowSums("data"), '/')

- Create a distribution file with the following command:

    d_data <- dist(data1, diag=FALSE, upper=FALSE, p=2)

- A new addition should now come up under "values" called d_data. Any name can be used instead of "d_data", though it's recommended that it be kept short.
- Create a cluster analysis file from the distribution file with the following command:

    c_data <- chclust(d_data, method = "coniss")

- A new addition should now come up under "values" called c_data. Again, any name can be used instead of "c_data".

- Plot the data using the following command:

plot(as.dendrogram(c_data))

- A dendrogram should now appear with the constrained cluster analysis.
- To change label font size, use the following command:

par(cex = X)

where X is a proportion of the font required (e.g. 0.75, 0.5, 0.2 etc.)

Detrended Correspondence Analysis

- Data to be used should be in .csv format (e.g. data1.csv)
- Package to be used is vegan. After installing the package, launch package with the following command:

Library(vegan)

- Import data using the same parameters described in the Constrained Cluster Analysis section, and convert to proportions using the same formula if required.
- Create a detrended correspondence analysis file from data1 using the following command:

DCA <- (data1, iweigh=0, iresc=4, ira=0, mk=26, short=0, before=NULL, after=NULL)

- A new addition should now come up under "values" called DCA. Again, any name can be used instead of "DCA".
- Plot the file using the following command:

plot(DCA)

- A plot of the detrended correspondence analysis should now be displayed. To narrow down the range of the plot, use the following command:

xlim = range(X:Y)
ylim = range(U:Z)
where X,Y, U and Z are coordinates on the graph (e.g. -1:1, -2:3 etc.)

Canonical Correspondence Analysis

- Data to be used should be in .csv format (e.g. data1.csv)
- Package to be used is vegan. After installing the package, launch package with the following command:

Library(vegan)

- Import data using the same parameters described in the Constrained Cluster Analysis section, and convert to proportions using the same formula if required. A separate file can be added that includes relevant statistical data, provided it is in the same format, with the same data points.

- Create a canonical correspondence analysis file from data1 using the following command:

  Ca <- cca("data1"~Param1 + Param2, data="source")
  where source is the name of the data file that includes the statistical data. This source could also be the original file (in this case, data1)

- A new addition should now come up under "values" called Ca. Again, any name can be used instead of "Ca".
- Plot the file using the following command:

  plot(Ca)

- Editing of these plots can be done with Adobe Illustrator. The following command can also be used to change labels and points:

Text(Ca, display=X, col=Y, cex=Z, type="point")

where X = "*sites*" or "*species*", Y = a desired colour (e.g. red), and Z = proportion of the font

required (e.g. 0.75, 0.5, 0.2 etc.)

Appendix V: Range chart and raw counts

This chart provides raw counts of all taxa recorded in the present study, including counts of in-situ and reworked dinoflagellate cysts, acritarchs, green algae and terrestrial palynomorphs. Also included are calculated ratios and indices as discussed in the text. A “+” indicates a taxon not recorded during the count, but registered during subsequent searching of the slide for rare specimens. The chart has been split into two sections, for display and printing purposes. The first chart shows raw counts of in-situ dinoflagellate cysts, and the second displays all other counts and calculations.

	Merksplas Formation																										Poederlee Formation									Kasterlee Formation											Diest Formation								
Slide Number	**1158**	**1159**	**1160**	**1161**	**1162**	**1163**	**1164**	**1165**	**1166**	**1167**	**1168**	**1169**	**1170**	**1171**	**1172**	**1173**	**1174**	**568**	**1175**	**1176**	**1177**	**1178**	**1179**	**1180**	**1181**	**1182**	**551**	**545**	**544**	**543**	**574**	**537**	**536**	**535**	**534**	**533**	**532**	**531**	**530**	**920**	**921**	**922**	**923**	**924**	**925**	**926**	**927**	**928**	**929**	**930**	**931**	**932**	**933**	**934**	**935**
Depth (m)	5.60	5.70	5.80	6.10	6.20	6.30	6.40	6.50	6.70	6.80	7.10	7.20	7.30	7.40	7.50	7.60	7.70	7.80	7.90	8.00	8.10	8.20	8.40	8.50	8.60	8.70	17.50	20.21	20.42	20.70	22.58	23.80	24.22	24.65	24.95	25.72	26.39	26.56	26.79	27.30	28.35	29.33	30.30	31.30	32.30	33.08	33.30	34.35	35.50	35.98	36.30	36.90	37.85	38.35	39.50
In-situ Dinoflagellate Cysts																																																							
Achomosphaera a. andalousiensis		3		2	+	1	1	+	1					1			+	2					1		1	5	1	2		2	2	3	5	5	2	1	3	1	2	4	1	1	1	2	1			2	+	2		6	2	1	
Achomosphaera a. suttonensis		2	2	2	1			+	3		+	+		1		1		+	1			+		3			+	3		2	3	4	1	1	3	2	3	+	2	1	3	2	6	2	4		2	1	1	3	1	7			
Achomosphaera sp. 1	1	2	6		+	2	+	1						3	2		1						+	+																															
Amiculosphaera umbraculum	1	8	11	5	3	1	1	3	6	1	5	18	2	6	2	10	4	3	3	2	2	2	4	2	3		+		2			+				1		1			1	1				1			1						
Apteodinium sp.																																					2	2	2												3				
Ataxiodinum choane			1		1			1	1	1	1			2		1	2	+				1	3	1	1	2						1	7	4	3	6	1	2	1	2		3	1		1							1			
Ataxiodinum zevenboomii		2																					1								2		2		1	3		+			2	1		1	3									3	
Barssidinium graminosum								1						1			2	+			1												1						1				1	2	1										
Barssidinium pliocenicum					2				1	1		1		3				2	2	1			3	1		1	2	3	4		6	+	1	4	10	6	7	18	15	5	6	3	2	7	13	15	2	4	17	8		7	1		
Batiacasphaera cf. *minuta*																																							1		2			1											
Batiacasphaera micropapillata																																					1	1	1																
Batiacasphaera sphaerica																																								1															
Bitectatodinium cf. *raedwaldii*	9	25	26	29	33	24	27	26	24	3	29	39	14	11	13	27	32	33	23	87	21	18	31	30	16	39	18	15	4	7	1	7	10	4	5	11	17	5	14	24	32	4	6	27	4	12	3	2	11	15		47	5	3	2
Bitectatodinium sp.				1																																		1						2					+	+					
Bitectatodinium tepikiense ?				1																																																			
Brigantedinium cariacoense																												+													1														
Brigantedinium sp.		1																9									2	9	7		11	+		4	13		6	6	5	4	21	1	13	16	7	46	10	1	17	37	2	86	1	1	
Capisocysta lyellii	1	2	7	15	17	7	5	4	3	3	11	12	7	32	56	20	19	18	12	23	18	7	6	3	10	10																													
Corrudinium ? sp.								1										+										+				2	2		1		1				1											1			
Dapsilidinium pastielsii		2									1																+	4	1	1	2	1		3	1		1			2		1		1			1	4	1	1	2		1		
Desotodinium wrennii												+	1										1			1																													
Dinocyst sp. 1																																	1	7	4	2	1	2																	
Dinocyst sp. 2																																		3			1		1																
Filisphaera filifera																																														3			1						
Filisphaera microornata																																				1																			
Gen. et sp. ind. A		2	3	3	2	1		1				3	1								1			1																															
Geonettia waltonensis			1	1				1						+	+			5																																					
Gramocysta verricula																																																+	2	1		11			
Habibacysta tectata																																																		1	1	6	5	1	
Heteraulacacysta sp. A of C & D			8	42	71	35	16	29	40	8	40	30	92	84	117	41	83	101	39	38	96	137	102	59	15	18	57	27	17	36	23	19	18	11	16	31	26	11	12	4	1	5	8	6	14	10	30	81	19	6		1	4	8	
Homotryblium sp.																				2																																			
Hystrichokolpoma rigaudiae	1	1			2		1			2	9	+			1		1	1		2					2		3	+	2		2					1				1							2	1	1	1	1	+	2		
Hystrichosphaeropsis obscura																																													2	1			1	1					
Hystrichosphaeropsis obscura ?																																										1			1										
Hystrichosphaeropsis sp.											1																																												
Invertocysta lacrymosa											2							3							1		2		+	3	+			2		4					3	7		3		1	1	2	1						
cf. *Labyrinthodinium t. truncatum*																																												1	2						1	1	1		
Lejunecysta sp.											1											1	2						2		1				1	2			1			1			2			1		1		4	1	6	1
Lingulodinium machaerophorum	1		2	1	2	1	2		2	+	2	1		+	2					2				1	1	2		+	1		1	1	26	51	22	47	26	26	23	15	3	2	7	2	3	1	1	4	1	1		1			9
Lingulodinium multivirgatum																																																							1
Lingulodinium sp.																																										5	1					1			4		6	1	
Medicodinium sp.																														2																									
Melitasphaeridium choanophorum																											2	4	7	5	9	14	11	9	6	2		1	1	1	5	2	3	2	1					5	2	4	1		2
Nematosphaeropsis labyrinthus										1													1				1				+	1																1							
Operculodinium centrocarpum		1	7	5	6	3	4	4	5	4	1	6	1	3	1	4	6		1	3	3	3	3	3		1		1	3		2	2	3	6	3	6	7	4	9	2		3	1	2	5	3	1	1	3		1		4	3	2
Operculodinium cf. *piaseckii*																																+																							
Operculodinium israelianum	14	37	16	16	29	10	8	11	23	5	9	12	14	12	12	11	11	9	13	7	13	10	10	4	8	6	1	2	4				4	15	14	13	38	22	20	12	11	4	8	9	7	22	11	12	23	25	2	7	2		3
Operculodinium tegillatum	1																																	1		1	7	5	9	5	3	24	41	42	48	32	48	31	96	67		3		4	1
Operculodinium ? *eirikianum*																										1	4	3	3	7	10	6	1		1	2		1	2	3	6	5	1	9	11	5	1		1	7	1	+		3	1
Pentapharsodinium dalei																											1	2	3		2	2	3	4	1	9	1	2	1	3	10	3	3	2						2		1			
Piccoladinium sp.																												+	+											2	2	1		3		1									
Piccoladinium ? sp.																					1																																		
Polysphaeridium zoharyi												1	2					+																		1			1										1			2			
Protoceratium reticulatum	3	34	45	27	34	45	27	86	46	14	35	52	36	42	12	40	38	24	35	13	24	35	30	18	13	30	27	26	23	35	24	34	16	17	15	18	21	5	7			2	2												
Pyxidinopsis cf. *braboi*	+	1	3	1	3	1	3	4	2		1		1	7	+	2	3			3	3	3	3	4	4	4																													
Pyxidinopsis sp.	+	5	4	2	1	2	3	9	3		1	4	2	3	2	4	8		3	+	2	3	1	4	1	6													1		5	4	3		5	+	1	7	+	2	4	2	4	7	
Pyxidinopsis ? sp.																																						1	1					1			1	1					2	1	
Reticulatosphaera actinocoronata																																					1	1	4	3	3	4	11	6	4	5	1	2	4	2		4	1	1	
Selenopemphix armageddonensis																																			2	2		2	1		1	3	1	3	5	3		1	2	4		6			+
Selenopemphix brevispinosa																											3		2		3	2		2			+	1	1	2	3	6	2	2	1				1			3		8	
Selenopemphix dionaeacysta																															1	1	2		1		2	3	2		1		2			1		1	1	1		4	27	5	1
Selenopemphix nephroides																											1	2	1	1		+	2					1				1	1	1	3	1	2			2		1	1		
Selenopemphix quanta								1																							2	+	2	1			2	1		1	3	1	1					2		1		5			
Selenopemphix sp.				1							1				1																																								
Spiniferites falcipedius																														+	2	1					+				+								1			2			
Spiniferites mirabilis																												2				2	+									1			2		1		1	+				3	
Spiniferites sp. 1	3	+	24	16	27	7	5	7	19	1	16	15	7	11	24	17	7	13	42	16	12	10	17	45	10	14			1	2	12	13	6	6	2																				
Spiniferites / Achomosphaera spp.	52	265	144	129	113	66	64	132	110	17	115	121	132	109	71	120	82	76	123	70	122	86	88	132	177	149	114	164	167	135	142	107	95	70	98	96	89	109	121	110	92	113	102	83	98	88	45	43	68	51	22	83	29	48	22
Tectatodinium pellitum	4	7	3	6	2	1		1	3		+	5	1	+	4	1	3	3	1	+	+	2	2	2	1	3	4		2	+		+		1		1		+	2					+		1	1		2	5	1	+			
Tectatodinium sp.	1							2	1						1		1				+																								1								1		
Trinovantedinium ferugnomatum																																																				1	1		
Trinovantedinium glorianum																													2	1	2	2		1	1			1		1					1	3			1	4		1			
Trinovantedinium sp.																																	1		3								1	1		1			2					3	
Trinovantedinium variabile																											1	1		2	1	2	2		2		1	3	3		3				2	4	1	2	10	14		1		2	
Tuberculodinium vancampoae	+	5	5	1	2	1	1	1	1		2	1	3	5	5	2	1	2	11	8	7	4	4	1	1	1												1	1	1							1								
Total In-situ	**92**	**405**	**318**	**307**	**351**	**208**	**168**	**325**	**294**	**62**	**283**	**321**	**316**	**336**	**326**	**301**	**304**	**304**	**309**	**277**	**326**	**322**	**313**	**314**	**265**	**293**	**244**	**270**	**258**	**241**	**266**	**227**	**222**	**232**	**231**	**269**	**265**	**240**	**268**	**209**	**225**	**215**	**229**	**239**	**252**	**260**	**167**	**209**	**291**	**270**	**51**	**309**	**103**	**113**	**45**
In-situ Concentration (cysts/g)	**61.51**	**145.98**	**230.30**	**178.65**	**325.80**	**196.03**	**85.09**	**373.53**	**252.47**	**19.54**	**181.34**	**198.94**	**261.49**	**1106.15**	**742.54**	**286.44**	**140.13**	**933.62**	**537.30**	**248.86**	**530.59**	**607.73**	**337.23**	**230.11**	**161.63**	**122.16**	**180.72**	**377.75**	**492.78**	**421.93**	**1192.16**	**1143.18**	**1336.27**	**2180.49**	**752.08**	**1671.17**	**1717.99**	**1668.28**	**1652.02**	**2158.66**	**2833.84**	**548.18**	**760.35**	**2455.01**	**1035.01**	**4320.48**	**184.75**	**131.47**	**1907.14**	**2379.58**	**70.23**	**1522.65**	**151.18**	**244.46**	**27.26**

	Merksplas Formation																									
Slide Number	1158	1159	1160	1161	1162	1163	1164	1165	1166	1167	1168	1169	1170	1171	1172	1173	1174	568	1175	1176	1177	1178	1179	1180	1181	1182
Depth (m)	5.60	5.70	5.80	6.10	6.20	6.30	6.40	6.50	6.70	6.80	7.10	7.20	7.30	7.40	7.50	7.60	7.70	7.80	7.90	8.00	8.10	8.20	8.40	8.50	8.60	8.70
Reworked Dinoflagellate Cysts																										
Cleistosphaeridium sp.	1	1	1	1			1	1		+	3		+	+						1						
Cordosphaeridium cf. *inodes*																										
Cordosphaeridium inodes																										
Cordosphaeridium sp.	1	2	3	2	+	1	2	2	1	1	4	2		1	+	1	1		2	4		2		3		2
Glaphyrocysta sp.				1						1		+		+	+	+										
Unidentified reworked cyst	7	1	3	4	5		4	1	5	2	12	2		1	1	3	2			6	4	2	6	4	2	4
Total Reworked	**9**	**4**	**7**	**7**	**5**	**1**	**7**	**5**	**6**	**3**	**19**	**4**	**0**	**2**	**1**	**4**	**3**	**0**	**2**	**11**	**4**	**4**	**6**	**7**	**2**	**6**
Reworked Concentration (cysts/g)	**6.02**	**1.44**	**5.07**	**4.07**	**4.64**	**0.94**	**3.55**	**5.75**	**5.15**	**0.95**	**12.17**	**2.48**	**0.00**	**6.58**	**2.28**	**3.81**	**1.38**	**0.00**	**3.48**	**9.88**	**6.51**	**7.55**	**6.46**	**5.13**	**1.22**	**2.50**
Acritarchs																										
Acritarch sp. 1																										
Acritarch sp. 2	1	2	1					+	1		1															1
Acritarch sp. 3			1	1	1	1	1				1			1						1	1		1			
Acritarch sp. 4		1					1						1													
Cyclopsiella sp.					1		1	3	1		4	1	2	2			1	2		1	1	1	3			
Cymatiosphaera sp.			1	2		1				1	2	2						1		1			1		1	
Cymatiosphaera ? invaginata					1		1	1	1																	
Halodinium sp.																										
Lavradosphaera sp.																										
Nanobarbophora walldalei		2																								
Paralecaniella indentata			+		2				1		2	1		1		2	2	2		1	+			3	1	1
Quadrina ? condita																										
Green Algae																										
Botryococcus					1													1		1						
Gelasinicysta vangeelii	1		1		1		1										1		1	1						
Pediastrum spp. ind.	1	1		1		2					4	2		1			2									
Sigmopollis	12	37	11	13	16	30	3		9	4	7	11	7	5	6	8	8	1	5		7	5	8	3	4	5
Tasmanites		1										1		1				1	2				1			1
Zygnemataceae	4	3	3	3	4	4	2	3	5	4	3	4	1	3	1	8	3		1		3	2	1	2		
Terrestrial Palynomorphs																										
Bisaccate Pollen	18	79	66	95	112	80	39	134	136	23	88	82	60	62	137	95	187	133	120	98	84	79	61	24	56	146
Fern Spore	2	20	6	9	16	18	2	13	13	7	12	7	13	5	6	19	13	6	4	21	15	14	10	7	2	10
Fungal Spore		4	2	1	5	1	4		3		5	3	5	7		2	3		2				4	6	1	2
Monosaccate Pollen		5	4		2	2			2		1	3	1	2	1	4	5	6	2	2			3		1	
Nonsaccate Pollen	238	497	357	334	364	435	220	215	337	168	411	218	144	112	146	328	292	78	181	517	320	193	201	162	81	292
Total	**258**	**605**	**435**	**439**	**499**	**536**	**265**	**362**	**491**	**198**	**517**	**313**	**223**	**188**	**290**	**448**	**500**	**223**	**309**	**638**	**419**	**286**	**279**	**199**	**141**	**450**
Total Pollen Concentration	**171.17**	**209.41**	**309.24**	**249.65**	**443.68**	**487.24**	**131.18**	**401.12**	**407.90**	**60.20**	**320.38**	**187.78**	**169.64**	**579.41**	**646.88**	**406.34**	**223.10**	**34151.06**	**526.87**	**554.32**	**657.54**	**513.36**	**285.52**	**136.31**	**84.17**	**182.62**
Pollen Ratios																										
D/Ap Ratio	0.264	0.411	0.427	0.417	0.423	0.287	0.393	0.482	0.382	0.245	0.361	0.514	0.607	0.656	0.534	0.413	0.386	0.583	0.505	0.310	0.447	0.542	0.542	0.628	0.658	0.401
D/Bp Ratio	0.836	0.837	0.828	0.764	0.758	0.722	0.812	0.708	0.684	0.729	0.763	0.797	0.840	0.844	0.704	0.760	0.619	0.696	0.720	0.739	0.795	0.803	0.837	0.929	0.826	0.667
D/Np Ratio	0.279	0.449	0.471	0.479	0.491	0.323	0.433	0.602	0.466	0.270	0.408	0.596	0.687	0.750	0.691	0.479	0.510	0.796	0.631	0.349	0.505	0.625	0.609	0.660	0.766	0.501
D/BpNp Ratio	0.264	0.413	0.429	0.417	0.424	0.288	0.393	0.482	0.383	0.245	0.362	0.517	0.608	0.659	0.535	0.416	0.388	0.590	0.507	0.311	0.447	0.542	0.544	0.628	0.659	0.401
Bp/Np Ratio	0.070	0.137	0.156	0.221	0.235	0.155	0.151	0.384	0.288	0.120	0.176	0.273	0.294	0.356	0.484	0.225	0.390	0.630	0.399	0.159	0.208	0.290	0.233	0.129	0.409	0.333
D/ApF Ratio	0.263	0.401	0.422	0.412	0.413	0.280	0.388	0.473	0.375	0.238	0.354	0.506	0.586	0.641	0.529	0.402	0.378	0.577	0.500	0.303	0.438	0.530	0.529	0.612	0.653	0.394
Other																										
Foraminiferal lining																										
Invertebrate remains	3		3	2	7	3	6	4	10	4	3	15			3		1					1				
Stoma	1																									
Sample Data																										
Lycopodium clavatum	577	1068	531	659	413	407	762	334	448	1221	601	623	465	117	168	405	829	161	222	424	234	204	357	520	631	914
Lycopodium tablets	2	2	2	2	2	2	2	2	2	2	2	2	2	2	2	2	2	2	2	2	2	2	2	2	2	2
Sample dry weight (g)	50.11	50.22	50.27	50.41	50.43	50.4	50.09	50.36	50.25	50.23	50.2	50.07	50.24	50.19	50.52	50.16	50.59	75.17	50.08	50.75	50.76	50.21	50.26	50.73	50.23	50.73
Lycopodium per tablet	9666	9666	9666	9666	9666	9666	9666	9666	9666	9666	9666	9666	9666	9666	9666	9666	9666	18584	9666	9666	9666	9666	9666	9666	9666	9666
Lycopodium tablet error	949	949	949	949	949	949	949	949	949	949	949	949	949	949	949	949	949	828	949	949	949	949	949	949	949	949
Standard deviation	1342.089	1342.089	1342.089	1342.089	1342.089	1342.089	1342.089	1342.089	1342.089	1342.089	1342.089	1342.089	1342.089	1342.089	1342.089	1342.089	1342.089	1170.969	1342.089	1342.089	1342.089	1342.089	1342.089	1342.089	1342.089	1342.089
Statistical Data																										
Richness	16	22	22	25	20	18	18	24	21	16	23	18	16	20	18	17	20	21	15	18	16	17	21	20	18	20
Error (%)	3.19	2.27	2.43	2.41	2.45	2.65	2.65	2.53	2.49	3.62	2.45	2.40	2.46	3.08	2.83	2.51	2.38	11.61	2.70	2.52	2.66	2.73	2.53	2.44	2.46	2.38
Standard Deviation (±)	1.96	3.31	5.60	4.30	8.00	5.20	2.26	9.47	6.29	0.71	4.44	4.77	6.43	34.07	21.01	7.18	3.33	108.36	14.52	6.28	14.12	16.58	8.52	5.61	3.98	2.91
Total marine palynomorphs (TMP)	91	407	319	309	355	209	170	330	297	63	291	325	318	339	326	303	307	309	309	280	327	323	317	317	267	294
Total protoperidinioid cysts	0	1	0	1	2	0	0	2	1	1	2	1	0	4	1	0	2	11	2	1	1	1	5	1	0	1
Total gonyaulacoid cysts	91	402	315	302	347	207	168	322	293	60	281	317	315	332	325	301	302	293	307	276	324	321	308	312	265	292
G/P	1.00	1.00	1.00	1.00	0.99	1.00	1.00	0.99	1.00	0.98	0.99	1.00	1.00	0.99	1.00	1.00	0.99	0.96	0.99	1.00	1.00	1.00	0.98	1.00	1.00	1.00
Shannon Index	1.76	1.44	2.07	2.12	2.11	1.97	2.07	1.88	2.08	2.26	2.15	2.05	1.65	2.03	1.90	1.99	2.09	1.51	1.92	2.08	1.83	1.76	2.02	1.88	1.43	1.85
Evenness	0.64	0.46	0.67	0.66	0.70	0.68	0.72	0.59	0.68	0.81	0.68	0.71	0.59	0.68	0.66	0.70	0.70	0.49	0.71	0.72	0.66	0.62	0.66	0.63	0.50	0.62
Cyst Ratios (VS Total Gonyaulacoid Cysts)																										
Bitectatodinium cf. *raedwaldii*	9.89	6.22	8.25	9.60	9.51	11.59	16.07	8.07	8.19	5.00	10.32	12.30	4.44	3.31	4.00	8.97	10.60	11.26	7.49	31.52	6.48	5.61	10.06	9.62	6.04	13.36
Capisocysta lyellii	1.10	0.50	2.22	4.97	4.90	3.38	2.98	1.24	1.02	5.00	3.91	3.79	2.22	9.64	17.23	6.64	6.29	6.14	3.91	8.33	5.56	2.18	1.95	0.96	3.77	3.42
Heteraulacacysta sp. A of C & D	0.00	0.00	2.54	13.91	20.46	16.91	9.52	9.01	13.65	13.33	14.23	9.46	29.21	25.30	36.00	13.62	27.48	34.47	12.70	13.77	29.63	42.68	33.12	18.91	5.66	6.16
Lingulodinium machaerophorum	1.10	0.00	0.63	0.33	0.58	0.48	1.19	0.00	0.68	0.00	0.71	0.32	0.00	0.00	0.62	0.00	0.00	0.00	0.00	0.72	0.00	0.00	0.00	0.32	0.38	0.68
Operculodinium israelianum	15.38	9.20	5.08	5.30	8.36	4.83	4.76	3.42	7.85	8.33	3.20	3.79	4.44	3.61	3.69	3.65	3.64	3.07	4.23	2.54	4.01	3.12	3.25	1.28	3.02	2.05
Operculodinium tegillatum	0.00	0.00	0.00	0.00	0.00	0.00	0.00	0.00	0.00	0.00	0.00	0.00	0.00	0.00	0.00	0.00	0.00	0.00	0.00	0.00	0.00	0.00	0.00	0.00	0.00	0.00
Protoceratium reticulatum	3.30	8.46	14.29	8.94	9.80	21.74	16.07	26.71	15.70	23.33	12.46	16.40	11.43	12.65	3.69	13.29	12.58	8.19	11.40	4.71	7.41	10.90	9.74	5.77	4.91	10.27
Spiniferites/Achomosphaera spp. indet.	61.54	67.66	55.87	49.34	40.63	36.71	41.67	43.48	45.39	30.00	46.62	42.90	44.13	37.65	29.85	45.85	29.80	0.00	54.07	31.16	41.36	29.91	34.42	57.69	70.94	57.53
AIN	1.10	1.99	3.49	1.66	0.86	0.48	0.60	0.93	2.05	3.33	2.49	5.68	0.63	1.81	0.62	3.32	1.32	2.05	0.98	0.72	0.62	0.62	1.62	0.64	1.51	0.00
Cymatiosphaera ? invaginata VS TMP	0.00	0.00	0.00	0.00	0.00	0.00	0.01	0.00	0.00	0.00	0.00	0.00	0.00	0.00	0.00	0.00	0.00	0.00	0.00	0.00	0.00	0.00	0.00	0.00	0.00	0.00
Acritarch sp. 1 VS TMP	0.00	0.00	0.00	0.00	0.00	0.00	0.00	0.00	0.00	0.00	0.00	0.00	0.00	0.00	0.00	0.00	0.00	0.00	0.00	0.00	0.00	0.00	0.00	0.00	0.00	0.00

	Poederlee Formation								
Slide Number	551	545	544	543	574	537	536	535	534
Depth (m)	17.50	20.21	20.42	20.70	22.58	23.80	24.22	24.65	24.95
Reworked Dinoflagellate Cysts									
Cleistosphaeridium sp.	2						1		
Cordosphaeridium cf. *inodes*		3		2					
Cordosphaeridium inodes	1	1	1	+	2	2	1		1
Cordosphaeridium sp.									
Glaphyrocysta sp.									
Unidentified reworked cyst	+	1	1			+		3	2
Total Reworked	**3**	**5**	**2**	**2**	**2**	**2**	**2**	**3**	**3**
Reworked Concentration (cysts/g)	**2.22**	**6.89**	**3.82**	**3.50**	**8.96**	**10.07**	**12.04**	**28.20**	**9.77**
Acritarchs									
Acritarch sp. 1						36	44	14	2
Acritarch sp. 2								1	4
Acritarch sp. 3				+				4	1
Acritarch sp. 4						1	+		
Cyclopsiella sp.	34	23	32	25	14	14	4	1	7
Cymatiosphaera sp.			1		1			1	
Cymatiosphaera ? invaginata	13	13	15	16	16	20	28	51	54
Halodinium sp.	1	5	2	5	1	1			
Lavradosphaera sp.			1			+	1	5	2
Nanobarbophora walldalei	1	3	4	3	5	9	5	3	3
Paralecaniella indentata		5	5	8					
Quadrina ? condita				1					
Green Algae									
Botryococcus		1	2		2	2	1	2	
Gelasinicysta vangeelii	2		2	1		3	3		
Pediastrum spp. ind.						4	1		
Sigmopollis	4	8	14	9	8	9	7	13	2
Tasmanites	1	1		1			1		1
Zygnemataceae	2		1	3	5	11	3	1	1
Terrestrial Palynomorphs									
Bisaccate Pollen	628	882	740	710	552	560	402	189	160
Fern Spore	29	31	19	27	12	56	36	8	7
Fungal Spore		4	14	16	8	27	13	3	3
Monosaccate Pollen	3	9	10	7	7	8	2	3	2
Nonsaccate Pollen	344	386	357	427	257	396	288	198	199
Total	**1004**	**1312**	**1140**	**1187**	**836**	**1047**	**741**	**401**	**371**
Total Pollen Concentration	**48882.17**	**72245.02**	**90641.68**	**89691.8**	**158890.9**	**201870.3**	**157841.4**	**112630.3**	**58815.8**
Pollen Ratios									
D/Ap Ratio	0.200	0.177	0.189	0.174	0.246	0.191	0.243	0.373	0.390
D/Bp Ratio	0.280	0.237	0.259	0.253	0.325	0.288	0.356	0.551	0.591
D/Np Ratio	0.415	0.415	0.420	0.361	0.509	0.364	0.435	0.540	0.537
D/BpNp Ratio	0.201	0.178	0.190	0.175	0.247	0.192	0.243	0.375	0.392
Bp/Np Ratio	0.646	0.696	0.675	0.624	0.682	0.586	0.583	0.488	0.446
D/ApF Ratio	0.196	0.173	0.185	0.169	0.241	0.178	0.231	0.367	0.384
Other									
Foraminiferal lining	1	1	1	6	6	2	1		
Invertebrate remains	10	11	5	5	7	9	11	4	4
Stoma	1	4	12	5	3	3	4		
Sample Data									
Lycopodium clavatum	666	613	406	424	124	111	103	78	154
Lycopodium tablets	2	2	2	2	2	2	2	2	2
Sample dry weight (g)	75.35	43.98	47.93	50.07	66.88	66.49	59.95	50.70	74.13
Lycopodium per tablet	18584	18584	18584	18584	18584	18584	18584	18584	18584
Lycopodium tablet error	828	828	828	828	828	828	828	828	828
Standard deviation	1170.969	1170.969	1170.969	1170.969	1170.969	1170.969	1170.969	1170.969	1170.969
Statistical Data									
Richness	21	23	23	17	26	29	25	24	26
Error (%)	9.78	9.62	10.15	10.24	12.57	13.19	13.48	14.53	12.16
Standard Deviation (±)	17.68	36.33	50.03	43.19	149.82	150.73	180.19	316.74	91.47
Total marine palynomorphs (TMP)	293	323	317	298	303	271	259	288	295
Total protoperidinioid cysts	9	15	18	4	27	7	12	22	37
Total gonyaulacoid cysts	235	259	240	237	239	220	210	210	194
G/P	0.96	0.95	0.93	0.98	0.90	0.97	0.95	0.91	0.84
Shannon Index	1.31	1.28	1.23	1.13	1.42	1.43	1.72	1.92	1.84
Evenness	0.43	0.41	0.39	0.40	0.44	0.42	0.53	0.60	0.56
Cyst Ratios (VS Total Gonyaulacoid Cysts)									
Bitectatodinium cf. *raedwaldii*	7.66	5.79	1.67	2.95	0.42	3.18	4.76	1.90	2.58
Capisocysta lyellii	0.00	0.00	0.00	0.00	0.00	0.00	0.00	0.00	0.00
Heteraulacacysta sp. A of C & D	24.26	10.42	7.08	15.19	9.62	8.64	8.57	5.24	8.25
Lingulodinium machaerophorum	0.00	0.00	0.42	0.00	0.42	0.45	12.38	24.29	11.34
Operculodinium israelianum	0.43	0.77	1.67	0.00	0.00	0.00	1.90	7.14	7.22
Operculodinium tegillatum	0.00	0.00	0.00	0.00	0.00	0.00	0.00	0.48	0.00
Protoceratium reticulatum	11.49	10.04	9.58	14.77	10.04	15.45	7.62	8.10	7.73
Spiniferites/Achomosphaera spp. indet.	0.00	0.77	0.00	0.00	0.00	0.91	0.00	0.00	0.00
AIN	1.28	1.54	0.83	1.27	0.00	0.45	0.00	0.95	0.00
Cymatiosphaera ? invaginata VS TMP	4.25	3.87	4.52	5.10	5.02	6.87	9.76	15.04	15.47
Acritarch sp. 1 VS TMP	0.00	0.00	0.00	0.00	0.00	11.73	14.52	4.64	0.67

	Kasterlee Formation										
Slide Number	533	532	531	530	920	921	922	923	924	925	926
Depth (m)	25.72	26.39	26.56	26.79	27.30	28.35	29.33	30.30	31.30	32.30	33.08
Reworked Dinoflagellate Cysts											
Cleistosphaeridium sp.										1	
Cordosphaeridium cf. *inodes*									1		
Cordosphaeridium inodes					1						+
Cordosphaeridium sp.											
Glaphyrocysta sp.											
Unidentified reworked cyst		4	1				27	7	1	10	1
Total Reworked	**0**	**4**	**1**	**0**	**1**	**0**	**27**	**7**	**2**	**11**	**1**
Reworked Concentration (cysts/g)	**0.00**	**25.93**	**6.95**	**0.00**	**10.33**	**0.00**	**68.84**	**23.24**	**20.54**	**45.18**	**16.62**
Acritarchs											
Acritarch sp. 1	9	2		1	118	463	874	276	425	149	233
Acritarch sp. 2	6	1	4		1	3	2		3	2	
Acritarch sp. 3	2						1	1	2		1
Acritarch sp. 4	1		1						1	2	
Cyclopsiella sp.	2	3	4	4	4	9	10	6	3		3
Cymatiosphaera sp.	21	2		1	1	1	13	1	1	3	
Cymatiosphaera ? invaginata	147	40	56	33	90	92	33	27	54	27	28
Halodinium sp.											
Lavradosphaera sp.	10	1	8	6	5	4	3	1	2	5	4
Nanobarbophora walldalei	4	2	6	2	3	2	2	5	2	1	6
Paralecaniella indentata			1			1	1	1		2	
Quadrina ? condita				2		2		1			
Green Algae											
Botryococcus								1			
Gelasinicysta vangeelii										1	
Pediastrum spp. ind.	1				+						
Sigmopollis	21	9	24	8	27	15	17	28	24	65	19
Tasmanites		1	1						1		2
Zygnemataceae	4		1		2		82	36	10	16	11
Terrestrial Palynomorphs											
Bisaccate Pollen	272	265	244	210	190	114	609	434	204	557	188
Fern Spore	13	11	7	13	7	5	6	7	9	10	8
Fungal Spore	5	7	3	3		1	3	2			2
Monosaccate Pollen	6		2				5	5	1	9	2
Nonsaccate Pollen	416	171	285	176	151	145	681	598	171	575	121
Total	**712**	**454**	**541**	**402**	**348**	**265**	**1304**	**1046**	**385**	**1151**	**321**
Total Pollen Concentration	**164265.4**	**106768**	**134893.1**	**92339.89**	**111796.9**	**90567.46**	**185102.7**	**178931.3**	**121372.6**	**226332.7**	**120291.8**
Pollen Ratios											
D/Ap Ratio	0.279	0.378	0.311	0.410	0.380	0.465	0.142	0.181	0.389	0.181	0.455
D/Bp Ratio	0.497	0.500	0.496	0.561	0.524	0.664	0.261	0.345	0.540	0.311	0.580
D/Np Ratio	0.393	0.608	0.457	0.604	0.581	0.608	0.240	0.277	0.583	0.305	0.682
D/BpNp Ratio	0.281	0.378	0.312	0.410	0.380	0.465	0.143	0.182	0.389	0.182	0.457
Bp/Np Ratio	0.395	0.608	0.461	0.544	0.557	0.440	0.472	0.421	0.544	0.492	0.608
D/ApF Ratio	0.274	0.369	0.307	0.400	0.375	0.459	0.142	0.180	0.383	0.180	0.448
Other											
Foraminiferal lining									1	1	1
Invertebrate remains	2	6	2	3		1	15	33	2	9	1
Stoma	1	1					1	1	1	2	
Sample Data											
Lycopodium clavatum	92	81	71	80	61	44	216	166	54	135	34
Lycopodium tablets	2	2	2	2	2	2	2	2	2	2	2
Sample dry weight (g)	65.03	70.78	75.31	75.37	66.18	75.24	75.71	75.65	75.17	75.20	73.80
Lycopodium per tablet	18584	18584	18584	18584	20848	20848	20848	20848	20848	20848	20848
Lycopodium tablet error	828	828	828	828	1546	1546	1546	1546	1546	1546	1546
Standard deviation	1170.969	1170.969	1170.969	1170.969	2186.374	2186.374	2186.374	2186.374	2186.374	2186.374	2186.374
Statistical Data											
Richness	25	26	33	32	24	28	31	26	29	29	24
Error (%)	13.62	14.17	14.91	14.21	17.94	19.54	14.24	14.63	18.36	14.96	21.04
Standard Deviation (±)	227.65	243.50	248.69	234.81	387.21	553.65	78.06	111.20	450.69	154.82	908.91
Total marine palynomorphs (TMP)	443	312	307	308	307	330	274	269	299	285	297
Total protoperidinioid cysts	12	20	38	30	13	39	16	24	32	35	74
Total gonyaulacoid cysts	257	245	202	238	196	186	199	205	207	217	186
G/P	0.96	0.92	0.84	0.89	0.94	0.83	0.93	0.90	0.87	0.86	0.72
Shannon Index	1.86	1.89	1.80	1.88	1.59	1.90	1.56	1.60	1.95	1.76	1.82
Evenness	0.58	0.58	0.52	0.54	0.50	0.57	0.46	0.49	0.58	0.52	0.57
Cyst Ratios (VS Total Gonyaulacoid Cysts)											
Bitectatodinium cf. *raedwaldii*	4.28	6.94	2.48	5.88	12.24	17.20	2.01	2.93	13.04	1.84	6.45
Capisocysta lyellii	0.00	0.00	0.00	0.00	0.00	0.00	0.00	0.00	0.00	0.00	0.00
Heteraulacacysta sp. A of C & D	12.06	10.61	5.45	5.04	2.04	0.54	2.51	3.90	2.90	6.45	5.38
Lingulodinium machaerophorum	18.29	10.61	12.87	9.66	7.65	1.61	1.01	3.41	0.97	1.38	0.54
Operculodinium israelianum	5.06	15.51	10.89	8.40	6.12	5.91	2.01	3.90	4.35	3.23	11.83
Operculodinium tegillatum	0.39	2.86	2.48	3.78	2.55	1.61	12.06	20.00	20.29	22.12	17.20
Protoceratium reticulatum	7.00	8.57	2.48	2.94	0.00	0.00	1.01	0.98	0.00	0.00	0.00
Spiniferites/Achomosphaera spp. indet.	0.00	0.00	0.00	0.00	0.00	0.00	0.50	0.00	0.00	0.92	0.00
AIN	1.95	0.00	0.50	0.00	0.00	2.15	4.02	0.00	1.45	0.00	1.08
Cymatiosphaera ? invaginata VS TMP	24.92	11.36	15.43	9.68	22.67	21.80	10.75	9.12	15.30	8.65	8.62
Acritarch sp. 1 VS TMP	1.99	0.64	0.00	0.32	27.76	58.39	76.13	50.64	58.70	34.33	43.96

	Diest Formation								
Slide Number	927	928	929	930	931	932	933	934	935
Depth (m)	33.30	34.35	35.50	35.98	36.30	36.90	37.85	38.35	39.50
Reworked Dinoflagellate Cysts									
Cleistosphaeridium sp.		1			1	+	1	1	
Cordosphaeridium cf. *inodes*		1			3		1		
Cordosphaeridium inodes						1			
Cordosphaeridium sp.									
Glaphyrocysta sp.									
Unidentified reworked cyst	24	16	3		13	2	12	19	
Total Reworked	**24**	**17**	**3**	**0**	**14**	**3**	**13**	**19**	**0**
Reworked Concentration (cysts/g)	**26.55**	**10.69**	**19.66**	**0.00**	**19.28**	**14.78**	**19.08**	**41.10**	**0.00**
Acritarchs									
Acritarch sp. 1	49	29	84	167	15	546	6	176	70
Acritarch sp. 2		2		1				1	
Acritarch sp. 3	1		1						
Acritarch sp. 4		2		3	1	3			
Cyclopsiella sp.	17	14	7	3	1	3	4	1	9
Cymatiosphaera sp.	1	3				1		1	4
Cymatiosphaera ? invaginata	7	7	8	31		14	2	24	2
Halodinium sp.	1								
Lavradosphaera sp.	2	1	1	4		14	1	2	
Nanobarbophora walldalei				1					
Paralecaniella indentata	7	5	1		2	+	4	3	238
Quadrina ? condita				1		1		1	
Green Algae									
Botryococcus									
Gelasinicysta vangeelii						2		2	1
Pediastrum spp. ind.							1	3	
Sigmopollis	7	10	15	24	4	40	2	16	4
Tasmanites	1	2		5	1	6		2	1
Zygnemataceae	17	12	4	32	7	50	11	52	1
Terrestrial Palynomorphs									
Bisaccate Pollen	123	65	148	252	33	445	87	276	7
Fern Spore	3	7	8	16	2	1	7	13	4
Fungal Spore	2	2	2	2			1	2	
Monosaccate Pollen	2		2	3	1	4	1	5	1
Nonsaccate Pollen	144	92	86	259	59	355	72	245	30
Total	**274**	**166**	**246**	**532**	**95**	**805**	**168**	**541**	**42**
Total Pollen Concentration	**19464.84**	**6878.721**	**61601.7**	**151589.6**	**8110.20**	**178744.8**	**14748.23**	**66485.07**	**1601.58**
Pollen Ratios									
D/Ap Ratio	0.383	0.571	0.552	0.344	0.354	0.278	0.392	0.177	0.542
D/Bp Ratio	0.576	0.763	0.663	0.517	0.607	0.410	0.542	0.290	0.865
D/Np Ratio	0.537	0.694	0.772	0.510	0.464	0.465	0.589	0.316	0.600
D/BpNp Ratio	0.385	0.571	0.554	0.346	0.357	0.279	0.393	0.178	0.549
Bp/Np Ratio	0.461	0.414	0.632	0.493	0.359	0.556	0.547	0.530	0.189
D/ApF Ratio	0.379	0.557	0.542	0.337	0.349	0.277	0.380	0.173	0.517
Other									
Foraminiferal lining	5	1		1	2		3	1	
Invertebrate remains		14	1	1	1		2	1	8
Stoma	1			1	1	1	1	1	
Sample Data									
Lycopodium clavatum	501	876	84	87	403	112	377	254	914
Lycopodium tablets	2	2	2	2	2	2	2	2	2
Sample dry weight (g)	75.23	75.67	75.74	54.38	75.13	75.55	75.35	75.88	75.30
Lycopodium per tablet	20848	20848	20848	20848	20848	20848	20848	20848	20848
Lycopodium tablet error	1546	1546	1546	1546	1546	1546	1546	1546	1546
Standard deviation	2186.374	2186.374	2186.374	2186.374	2186.374	2186.374	2186.374	2186.374	2186.374
Statistical Data									
Richness	22	25	32	30	15	33	22	20	12
Error (%)	13.78	13.01	16.23	16.19	18.52	15.22	15.31	15.45	18.52
Standard Deviation (±)	25.45	17.10	309.52	385.14	12.24	231.74	22.93	37.43	5.05
Total marine palynomorphs (TMP)	200	238	307	305	51	327	112	141	298
Total protoperidinioid cysts	15	12	51	72	2	119	32	25	2
Total gonyaulacoid cysts	152	197	240	198	46	190	70	87	43
G/P	0.91	0.94	0.82	0.73	0.96	0.61	0.69	0.78	0.96
Shannon Index	1.46	1.51	1.83	2.13	1.55	1.81	1.53	1.77	1.08
Evenness	0.47	0.47	0.53	0.63	0.57	0.52	0.49	0.59	0.43
Cyst Ratios (VS Total Gonyaulacoid Cysts)									
Bitectatodinium cf. *raedwaldii*	1.97	1.02	4.58	7.58	0.00	24.74	7.14	3.45	4.65
Capisocysta lyellii	0.00	0.00	0.00	0.00	0.00	0.00	0.00	0.00	0.00
Heteraulacacysta sp. A of C & D	19.74	41.12	7.92	3.03	0.00	0.53	5.71	9.20	0.00
Lingulodinium machaerophorum	0.66	2.03	0.42	0.51	0.00	0.53	0.00	0.00	20.93
Operculodinium israelianum	7.24	6.09	9.58	12.63	4.35	3.68	2.86	0.00	6.98
Operculodinium tegillatum	31.58	15.74	40.00	33.84	0.00	1.58	0.00	4.60	2.33
Protoceratium reticulatum	0.00	0.00	0.00	0.00	0.00	0.00	0.00	0.00	0.00
Spiniferites/Achomosphaera spp. indet.	0.66	0.00	0.42	0.00	0.00	0.00	0.00	3.45	0.00
AIN	0.66	1.52	0.83	0.00	0.00	0.00	0.00	0.00	0.00
Cymatiosphaera ? invaginata VS TMP	3.38	2.86	2.54	9.23	0.00	4.11	1.75	14.55	0.67
Acritarch sp. 1 VS TMP	19.68	10.86	21.48	35.38	22.73	62.54	5.08	55.52	19.02